ISSN 2636-8498

Environmental Research & Technology

Year 2022
Volume 5
Number 4

YTU PRESS

www.ert.yildiz.edu.tr

ISSN 2636-8498

Environmental Research & Technology

Volume 5 Number 4 Year 2022

ISSN 2636-8498

Environmental Research & Technology

Volume 5 Number 4 Year 2022

ISSN 2636-8498

Environmental Research & Technology

Volume 5 Number 4 Year 2022

CONTENTS

Environ Res Tec, Vol. 5, Issue. 4, pp. 289–295, December 2022

Environmental Research and Technology
https://ert.yildiz.edu.tr - https://dergipark.org.tr/tr/pub/ert
DOI: https://doi.org/10.35208/ert.1117728

Environmental Research & Technology

Research Article

Comparison of mechanical and physical properties of screed with and without expanded polystyrene (EPS) particles

Fikret Merih KILIÇ[1], Hediye YORULMAZ[*2], Sümeyye ÖZUZUN[1], Uğur DURAK[1], Serhan İLKENTAPAR[1], Okan KARAHAN[1], Cengiz Duran ATİŞ[1]

[1]Department of Civil Engineering, Erciyes University, Kayseri, Türkiye
[2]Department of Civil Engineering, Abdullah Gül University, Kayseri, Türkiye

ARTICLE INFO

Article history
Received: 20 May 2022
Revised: 30 July 2022
Accepted: 03 November 2022

Key words:
EPS; Light-weight screed; Screed; Strength

ABSTRACT

In this study, in order to observe the mechanical and physical properties of ordinary screed, sandy-lightweight screed and lightweight screed samples, expanded polystyrene (EPS) was used as fine aggregate and lightweight screed systems were produced by replacing sand at 100%, 50% and 0%. Samples of cement dosages of 250, 300, 350 kg/m^3 were produced for lightweight screeds, sandy-lightweight screeds and ordinary screeds. Unit weight, water absorption capacity, flexural strength, compressive strength, fire resistance, abrasion and thermal conductivity tests were performed on the produced screed systems. As a result of the research, it was determined that as EPS ratio increases in screed system; unit weights decreased, water absorption rates increased. Besides, the flexural and compressive strengths, fire and abrasion resistance are also decreased. However, it was observed that the thermal conductivity coefficient reduced with the increment of EPS particles in the screed. In normal, sandy-lightweight and lightweight screeds, it was determined that as the cement dosage increased; the unit weights, flexural and compressive strengths, fire and abrasion resistance increased, water absorption capacity and the thermal conductivity coefficient decreased.

Cite this article as: Kılıç FM, Yorulmaz H, Özuzun S, Durak U, İlkentapar S, Karahan O, Atiş CD. Comparison of mechanical and physical properties of screed with and without expanded polystyrene (EPS) particles. Environ Res Tec 2022;5:4:289–295.

INTRODUCTION

A traditional screed mixture consists of cement, aggregate and water. As heat and sound insulation rules have gotten more strict, it has been suggested that new goods must be developed that can compete in terms of performance with existing products [1]. In general, lightweight aggregates are divided into 2 classes: natural and artificial. Diatomite, pumice and volcanic slag are examples of natural aggregates, while clay, expanded shales, and perlite are examples of artificial aggregates [2]. Lightweight aggregates can affect both fresh and hardened state properties of concrete in different ways, depending on their origin and qualities [3]. Because the aggregate is stronger than the transition zone

***Corresponding author.**
*E-mail address: hediye.yorulmaz@agu.edu.tr

Table 1. Chemical composition of Portland cement (%)

Oxide	SiO_2	Al_2O_3	Fe_2O_3	CaO	MgO	SO_3	$Na_2O+0,658K_2O$	Cl^-	Free CaO	LOI
Portland cement	18.80	5.81	2.61	62.90	1.29	2.74	0.74	0.033	0.70	3.27

and matrix, aggregate strength has no effect on concrete strength in normal weight concrete. But, since lightweight aggregate's strength is generally lower than the strength of the other 2 phases, the concrete's strength depends on the lightweight aggregate's strength [4]. Lightweight concrete is usually used to decrease a dead mass of the structure and to decrease the potential of earthquake damage. Because the earthquake forces affecting the structures are directly proportional to the mass of the structures. Therefore, if the weight of the structure is decreased, it is possible to decrease the risks caused by the acceleration of earthquake [5]. It is known that lightweight concrete is approximately 28% lighter than normal concrete [6]. Additionally, low density aggregates result in reduced stress concentrations in concrete and cause less micro cracks in the cement paste matrix compared to normal density aggregates. When compared to conventional concrete, lightweight concrete has a more uniform stress distribution at the micro level, resulting in greater endurance in hard conditions and increased concrete impermeability [6].

Polystyrene beads are a type of aggregate commonly used and easily added to system to obtain lightweight concrete in a variety of densities. Expanded polystyrene(EPS) is a stable low density foam with separate air gaps in the polymer matrix [7]. Small polystyrene beads generated from the styrene via polymerization process make up EPS [8]. It has been stated in previous publications that with altering the volume proportion in mortar or concrete, EPS can be utilized as an ultra-lightweight aggregate appropriate for not only structural but also non-structural purposes [9]. EPS is a material that attracts attention in construction applications thanks to its many advantages [10–13]. These advantages are can be listed; good performance, less material usage and cost of installation, resistance to moisture penetration and biodegradation [10]. Brás et al. [12] noted that the water produced by the EPS beads in EPS bead mortar samples allowed the workability to rise, notably between 5 and 15 minutes, and this had a favorable impact on the workability of the mortar mixes. Besides, it is constructed of pre-expanded polystyrene beads, which have excellent thermal insulation qualities [12]. Its availability in a large variety of densities and sizes is another positive property [10]. Unlike other artificial lightweight materials, EPS aggregates are commercially accessible all around the world [14].

In this study, the properties of normal screed (NS), sandy-lightweight screed (SLS) and EPS granular lightweight screed (LS) samples were examined and compared with each other. Normal screed prepared with sand as fine aggregate, sandy-lightweight screed prepared using 50% less sand and adding 5 grams of EPS particles and lightweight screed samples prepared by adding 10 grams of EPS particles without using any sand were investigated. Normal screed, known as traditional screed, contains sand, cement and water. EPS particles used in lightweight screed production are combined with agents, which are a special additive material, under the factory conditions. Lightweight screed is produced by mixing EPS particles with Portland cement and water in certain proportions in the construction site environment.

For this research, normal screed, sandy-lightweight screed and lightweight screed samples produced with cement dosages of 250, 300, 350 kg/m^3 were adjusted to almost the same workability. The amount of EPS added was calculated by reducing the volume according to the amount of sand. The prepared samples were cured in water at room conditions. Unit volume weight, water absorption and void ratio, flexural strength, compressive strength, abrasion resistance, fire resistance and thermal conductivity properties were examined in screed samples.

MATERIALS AND METHODS

Materials

Portland cement (PC) CEM I 42,5R was used in this study. Chemical composition of PC is given in the Table 1. Specific gravity of cement is 3.15 g/cm^3, and its specific surface area is 3561 cm^2/g. Normal screed samples were prepared by using 0–4 mm natural river sand as fine aggregate. The properties of the fine aggregate obtained as a result of the experiments on fine aggregate are presented in Table 2. The properties of EPS particles used in the research are given in Table 3. EPS materials are combined with a concrete additive material called an agent in order to form a bond between EPS particles and cement mortar in the factory environment.

Mix Proportion

A total of 9 different mixes were prepared with the constant water/binder ratio of 0.6. Normal screed (NS), sandy-lightweight screed (SLS) and lightweight screed (LS) systems were produced. Normal screed, sandy-lightweight screed and lightweight screed specimens are produced at 250, 300, 350 kg/m^3 cement dosages. Mixing ratios for mortar samples are presented in Table 4. The mixtures were casted into molds of 40×40×160 mm^3, 71×71×71 mm^3 and 500×500×50 mm^3 and they were re-

Table 2. Properties of natural river sand

	Specific gravity (SSD) (g/cm³)	Water absorption capacity (%)	Fineness modulus	Amount of filler (%)	Loose unit weight (g/cm³)	Strict unit Weight (g/cm³)
River sand	2.32	4.61	2.39	0.20	1.653	1.784

Table 3. Properties of EPS particles

	Thermal conductivity (W/mK)	Cohesion (kPa)	Modulus of Elasticity	Permeability	Acoustic performance (dB)	Flexural strength (MPa)	Compressive strength (MPa)
EPS	0.067	82.62	–	11.50	14	0.46	0.83

moved from the molds after 24 hours and cured in water at room conditions (21±1 °C) until the test days.

Methods

The 40×40×160 mm³ prismatic specimens were cured in water for 28 days and then removed from the water and dried in an oven, and specimen's weight were measured. The unit weights of the mortars were determined by dividing the weight of the samples by their volume. Water absorption capacity was determined on prismatic samples of 40×40×160 mm³ cured in water for 28 days. The samples, which were kept at 105±5 °C for 24 hours in an oven, were kept at room temperature at the end of 24 hours and their oven dry weights were measured. Then, the samples were kept in water at room temperature (21±1 °C) for 24 hours. After 24 hours, the samples were taken out of the water, the outer surfaces of the samples were dried and their saturated surface dry (SSD) weights were determined. The water absorption capacity (%) can be determined by dividing the difference between the SSD weight of the sample and the oven dry weight of the sample by the dry weight of the sample, multiplying the result by 100. The flexural and compressive strength of 40x40x160 mm³ prismatic screed samples were determined on the 7 and 28 days in accordance with TS EN 1015-11 [15]. The prismatic screed specimens, which were cured in water for 28 days, were removed from the water and dried by furnace at 105±5 °C for 24 h. Then it was exposed to high temperatures of 300 °C in the oven. The temperature increase rate of the oven was set as 1 °C/min. After the furnace was kept at these 300 °C for 1 hour, the furnace was turned off and the specimens were left to cool in the furnace in order not to expose the samples to the effect of sudden temperature changes. Flexural strength and compressive strength tests were performed after the screed samples were allowed to cool down to room temperature. To determine the abrasion resistance of the systems, 71×71×71 mm³ cubic screed samples were produced and determined in accordance with TS 2824 EN 1338 [16]. The average of three samples was taken for result of all experiments. The brand of the device for which the thermal conductivity test is performed is "Thermtest", and the model is the "heat flow meter". The thermal conductivity coefficient of the 500×500×50 mm³ sized samples was determined by using the enclosed plate device. Surface temperatures are controlled by foils with thermocouples placed on both surfaces of the samples. Temperature changes were recorded from the cooler and heating plate by means of thermocouples and calibrated cables.

Table 4. Mixing ratios for 1 m³ of samples

Sample name	Cement (g)	Sand (g)	EPS granule (g)	Water (g)
NS 250	250	1883	–	150
NS 300	300	1776	–	180
NS 350	350	1649	–	210
SLS 250	250	942	5	150
SLS 300	300	883	5	180
SLS 350	350	825	5	210
LS 250	250	–	10	150
LS 300	300	–	10	180
LS 350	350	–	10	210

3. RESULTS AND DISCUSSION

Unit Weight, Water Absorption and Thermal Conductivity

The results of measurement of unit weight, water absorption and thermal conductivity coefficient are presented in Table 5. Considering the results shown in Table 5 and Figure 1, unit weights of hardened screed samples were found to be between 0.26 and 2.22 g/cm³. The increase in the amount of cement in the screed samples causes the unit weight values to increase. For example, the unit weights of the SLS 250, SLS 300 and SLS 350 samples are 1.26, 1.30 and 1.4 g/cm³, respectively, and this behavior is similar in the other sample series. However, the use of EPS particles instead of sand aggregate in the mixture causes a decrease in unit weight.

Table 5. Unit weight, water absorption and thermal conductivity coefficient

Sample code	Unit weight g/cm³	Absorption %	Thermal conductivity W/mK
NS 250	2.13	7	0.575
NS 300	2.17	6.7	0.752
NS 350	2.22	5.4	0.784
SLS 250	1.26	11.9	0.296
SLS 300	1.3	10.6	0.344
SLS 350	1.4	9.3	0.392
LS 250	0.26	46.8	0.073
LS 300	0.28	40.8	0.083
LS 350	0.32	39.1	0.091

Table 6. Abrasion results of all specimens

Sample code	Abrasion (mm³/5000 mm²)	Weight loss (%)
NS 250	19570	5.5
NS 300	9987	2.8
NS 350	7008	2.4
SLS 250	24568	6.6
SLS 300	13270	3.7
SLS 350	10938	3.0
LS 250	63324	18.3
LS 300	40786	12.1
LS 350	29805	8.4

The unit weights of NS 250, SLS 250 and LS 250 samples with the same cement values were 2.13, 1.26 and 0.26 g/cm³; the unit weights of the NS 300, SLS 300 and LS 300 samples were 2.17, 1.30 and 0.28; the unit weights of NS 350, SLS 350 and LS 350 samples are 2.22, 1.4 and 0.32 g/cm³, respectively. According to the Table 5, the EPS particles increases the water absorption capacity and the highest water absorption percentages are 46.8%, 40.8% and 39.1% for the LS 250, LS 300 and LS 350 samples, respectively. At the same time, the increase in cement in all screed mixtures reduces the water absorption capacity.

Moreira et. al [1] also showed this inverse ratio between the cement amount in the mixture and the water absorption capacity in the literature. The amount of heat transmitted from the unit thickness and unit temperature gradient in a direction perpendicular to the unit area surface is the thermal conductivity of the material. Porosity is one of the characteristics that has a substantial impact on the sample's thermal conductivity and due to the poor thermal conductivity of air, closed pores decrease the conductivity [17–19].

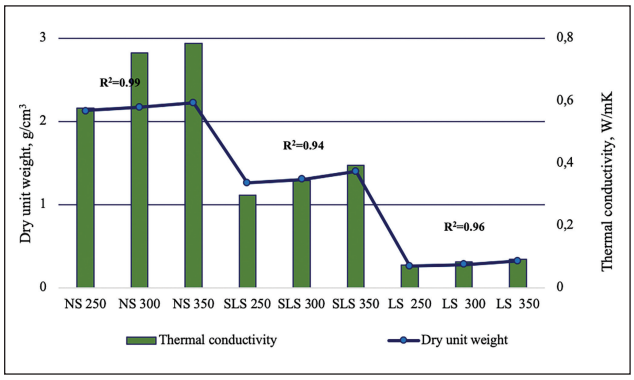

Figure 1. Unit weight and thermal conductivity.

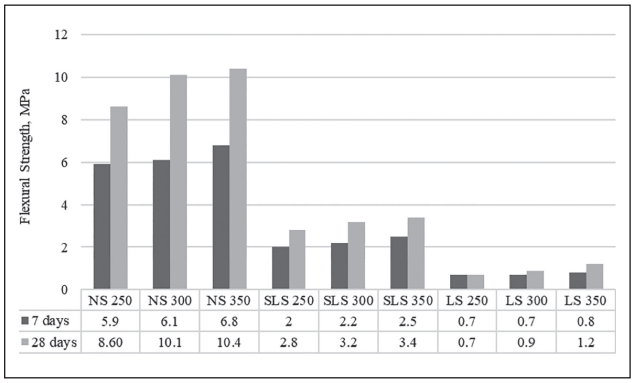

Figure 2. Flexural strengths of the screed mixtures.

The linear relationship between unit weight and thermal conductivity is shown in Figure 1. Replacing the aggregate with the EPS particles increased the total porosity of the samples and decreased the thermal conductivity. This results is in line with the literature [20]. Thus, as seen in Figure 1, there is a linear relationship between the unit weights of the samples and their thermal conductivity, as in many studies [19, 21]. Based on Figure 1, the correlation coefficient of the linear relationship between unit weight and thermal conductivity is 0.99, 0.94, 0.96, respectively. The variations obtained are similar to those reported in previous studies of lightweight concretes [19, 21–23].

According to many studies, the inclusion of lightweight aggregates in cementitious systems results in a decrease in the thermal conductivity of the lightweight composite cementitious system [1, 22–24]. The addition of EPS causes a decrease of 49% for SLS 250 and 75% for LS 250 in the use of 250 kg/m³ cement compared to references in thermal conductivity coefficients. Similar reduction percentages are also encountered in the use of 300 kg/m³ and 350 kg/m³ cement. It is seen that the thermal conductivity of the NS 350, SLS 350, LS 350 samples, each of which contains 350 kg/m³ cement in three different series, is higher than the others, that is, the low cement content reduces the thermal conductivity.

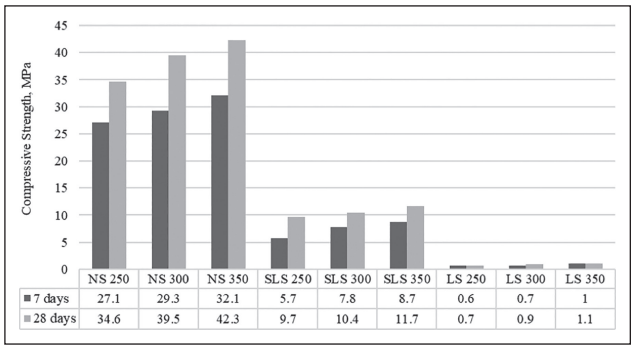

Figure 3. Compressive strength of the screed mixtures.

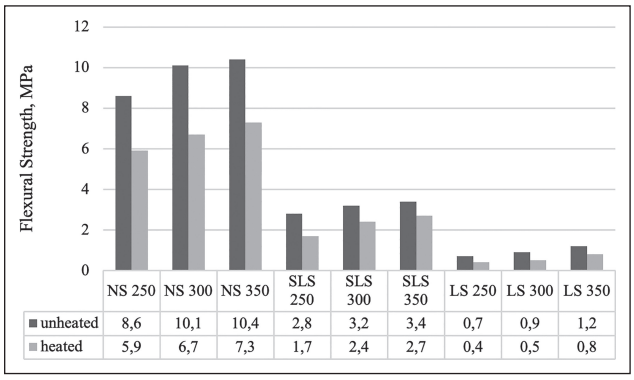

Figure 4. Comparison between heated and non-heated flexural strength of specimens.

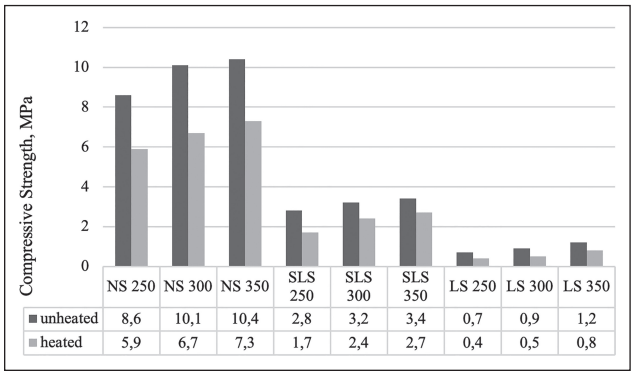

Figure 5. Comparison between heated and non-heated compressive strength of specimens.

Flexural and Compressive Strength Results

Figure 2 and Figure 3 demonstrated that flexural strength and compressive strength of the screed mixtures prepared with and without EPS was compared at 7 and 28 days, respectively. As shown in Figure 2, 7 day flexural strength values of NS screed mixtures prepared without EPS addition are 5.9, 6.1, 6.8, while the values of SLS screed mixtures are 2.0, 2.2, 2.5, and the values of LS screed samples are 0.7, 0.7, 0.8. Similar behavior is also present at 28-day flexural strength values. On the other hand, in Figure 3, the 7 day compressive strength values of NS screed mixtures prepared without EPS addition are 27.1, 29.3, 32.1, while the values of SLS screed mixtures are 5.7, 7.8, 8.7 and the values of LS samples are 0.6, 0.7, 1.0. Likewise, a similar situation was observed at 28-day values. These strength values show a decrease with EPS added to the mixtures and therefore the lowest strength values belong to LS 250, LS 300 and LS 350. The results of the flexural and compressive strength of the screed samples increased in direct proportion to the cement content. Due to the presence of EPS particles, the flexural cross-section height decreases and the flexural strength decreases [19, 25].

Fire Resistance

The high-temperature (300 °C) heating impact on the compressive and flexural strength of NS, SLS and LS specimens are displayed in Figure 4 and Figure 5. After applying high temperature to the samples, the use of lightweight aggregate in the screed mixtures causes a decrease in the structural strength and it has been observed that the samples containing lightweight aggregate, namely SLS and LS, have a higher fire resistance. The porosity formed during production of EPS results in a lower thermal conductivity and coefficient of thermal expansion, and they show less loss of strength in the fire resistance test.

Abrasion Resistance

The measurement results of the screed specimens are presented in Table 6. The results show that the addition of lightweight aggregate to the mixture of screed specimens reduces the abrasion resistance, that is, it has the highest abrasion value and the highest weight loss. The increase in cement content of the screed samples decreased the amount of abrasion and weight loss. In other words, the lowest ones in each series are NS 350, SLS 350 and LS 350. The increase in cement content of the screed samples decreased the amount of abrasion and weight loss. The increment in cement content of the screed samples decreased the amount of abrasion and weight loss, which was observed in three group sample series.

CONCLUSIONS

Based on the experimental results of the use of EPS in the screed mixtures formed in this study, the following conclusions can be drawn:

1. It has been observed that the unit weight of the NS samples is higher than the LS containing EPS particles and the SLS samples, and this is due to the porous structure of the replaced EPS particles instead of the aggregate. Increasing the EPS volume in the mix reduces the unit weight of the sample due to the higher air content. Due to this porous structure, water absorption increases and since the pores prevent heat

conduction, it reduces thermal conductivity. That is, unit weight and thermal conductivity behave in direct proportion to each other. The increase in the amount of cement in the mixture limited the porous structure. The unit weight of the LS samples of the porous structure formed due to the addition of EPS particles to the mixtures are smaller than SLS and NS samples. With the effect of the pores in this structure, the thermal conductivity properties are likewise NS, SLS and LS, from largest to smallest, respectively.

2. The expected strength loss has occurred due to the material structure of the EPS particles and the amount of air entering the mixture with the addition. Therefore, NS samples were found to have higher flexural and compressive strengths than SLS and LS samples containing EPS particles. Among the two, LS samples have the lowest strength values since they contain the most EPS. In addition, the increase in the amount of binder material in the mixture within the sample groups increased the strength values slightly.
3. The porosity that occurs in the use of EPS particles relative to their fire resistance values results in a lower thermal conductivity and thermal expansion coefficient, and they show less strength loss in fire resistance testing. NS samples without EPS particles showed greater differences when exposed to 300 °C. The increase the increase in the amount of binder provided a slight increase in the fire resistance values.
4. It has been observed that EPS particles reduce the abrasion resistance of the samples due to the material structure and the porosity caused in the samples. NS samples are more resistant to abrasion than LS and SLS samples containing EPS particles. The reason for this is that the aggregate is more resistant to abrasion than EPS particles. It was clearly seen that the increase in binder in the mixture increased the abrasion resistance in all samples.

DATA AVAILABILITY STATEMENT

The authors confirm that the data that supports the findings of this study are available within the article. Raw data that support the finding of this study are available from the corresponding author, upon reasonable request.

CONFLICT OF INTEREST

The authors declared no potential conflicts of interest with respect to the research, authorship, and/or publication of this article.

ETHICS

There are no ethical issues with the publication of this manuscript.

REFERENCES

[1] A. Moreira, J. António, and A. Tadeu, "Lightweight screed containing cork granules: Mechanical and hygrothermal characterization," Cement and Concrete Composites, Vol. 49, pp. 1–8, 2014. [CrossRef]

[2] B. Chen, and N. Liu, "A novel lightweight concrete-fabrication and its thermal and mechanical properties," Construction and Building Materials, Vol. 44, pp. 691–698, 2013. [CrossRef]

[3] A. Ben Fraj, M. Kismi, and P. Mounanga, "Valorization of coarse rigid polyurethane foam waste in lightweight aggregate concrete," Construction and Building Materials, Vol. 24(6), pp. 1069–1077, 2010. [CrossRef]

[4] C. Yang, and R. Huang, "Approximate strength of lightweight aggregate using micromechanics method," Advanced Cement Based Materials, Vol. 7, pp. 133–138, 1998. [CrossRef]

[5] E. Yasar, C. D. Atis, A. Kilic, and H. Gulsen, "Strength properties of lightweight concrete made with basaltic pumice and fly ash," Materials Letters, Vol. 57(15), pp. 2267–2270, 2003. [CrossRef]

[6] T. W. Bremner, "Environmental Aspects of Concrete: Problems and Solutions," Proc. First Russ. Conf. Concr. Reinf. Concr. Probl, no. Moscow, Russia, pp. 232–246, 2001.

[7] R. Sri Ravindrarajah, and A. J. Tuck, "Properties of hardened concrete containing treated expanded polystyrene beads," Cement and Concrete Composites, Vol. 16(4), pp. 273–277, 1994. [CrossRef]

[8] N. H. Ramli Sulong, S. A. S. Mustapa, and M. K. Abdul Rashid, "Application of expanded polystyrene (EPS) in buildings and constructions: A review," Journal of Applied Polymer Science, Vol. 136(20), pp. 1–11, 2019. [CrossRef]

[9] D. S. Babu, K. Ganesh Babu, and T. H. Wee, "Properties of lightweight expanded polystyrene aggregate concretes containing fly ash," Cement and Concrete Research, Vol. 35(6), pp. 1218–1223, 2005. [CrossRef]

[10] S. Doroudiani, and H. Omidian, "Environmental, health and safety concerns of decorative mouldings made of expanded polystyrene in buildings," Building and Environment, Vol. 453, pp. 647–654, 2010. [CrossRef]

[11] K. Miled, K. Sab, and R. Le Roy, "Particle size effect on EPS lightweight concrete compressive strength: Experimental investigation and modelling," Mechanics of Materials, Vol. 39(3), pp. 222–240, 2007. [CrossRef]

[12] A. Brás, M. Leal, and P. Faria, "Cement-cork mortars for thermal bridges correction. Comparison with cement-EPS mortars performance," Construction and Building Materials, Vol. 49, pp. 315–327, 2013. [CrossRef]

[13] D. P. P. Meddage, A. Chadee, M. T. R. Jayasinghe, and U. Rathnayake, "Exploring the applicability of expanded polystyrene (EPS) based concrete panels as roof slab insulation in the tropics," Case Studies in Construction Materials, Vol. 17, Article e01361, 2022. [CrossRef]

[14] D. S. Babu, K. Ganesh Babu, and W. Tiong-Huan, "Effect of polystyrene aggregate size on strength and moisture migration characteristics of lightweight concrete," Cement and Concrete Composites, Vol. 28(6), pp. 520–527, 2006. [CrossRef]

[15] TS EN 1015-11, "Methods of test for mortar for masonry- Part 11: Determination of flexural and compressive strength of hardened mortar," TSE, 2020.

[16] TS 2824 EN 1338, "Concrete paving blocks - Requirements and test methods," TSE, 2005.

[17] E. K. Akpinar, and F. Koçyigit, "Thermal and mechanical properties of lightweight concretes produced with pumice and tragacanth," Journal of Adhesion Science and Technology, Vol. 30(5), pp. 534–553, 2016. [CrossRef]

[18] H. Oktay, R. Yumrutaş, and A. Akpolat, "Mechanical and thermophysical properties of lightweight aggregate concretes," Cement and Concrete Composites, Vol. 96, pp. 217–225, 2015. [CrossRef]

[19] O. Sengul, S. Azizi, F. Karaosmanoglu, and M. A. Tasdemir, "Effect of expanded perlite on the mechanical properties and thermal conductivity of lightweight concrete," Energy and Buildings, Vol. 43(2–3), pp. 671–676, 2011. [CrossRef]

[20] M. Mohammad, E. Masad, T. Seers, and S. G. Al-Ghamdi, "Properties and microstructure distribution of high-performance thermal insulation concrete," Materials (Basel), Vol. 13(9), 2020. [CrossRef]

[21] R. Demirboğa, and R. Gül, "The effects of expanded perlite aggregate, silica fume and fly ash on the thermal conductivity of lightweight concrete," Cement and Concrete Research, Vol. 33(5), pp. 723–727, 2003. [CrossRef]

[22] R. Demirboğa, and R. Gül, "Thermal conductivity and compressive strength of expanded perlite aggregate concrete with mineral admixtures," Energy and Buildings, Vol. 35, no. 11, pp. 1155–1159, 2003. [CrossRef]

[23] J. Khedari, B. Suttisonk, N. Pratinthong, and J. Hirunlabh, "New lightweight composite construction materials with low thermal conductivity," Cement and Concrete Composites, Vol. 23(1), pp. 65–70, 2001. [CrossRef]

[24] D. K. Panesar, and B. Shindman, "The mechanical, transport and thermal properties of mortar and concrete containing waste cork," Cement and Concrete Composites, vol. 34(9), pp. 982–992, 2012. [CrossRef]

[25] N. Liu, and B. Chen, "Experimental study of the influence of EPS particle size on the mechanical properties of EPS lightweight concrete," Construction and Building Materials, Vol. 68, pp. 227–232. [CrossRef]

Environ Res Tec, Vol. 5, Issue. 4, pp. 296–304, December 2022

Environmental Research and Technology
https://ert.yildiz.edu.tr - https://dergipark.org.tr/tr/pub/ert
DOI: https://doi.org/10.35208/ert.1144689

Environmental Research & Technology

Research Article

Exploring hexagonal boron nitride (BN) as an efficient visible light-induced catalyst for the remediation of recalcitrant antibiotics from aqueous media

Zeynep BALTA[*1], Esra BİLGİN ŞİMŞEK[2]

[1]*Department of Chemical and Process Engineering, Yalova University, Institute of Science, Yalova, Türkiye*
[2]*Department of Chemical Engineering, Yalova University, Faculty of Engineering, Yalova, Türkiye*

ARTICLE INFO

Article history
Received: 17 July 2022
Revised: 02 September 2022
Accepted: 11 October 2022

Key words:
Degradation; Hexagonal boron nitride; Photocatalysis, Whisker; Tetracycline

ABSTRACT

Hexagonal boron nitride (h-BN) is a novel non-metallic material which is newly discovered in the field of photocatalysis due to its high surface area, excellent optical features and high electrical conductivity. Herein, hexagonal boron nitride whiskers were fabricated by using the polymeric precursor method and, the photocatalytic degradation performance was measured towards tetracycline antibiotic under visible-light-illumination. The morphological, physical, and optical features of the catalyst were identified by several characterization analyses. The characteristic peaks associated with the hexagonal phase of boron nitride were determined and high crystallinity of h-BN was confirmed by X-ray diffraction analysis. The characteristic B–N absorption peaks were detected in the Fourier transfer infrared spectrum. Brunauer–Emmet–Teller specific surface area of the boron nitride catalyst was calculated as 1019 m^2/g which was relatively high, supplying abundant active regions to interact with the target pollutant. In photocatalytic degradation experiments, 91.9% of tetracycline decomposition was achieved within 180 min with a catalyst dosage of 0.2 g/L and initial concentration of 10 mg/L. The outstanding catalytic activity of the h-BN catalyst was attributed to the high surface area and negatively charged groups on the surface which captured the photo-induced holes and inhibited the recombination rate of charge carriers. These findings highlight the potential application of h-BN in the field of photocatalytic processes.

Cite this article as: Balta Z, Bilgin Şimşek E. Exploring hexagonal boron nitride (BN) as an efficient visible light-induced catalyst for the remediation of recalcitrant antibiotics from aqueous media. Environ Res Tec 2022;5:4:296–304.

INTRODUCTION

Until now, environmental pollution has been considered a crisis that threatened human health and the ecosystem. Particularly, organic pollutants from the pharmaceutical industry and hospital effluents can be persistent in the aquatic environment [1]. Tetracycline (TC) is a member of polyketide antibiotics and commonly used in veterinary, animal farm, aquaculture and human medicines to prevent bacterial infections [2]. TC is detected in the

***Corresponding author.**
*E-mail address: zeyneppbalta@gmail.com, 165107001@ogrenci.yalova.edu.tr

aquatic medium because of the wide utilization and inefficient treatment by biological techniques. Tetracycline contamination is a serious problem due to harmful impacts on microorganism structure and wildlife. Additionally, exposure high levels of TC cause an increase in diseases in human life. Therefore, the removal of TC from water environment is significantly matter in recent years. Unfortunately, elimination of the pharmaceutical molecules is generally complicated and high cost by physical, chemical, or other traditional methods. So, various green technologies have been suggested by researchers. In this regard, photocatalytic remediation is sustainable, cost-effective and environmentally friendly technique and thus, attracted extensive attention due to its solar energy utilization [1]. In a typical photocatalytic process, photons are first absorbed with energy higher than the band gap energy of semiconductor material. Then, the photo-excited electrons (e^-) are transported from the valence band (VB) to the conduction band (CB) of the semiconductor, while positively charged holes (h^+) in the VB induce the formation of electron/hole pairs. This pair generates highly reactive superoxide and hydroxyl radicals which react with contaminants to convert them to non-toxic small molecules [3]. Inspired from this perspective, discovering and application of an effective and eco-friendly photocatalyst play a strategic role in the remediation of the persistent molecules from contaminated water. As an example, Luo and co-workers used photocatalysis process to efficiently remove tetracycline by $LaMnO_3$/g-C_3N_4 hybrid catalyst and they achieved 61.4% TC degradation after 120 min visible light irradiation [4]. Recently, Jiang et al. [5] constructed sulphur-doped g-C_3N_4 and evaluated its catalytic activity towards TC antibiotic. They reported that 34.7% TC removal was obtained in 60 min with bulk g-C_3N_4 while it increased to 78% with sulphur-doped g-C_3N_4. Yan et al. [6] reported that Bi_2WO_6/boron nitride heterojunction demonstrated 99.1% photodegradation degree of TC within 120 min. They mentioned that the boron nitride supplied more active sites and boosted the separation rate of electron/hole.

Hexagonal boron nitride (h-BN) is a non-oxide and non-metallic substance including equal boron and nitrogen atoms. In the structure, these atoms are covalently bonded via sp^2 bonds and the two-dimensional layers are linked together via van der Waals forces [7]. h-BN is also named as "white graphene" due to their similar structures. In recent years, h-BN is widely used in several fields such as photocatalysis, adsorption, biomedical applications and hydrogen storage according to its high surface area, high electrical insulation, good temperature resistance, biocompatibility and thermal conductivity [8, 9]. Due to the hydrophobicity and π conjugation in its structure, h-BN could easily connect with the aromatic rings of organic pollutants via π-π and hydrophobic interactions [10]. Therefore, h-BN has gained the attention of researchers in recent years to remove contaminants from water media. Li et al. [8] explored the adsorption ability of h-BN and observed that the color of methylene blue almost disappeared and 98% methylene blue was removed within 5 min. Fu et al. [11] prepared h-BN/TiO_2 samples for the photocatalytic removal of dye molecules and they observed that with the increasing of h-BN amount, degradation efficiencies were remarkably enhanced. Shenoy et al. [12] prepared α-Fe_2O_3/h-BN composites and they reported that the photodegradation efficiencies towards Methylene Blue increased from 51% to 91% after the introduction of h-BN into the structure. The enhancement was ascribed to the electrostatic interaction between boron nitride and photo-generated holes and thus inhibited the recombination rate of charge pairs.

Based on this background, herein, novel whisker-type h-BN was synthesized via polymeric precursor technique to clarify their photocatalytic degradation performance towards tetracycline which is one of the most commonly used antibiotics in the pharmaceutical industry. Characterization techniques such as Scanning electron microscopy (SEM), X-ray powder diffraction (XRD), Fourier transfer infrared (FTIR), Photoluminescence (PL), UV-vis diffuse reflectance spectra (DRS) were used to identify the catalyst structure. The influence of the pH value of the solution on the photocatalytic process was examined. The photocatalytic removal mechanism was explored with radical scavenging experiments. This study provides a novel and applicable usage of a hexagonal phase of boron nitride as a highly active photocatalyst.

MATERIALS AND METHOD

Chemicals

All chemicals were supplied commercially and used as received. Boric acid and melamine were obtained from Isolab. Benzoquinone (BQ), isopropanol (IPA), and Ethylene diamine tetra acetic acid disodium salt (EDTA) were obtained from the company of Sigma-Aldrich.

Fabrication of h-BN

Hexagonal boron nitride (h-BN) particles were fabricated by using H_3BO_3 (boric acid) and polymeric precursor namely melamine ($C_3N_6H_6$) [8]. Firstly, H_3BO_3 and $C_3N_6H_6$ with a molar ratio of 1:1 were magnetically stirred in 400 mL distilled water for 30 min at 90 °C and then the suspension was stirred at ~25 °C for 18 h. After that, a white precipitate was collected and dried at 60 °C for 5–6 h. Then, the product was moved in a tube furnace under an H_2 (5%)/N2 atmosphere and heated at 900 °C for 3 h. Finally, the white powders were obtained.

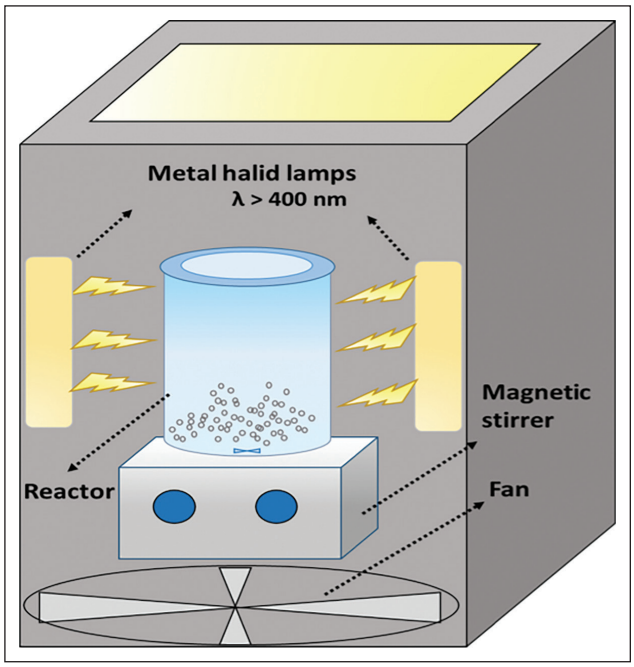

Figure 1. Schematic illustration of photochemical reactor.

Characterization

The morphological structure of boron nitride was examined by using the scanning electron microscopy (SEM) technique with Philips XL30 ESEM-FEG/EDAX equipment. Fourier transfer infrared (FTIR, Perkin Elmer Spectrum One-ATR) spectra were applied to investigate the structural groups of hexagonal boron nitride. The crystallinity phase structure was determined by X-ray powder diffraction (XRD, Panalytical X'Pert PRO). The specific surface area was obtained with Brunauer-Emmett-Teller (BET) technique by using a Quadrasorb SI-MP analyzer at 77 K. Photoluminescence (PL) data was obtained by Perkin Elmer FL6500 spectrophotometer with an excitation wavelength of 325 nm for h-BN. Perkin-Elmer Lambda 750 spectrophotometer was used to perform UV-vis diffuse reflectance spectra (DRS) analysis. The band gap energy of hexagonal boron nitride was calculated by using the Kubelka-Munk equation and Tauc plot technique.

Photocatalytic Degradation Tests

In this study, photocatalytic decomposition of tetracycline antibiotic (TC) was investigated under solar light irradiation in a square-shaped reactor (Fig. 1) equipped with metal halide lamps (Osram 150 W, 100 mW cm^{-2}) with a wavelength of λ: 400–800 nm. A fan was used to keep the temperature of the system constant during the photochemical process. In each experiment, the h-BN catalyst with the dosage of 0.2 g/L was first dispersed in a TC solution ($C_{initial}$: 10 mg/L; pH: 6.7) and the suspension was kept stirred magnetically with 500 rpm at room temperature (25 °C). In pH experiments, the initial solution pH of the TC solution was changed by using 0.1 M HCl and 0.1 M NaOH. To perform scavenger tests, EDTA, IPA and BQ agents were spiked into the initial TC solution. After the lights were opened and 4 mL of aliquots were collected and filtered with a syringe filter (0.20 μm). Finally, the residual antibiotic concentration was analyzed by using UV–vis spectrophotometer at the wavelength of 360 nm. Adsorption tests were also performed in dark to clarify the adsorption role in the removal mechanism.

RESULTS AND DISCUSSION

Characterization

The morphological feature of h-BN was examined by using the SEM technique. As shown in Figure 2, hexagonal boron nitride presented a short fibre and whiskers-like shape which was located randomly. Also, some defects were observed as graben on the h-BN surface which can act as interaction sites for the target pollutants. The obtained SEM images are in good agreement with previous reports in which h-BN whiskers were observed as nonuniform morphology [8, 13].

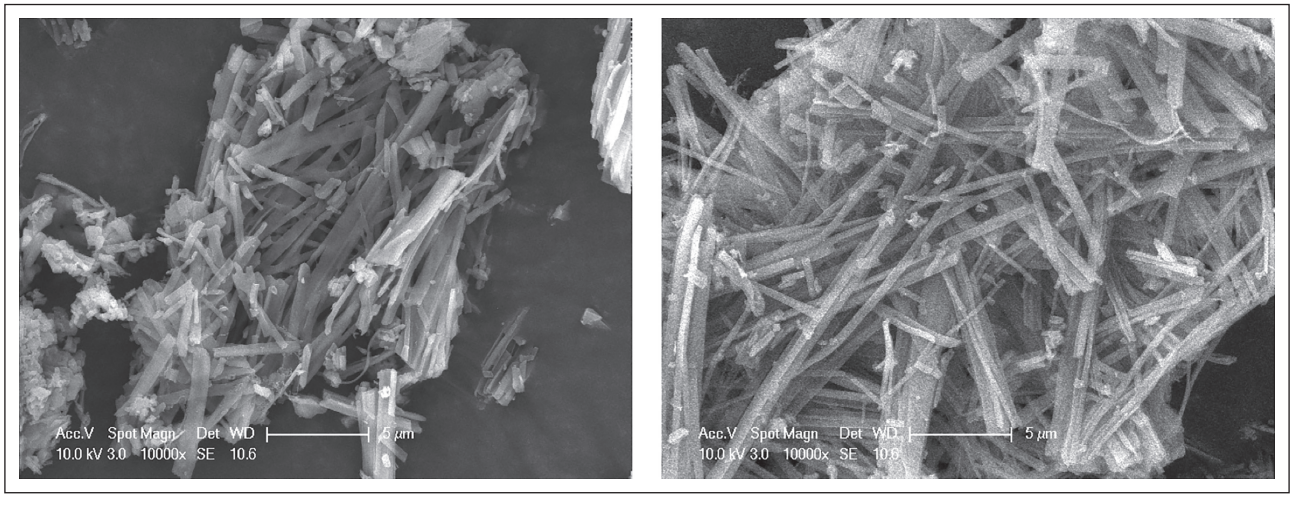

Figure 2. SEM images of h-BN.

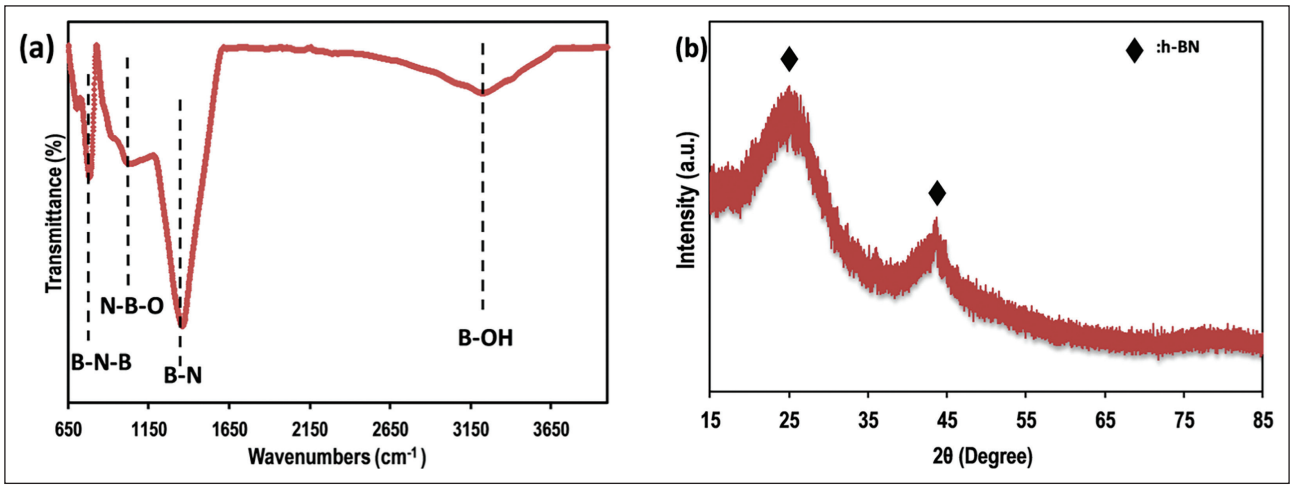

Figure 3. FTIR spectrum **(a)** and XRD pattern **(b)** of h-BN.

To identify surface functional groups in the structure, FTIR analysis was performed. In Figure 3a two peaks examined at 783 cm^{-1} and 1363 cm^{-1} were associated with δ(B–N–B) and ν(B–N) stretching vibrations, respectively [14]. The peak observed at 3400 cm^{-1} was assigned to the hydroxyl groups and adsorbed water [15]. Moreover, the peak located at 3261 cm^{-1} corresponded to the hydroxyl groups on the surface of h-BN with the bonds of B–OH [16]. Meanwhile, the boron oxynitride (N–B–O) bond was detected at around 900–1100 cm^{-1} [17]. The characteristic IR absorption peaks of the hexagonal phase of boron nitride indicated successful preparation of the h-BN with the polymeric precursor technique [8]. Moreover, no other peaks were found revealing that the precursors transformed to the h-BN sample. The obtained characteristic FTIR peaks were in agreement with previous studies in the literature [18, 19]. İkram et al. [16] observed boron oxynitride bond in h-BN structure. Moreover, Shenoy et al. [12] proved pure h-BN structure with an observation of B–N–B and B–N bonds in the h-BN structure via FTIR analysis. Similarly, Li and co-workers observed absorption peaks of the δ(B–N–B) and ν(B–N) bonds in the h-BN whisker [8]. The hydroxyl groups on the h-BN surface were also detected by Liu et al. [9] at around of 3200 cm^{-1}. According to all these results, the successful preparation of the hexagonal phase of boron nitride was proved by the FTIR analysis.

The phase composition and crystallographic structure of hexagonal boron nitride were examined by XRD analysis, and the result was represented in Figure 3b. The characteristic peaks of h-BN were fitted to the hexagonal phase of BN using the Joint Committee on Powder Diffraction Standards (JCPDS 73-2095) [8]. Also, the graphitic phase of boron nitride was demonstrated by the detection of 41.6° peak which corresponds to the (100) plane (JCPDS card No. 34-0421) [20]. Other peaks were not observed in the XRD spectrum, which confirmed that high purity of crystal h-BN was achieved via the polymeric precursor method.

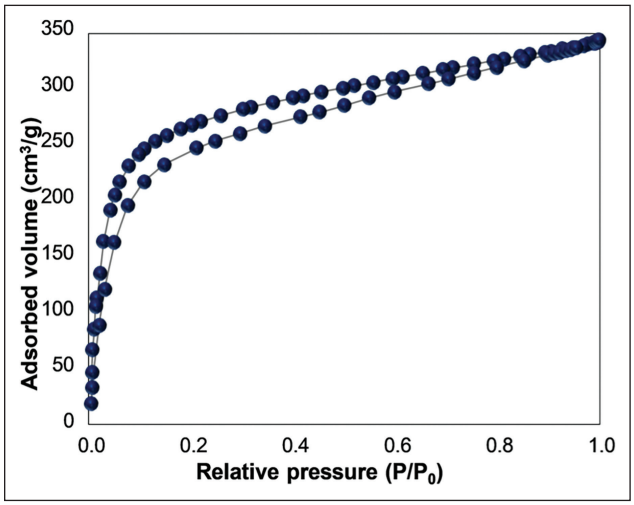

Figure 4. Nitrogen adsorption-desorption isotherm of h-BN.

The Brunauer–Emmett–Teller (BET) surface area of the material was calculated as 1050.1 m^2/g, which was found much greater than commercial boron nitride powder (25 m^2/g) [8]. The high surface area supplies many regions to contact with pollutants, leading to enhanced photocatalytic degradation performance. Similarly, Li et. al. also prepared whisker-shaped boron nitride and calculated the surface area as 964.4 m^2/g [8]. Similarly, Luo et al. [13] fabricated the hexagonal phase of boron nitride by polymeric precursor technique and they found the surface area as 964.3 m^2/g. Figure 4 shows the nitrogen adsorption-desorption isotherms of hexagonal boron nitride. According to result, the isotherms are closely be classified as the combination of characteristic type I, type II and H4 loops based on the International Union of Pure and Applied Chemistry (IUPAC) classification. This indicates that microporous and macroporous coexist in as-obtained h-BN. Additionally; H4 hysteresis indicated that the narrow slit pores [21].

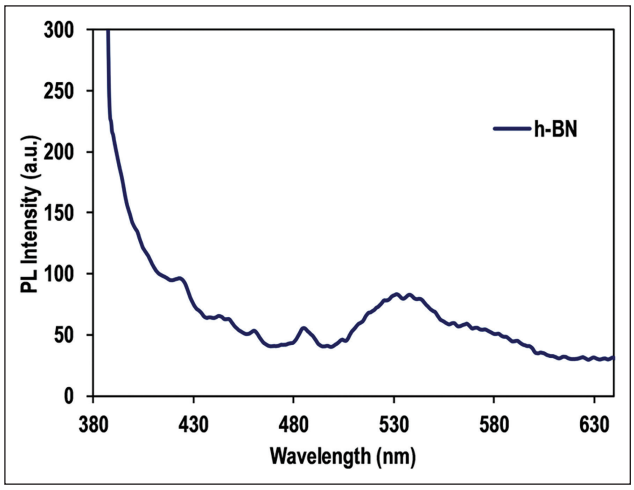

Figure 5. PL spectrum of h-BN.

The optical properties of h-BN were explored by PL and UV-vis DRS techniques and the results were shown in Figures 5, 6. PL spectra were obtained to explore the recombination issue and migration feature of the catalyst (Fig. 5) and it was shown that h-BN presented an excitation wavelength of 530 nm. It is known the PL intensity indicates the electron/hole recombination rate in which the peak intensity of h-BN was found relatively lower revealing enhanced separation of charge carriers and hindered recombination rate. Besides, the band gap feature of h-BN was investigated by DRS analysis. UV-Vis absorption spectrum and Kubelka-Munk function plot ($(aE)^2$) vs. photon energy (hv) were shown in Figure 6. The absorption edge of h-BN was determined as approximately 310 nm and the band gap energy of h-BN was determined as 4.5 eV which were in accordance with the literature [22]. Similarly, Gu et al. [1] reported the band gap energy of BN as 4.41 eV while He et al. [23] reported it as 3.98 eV.

Photocatalytic Activity Measurements

Tetracycline hydrochloride (TC) is the commonly used antibiotics to inhibit gram-positive and gram-negative bacteria [24, 25]. The occurrence of TC in the environment through contaminative wastewater is a serious threat to human health and the ecological system. Therefore, removal of TC from wastewater is a global concern and requires to be arranged immediately. In the present work, the photocatalytic efficiency of h-BN sample was tested for the elimination of tetracycline antibiotic. Both adsorption and photocatalytic tests were conducted. As shown in Figure 7a, the adsorptive removal of tetracycline was calculated as 20% within 180 min. In the tetracycline structure, NH_2 and OH groups are some of the functional states while boron nitride structure consists of abundant hydroxyl groups. The adsorption of tetracycline on the boron nitride surface could be via interactions between antibiotic molecules and hydroxyl groups of h-BN [26]. Under visible light illumination, 85.7% and 91.9% photocatalytic removal of TC were observed within 60 min and 180 min, respectively (Fig. 7b). Since the similar efficiencies of 60 min and 180 min, parameter experiments were performed for 60 min. Considering the insignificant adsorption performance of h-BN, the TC removal could be accomplished by the photocatalytic degradation reaction. Despite the wide band gap energy of boron nitride, the high degradation performance could be related to its positively charged hole capturing effect owing to negatively charged groups on the surface of h-BN. The great photocatalytic activity of h-BN towards TC elimination indicated that it could be a good alternative to remove organic contaminants from wastewater. On the other hand, h-BN by itself could be also used to boost catalytic activities of other semiconductors in the field of photocatalysis. For instance, Fu et al. [27] prepared h-BN/ZnO composite for the photocatalytic degradation of Rhodamine B and Methylene Blue dyes and reported that the introduction of boron nitride

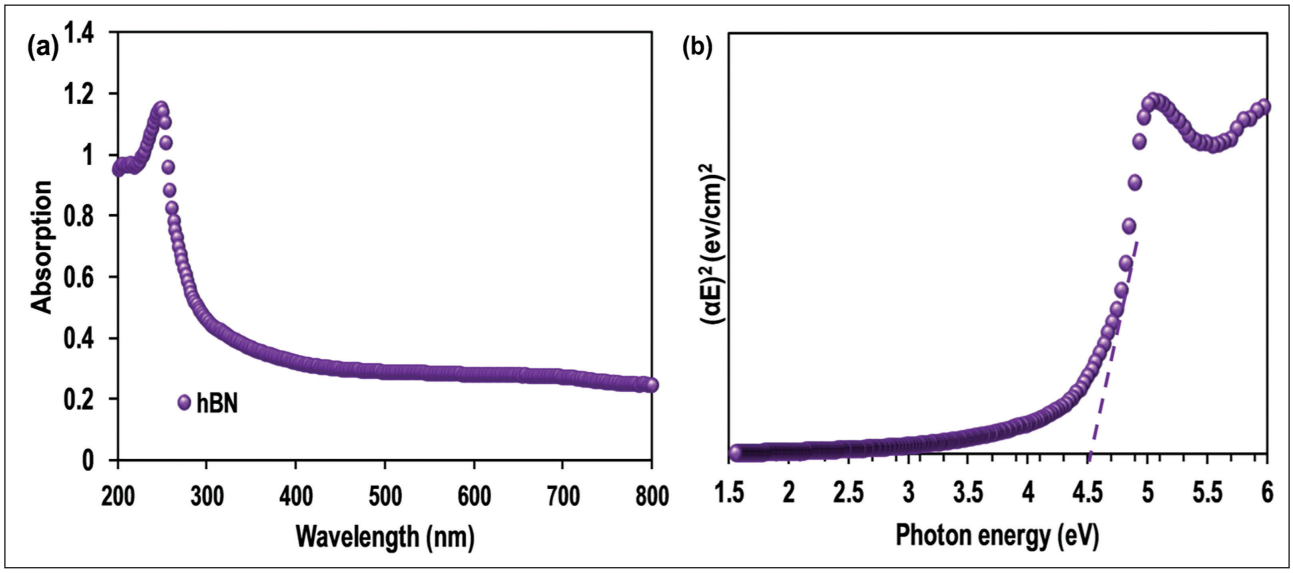

Figure 6. UV-Vis diffuse reflectance spectra **(a)** and Kubelka-Munk spectrum **(b)** of h-BN.

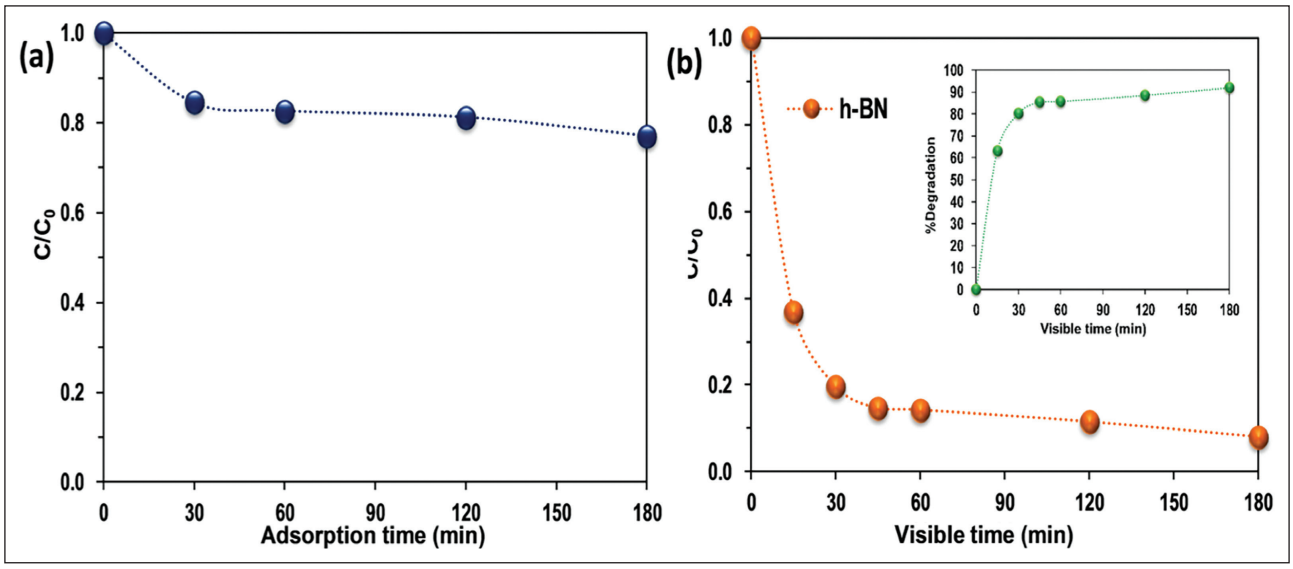

Figure 7. Adsorption **(a)** and photocatalytic **(b)** performance of h-BN.

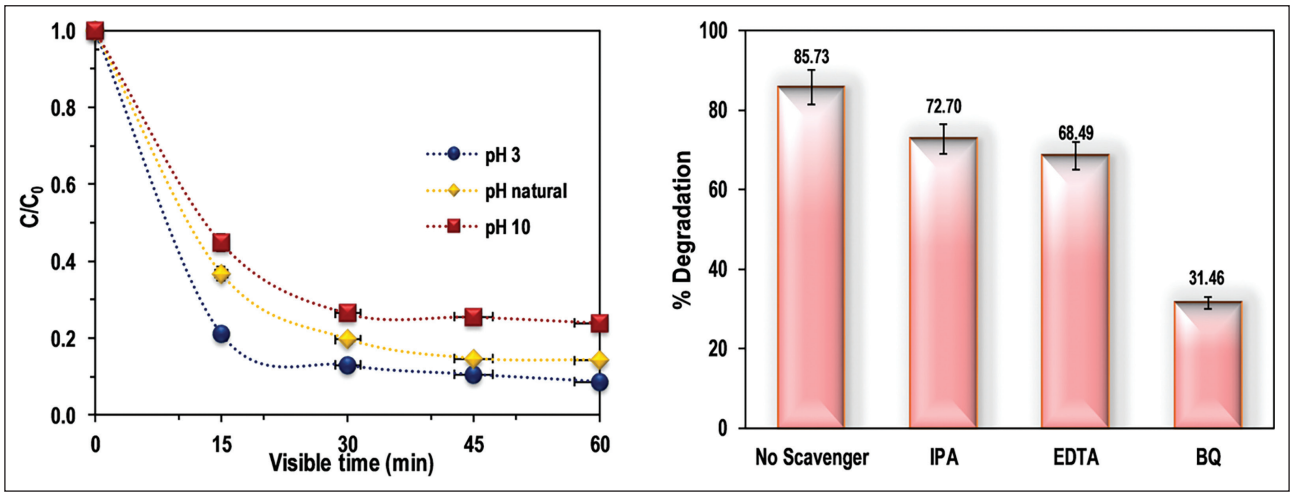

Figure 8. The effect of solution pH on TC removal **(a)** and radical trapping experiments **(b)**.

greatly increased the catalytic performance of raw ZnO. They attributed the enhancement to the hole transfer of h-BN and extra regions for the adsorption of pollutants via electrostatic forces. Lv et al. [28] mentioned that the photocatalytic activity of Ag_3VO_4 was considerably promoted after addition of the h-BN and the rate constant of the composite was detected six times higher than pure Ag_3VO_4. According to a study in 2017, the photocatalytic efficiency of $Bi_4O_5Br_2$ was increased from 55% to 97% with the loading of h-BN (1 wt %), which was assigned to the enhanced conductivity of heterojunction for electron-hole separation [29].

Influence of Solution pH on TC degradation

Initial solution pH is a significant parameter in photocatalytic processes, so the TC degradation over h-BN whiskers was investigated at three pH conditions (3, natural 6.7, 10). As shown in Figure 8a, 85.7% of the degradation rate was achieved at the initial pH 6.7 while the removal efficiencies increased to 91.3% (pH 3) and decreased to 76.0% (pH 10). It was observed that the degradation was inhibited in an alkaline medium while it favored acidic conditions. The TC molecule has three different pK_a values namely 3.30, 7.68 and 9.69 and it is significantly influenced by the initial solution pH value [30]. At pH values lower than 3.3, the cationic form TCH^{3+}, TCH_2° forms at pH values of between 3.4–9.7, and anionic TCH^- and TC^{2-} species were dominant at pH values higher than 9.7 [31, 32]. As reported in previous studies, the isoelectric point of h-BN is 2.7 [33]. So, the enhancement of TC degradation in acidic conditions could be ascribed to the electrostatic attraction between the negatively charged h-BN surface and protonated form of TC. By the way in alkaline conditions, the TC molecule exists in anionic form and electrostatic repulsion occurred between negatively charged h-BN surface and TC molecule resulting in low

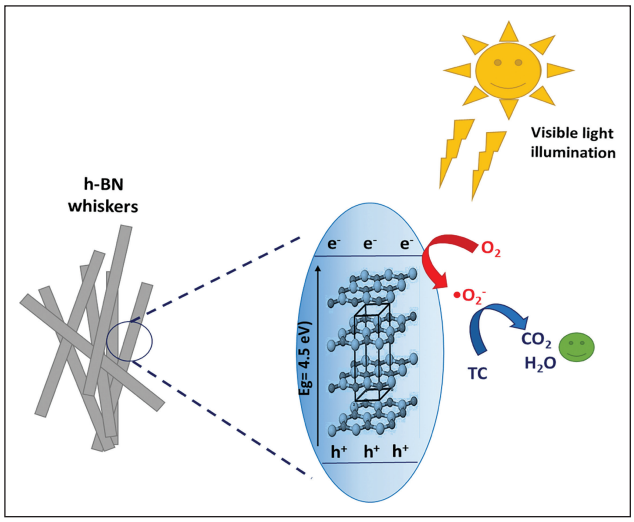

Figure 9. The possible photocatalytic degradation mechanism of TC on h-BN.

degradation efficiency. As a result, due to the surface charge of h-BN and TC chemical states, the initial solution pH was defined as a significant parameter and acidic media was determined as optimum condition to remove TC on h-BN.

Investigation of Active Radical Species

During photocatalytic reaction, various active substances were produced such as hydroxyl radicals (•OH), photoinduced holes (h^+) and superoxide anions ($\bullet O_2^-$). In order to understand the main active species in the TC degradation over h-BN whiskers, different reagents namely IPA, EDTA and BQ were added to the solution which acted as scavengers of •OH, h^+ and $\bullet O_2^-$, respectively. As depicted in Figure 8b, IPA and EDTA restricted removal rate from 85.7% to 72.7% and 68.4%, respectively. The degradation was significantly inhibited with the addition of BQ, and the removal efficiency was decreased to 31.4%, referring that superoxide anions were the key radicals in the TC degradation system. These results indicate that the possible mechanism of TC degradation onto h-BN dominantly triggered by superoxide anions and this process was schematized in Figure 9. When the catalyst is exposed to the light which has a higher wavelength than the band gap (E_g) of catalyst, the photoexcited electrons are occurred and transfer to the conduction band of the catalyst. Due to the transfer of the electrons, positively charged holes occur at the valence band (Eq. 1). Photo-induced electrons and holes take part in the reduction and oxidation reactions, respectively. In general, electron-hole pairs tend to recombine. But in this process, positively charged holes are captured by negatively charged hydroxyl groups on the surface of h-BN which was detected by FTIR analysis. Owing to the occupation of holes, recombination of pairs is inhibited, and electrons could be free and generate reactive radicals. Photo–induced electron in the conduction band of h-BN reduce the adsorbed oxygen molecules to generate superoxide radicals (Eq. 2). After that, the as-produced $\bullet O_2^-$ can oxidize the adsorbed TC molecules into CO_2 and H_2O (Eq. 3) [34].

$$\text{h-BN}+h\nu \rightarrow e^- + h^+ \quad \text{(Eq. 1)}$$

$$(O_2)_{ads} + e^- \rightarrow \bullet O_2^- \quad \text{(Eq. 2)}$$

$$\text{Pollutant molecules} + \bullet O_2^- \rightarrow CO_2 + H_2O \quad \text{(Eq. 3)}$$

CONCLUSIONS

Herein, the hexagonal phase of boron nitride was synthesized to investigate the photocatalytic ability for the degradation of TC antibiotics. The randomly located whisker shape of h-BN was observed by SEM technique. 20% adsorptive removal of TC was obtained via interactions between hydroxyl groups of boron nitride and functional groups of antibiotic molecule. Photocatalytic degradation efficiency reached 91% with visible light irradiation within 180 min (catalyst dosage: 0.2 g/L; initial pollutant concentration: 10 mg/L). The considerably high photocatalytic efficiency of h-BN was assigned to the excellent surface area and low recombination rate of h-BN. According to pH studies, it was observed that the optimum performance was obtained in acidic conditions. Tetracycline degradation was inhibited at higher pH while it favored lower pH values owing to the electrostatic repulsion and attraction circumstances, respectively. In the radical trapping experiments, superoxide radicals were detected as the vital active species for tetracycline degradation on the h-BN catalyst. According to the possible mechanisms, the photo-induced electrons generated $\bullet O_2^-$ anions which subsequently converted TC molecules to non-toxic products. This study provides a guide for the production of h-BN with outstanding photocatalytic performance to urgently solve water pollution globally.

ACKNOWLEDGMENT

The Scientific and Technological Research Council of Türkiye (TÜBİTAK, project no. 120Y369) financially supported the presented study. The authors are also thankful to the Research fund of the Yalova University, Türkiye for financial support under project no. 2020/DR/0001.

DATA AVAILABILITY STATEMENT

The authors confirm that the data that supports the findings of this study are available within the article. Raw data that support the finding of this study are available from the corresponding author, upon reasonable request.

CONFLICT OF INTEREST

The authors declared no potential conflicts of interest with respect to the research, authorship, and/or publication of this article.

ETHICS

There are no ethical issues with the publication of this manuscript.

REFERENCES

[1] J. Gu, J. Yan, Z. Chen, H. Ji, Y. Song, Y. Fan, H. Xu, and H. Li, "Construction and preparation of novel 2D metal-free few-layer BN modified graphene-like g-C_3N_4 with enhanced photocatalytic performance," Dalton Transactions, Vol. 46, pp. 11250–11258, 2017. [CrossRef]

[2] H. Cai, X. Li, D. Ma, Q. Feng, D. Wang, Z. Liu, X. Wei, K. Chen, H. Lin, S. Qin, and F. Lu, "Fe_3O_4 submicrospheres with SiO_2 coating for heterogeneous Fenton-like reaction at alkaline condition," Science of the Total Environment, Vol. 764, Article 144200. [CrossRef]

[3] G. Jácome-Acatitla, M. Álvarez-Lemus, R. López-González, C. García-Mendoza, A. Sánchez-López, and D. Hernández-Acosta, "Photodegradation of 4-chloropehol in aqueous media using $LaBO_3$ (B = Fe, Mn, Co) perovskites: Study of the influence of the transition metal ion in the photocatalytic activity," Journal of Photochemistry and Photobiology A: Chemistry, Vol. 390, Article 112330. [CrossRef]

[4] J. Luo, J. Chen, R. Guo, Y. Qiu, W. Li, X. Zhou, X. Ning, and L. Zhan, "Rational construction of direct Z-scheme $LaMnO_3$/g-C_3N_4 hybrid for improved visible-light photocatalytic tetracycline degradation," Separation and Purification Technology, Vol. 211, pp. 882–894, 2019. [CrossRef]

[5] X. Jiang, K. Qiao, Y. Feng, L. Sun, N. Jiang, and J. Wang, "Self-assembled synthesis of porous sulfur-doped g-C_3N_4 nanotubes with efficient photocatalytic degradation activity for tetracycline," Journal of Photochemistry and Photobiology A: Chemistry, Vol. 433, Article 114194, 2022. [CrossRef]

[6] T. Yan, Z. Du, J. Wang, H. Cai, D. Bi, Z. Guo, Z. Liu, C. Tang, and Y. Fang, "Construction of 2D/2D Bi_2WO_6/BN heterojunction for effective improvement on photocatalytic degradation of tetracycline," Journal of Alloys and Compounds, Vol. 894, Article 162487, 2022. [CrossRef]

[7] Ö. Şen, M. Emanet, and M. Çulha, "One-step synthesis of hexagonal boron nitrides, their crystallinity and biodegradation," Frontiers in Bioengineering and Biotechnology, Vol. 6, Article 83, 2018. [CrossRef]

[8] Q. Li, T. Yang, Q. Yang, F. Wang, K.C. Chou, and X. Hou, "Porous hexagonal boron nitride whiskers fabricated at low temperature for effective removal of organic pollutants from water," Ceramics International, Vol. 42, pp. 8754–8762, 2016. [CrossRef]

[9] Z. Liu, K. Zhao, J. Luo, and Y. Tang, "Highly efficient synthesis of hexagonal boron nitride short fibers with adsorption selectivity," Ceramics International, Vol. 45, 22394–22401, 2019. [CrossRef]

[10] S. Yu, X. Wang, H. Pang, R. Zhang, W. Song, D. Fu, T. Hayat, and X. Wang, "Boron nitride-based materials for the removal of pollutants from aqueous solutions: A review," Chemical Engineering Journal, Vol. 333, pp. 343–360, 2018. [CrossRef]

[11] X. Fu, Y. Hu, Y. Yang, W. Liu, and S. Chen, "Ball milled h-BN: An efficient holes transfer promoter to enhance the photocatalytic performance of TiO_2," Journal of Hazardous Materials, Vol. 244–245, pp.102–110, 2013. [CrossRef]

[12] M.R. Shenoy, S. Ayyasamy, V. Bhojan, R. Swaminathan, N. Raju, P. Senthil Kumar, M. Sasikumar, G. Kadarkarai, S. Tamilarasan, S. Thangavelu, and S. J, M. V. Reddy, "Visible light sensitive hexagonal boron nitride (hBN) decorated Fe_2O_3 photocatalyst for the degradation of methylene blue," Journal of Materials Science: Materials in Electronics, Vol. 32, pp. 4766–4783, 2021. [CrossRef]

[13] W. Luo, T. Yang, L. Su, K.C. Chou, and X. Hou, "Preparation of hexagonal BN whiskers synthesized at low temperature and their application in fabricating an electrochemical nitrite sensor," RSC Advances, Vol. 6, pp. 27767–27774, 2016. [CrossRef]

[14] C. Zhu, J. Zheng, L. Fang, P. Hu, Y. Liu, X. Cao, and M. Wu, "Advanced visible-light driven photocatalyst with enhanced charge separation fabricated by facile deposition of Ag_3PO_4 nanoparticles on graphene-like h-BN nanosheets," Journal of Molecular Catalysis A: Chemical, Vol. 424, pp. 135–144, 2016. [CrossRef]

[15] T. Chen, Q. Zhang, Z. Xie, C. Tan, P. Chen, Y. Zeng, F. Wang, H. Liu, Y. Liu, G. Liu, and W. Lv, "Carbon nitride modified hexagonal boron nitride interface as highly efficient blue LED light-driven photocatalyst," Applied Catalysis B: Environmental, Vol. 238, pp. 410–421, 2018. [CrossRef]

[16] M. Ikram, J. Hassan, M. Imran, J. Haider, A. Ul-Hamid, I. Shahzadi, M. Ikram, A. Raza, U. Qumar, and S. Ali, "2D chemically exfoliated hexagonal boron nitride (hBN) nanosheets doped with Ni: synthesis, properties and catalytic application for the treatment of industrial wastewater," Applied Nanoscience, Vol. 10, pp. 3525–3528, 2020. [CrossRef]

[17] V. Kumar, K. Nikhil, P. Roy, D. Lahiri, and I. Lahiri, "Emergence of fluorescence in boron nitride nanoflakes and its application in bioimaging," RSC Advances, Vol. 6, pp. 48025–48032, 2016. [CrossRef]

[18] K. Ren, W. Zhao, Z. Zhai, T. Han, and H. Shi, "2D/0D Bi2MoO6 nanosheets/BN quantum dots photocatalysts with enhanced charge separation for efficient elimination of antibiotic," Applied Surface Science, Vol. 562, Article 150144, 2021. [CrossRef]

[19] J. Yan, J. Gu, X. Wang, Y. Fan, Y. Zhao, J. Lian, Y. Xu, Y. Song, H. Xu, and H. Li, "Design of 3D WO3/h-BN nanocomposites for efficient visible-light-driven photocatalysis," RSC Advances, Vol. 7, pp. 25160–25170, 2017. [CrossRef]

[20] M. Wang, M. Li, L. Xu, L. Wang, Z. Ju, G. Li, and Y. Qian, "High yield synthesis of novel boron nitride submicro-boxes and their photocatalytic application under visible light irradiation," Catalysis Science & Technology, Vol. 1, pp. 1159–1165, 2011. [CrossRef]

[21] Z.A. Alothman, "A review: Fundamental aspects of silicate mesoporous materials," Materials (Basel), Vol. 5, pp. 2874–2902, 2012. [CrossRef]

[22] J. Zupan, and D. Kolar, "Optical properties of graphite and boron nitride," Journal of Physics C: Solid State Physics, Vol. 5, pp. 3097–3100, 1972. [CrossRef]

[23] Z. He, C. Kim, L. Lin, T.H. Jeon, S. Lin, X. Wang, and W. Choi, "Formation of heterostructures via direct growth CN on h-BN porous nanosheets for metal-free photocatalysis," Nano Energy, Vol. 42, pp. 58–68, 2017. [CrossRef]

[24] F. Sa'adah, H. Sutanto, and D. Hadiyanto, "Optimization of the Bi_2O_3/Cu synthesis process using response surface methodology as a tetracycline photodegradation agent," Results in Engineering, Vol. 16, Article 100521. [CrossRef]

[25] R. Zhang, Y. Li, W. Zhang, Y. Sheng, M. Wang, J. Liu, Y. Liu, C. Zhao, and K. Zeng, "Fabrication of Cu_2O/Bi_2S heterojunction photocatalysts with enhanced visible light photocatalytic mechanism and degradation pathways of tetracycline," Journal of Molecular Structure, Vol. 1229, Article 129581, 2021. [CrossRef]

[26] Y. Guo, C. Yan, P. Wang, L. Rao, and C. Wang, "Doping of carbon into boron nitride to get the increased adsorption ability for tetracycline from water by changing the pH of solution," Chemical Engineering Journal, Vol. 387, Article 124136, 2020. [CrossRef]

[27] X. Fu, Y. Hu, T. Zhang, and S. Chen, "The role of ball milled h-BN in the enhanced photocatalytic activity: A study based on the model of ZnO," Applied Surface Science, Vol. 280, pp. 828–835, 2013. [CrossRef]

[28] X. Lv, J. Wang, Z. Yan, D. Jiang, and J. Liu, "Design of 3D h-BN architecture as Ag_3VO_4 enhanced photocatalysis stabilizer and promoter," Journal of Molecular Catalysis A: Chemical, Vol. 418–419, pp. 146–153, 2016. [CrossRef]

[29] S. Ding, D. Mao, S. Yang, F. Wang, L. Meng, M. Han, H. He, C. Sun, and B. Xu, "Graphene-analogue h-BN coupled Bi-rich $Bi_4O_5Br_2$ layered microspheres for enhanced visible-light photocatalytic activity and mechanism insight," Applied Catalysis B: Environmental, Vol. 210, pp. 386–399, 2017. [CrossRef]

[30] V.H. Tran Thi, and B.K. Lee, "Great improvement on tetracycline removal using ZnO rod-activated carbon fiber composite prepared with a facile microwave method," Journal of Hazardous Materials, Vol. 324, pp. 329–339, 2017.

[31] R. Ocampo-Pérez, R. Leyva-Ramos, J. Rivera-Utrilla, J. V. Flores-Cano, and M. Sánchez-Polo, "Modeling adsorption rate of tetracyclines on activated carbons from aqueous phase," Chemical Engineering Research and Design, Vol. 104, pp. 579–588, 2015. [CrossRef]

[32] K. Liu, Z. Tong, Y. Muhammad, G. Huang, H. Zhang, Z. Wang, Y. Zhu, and R. Tang, "Synthesis of sodium dodecyl sulfate modified BiOBr/magnetic bentonite photocatalyst with Three-dimensional parterre like structure for the enhanced photodegradation of tetracycline and ciprofloxacin," Chemical Engineering Journal, Vol. 388, Article 124374, 2020. [CrossRef]

[33] C. Xiong, and W. Tu, "Synthesis of water-dispersible boron nitride nanoparticles," European Journal of Inorganic Chemistry, Vol. 2014(19), pp. 3010–3015, 2014. [CrossRef]

[34] J. Kong, T. Yang, Z. Rui, and H. Ji, "Perovskite-based photocatalysts for organic contaminants removal : Current status and future perspectives," Catalysis Today, Vol. 327, pp. 47–63, 2019. [CrossRef]

Environ Res Tec, Vol. 5, Issue. 4, pp. 305–314, December 2022

Environmental Research and Technology
https://ert.yildiz.edu.tr - https://dergipark.org.tr/tr/pub/ert
DOI: https://doi.org/10.35208/ert.1097795

Environmental Research & Technology

Review Article

Appraising the current state of irrigation schemes in northern Nigeria using sustainability pillars

Nura Jafar SHANONO*, Nuraddeen Mukhtar NASİDİ, Nura Yahaya USMAN

Department of Agricultural and Environmental Engineering, Bayero University Kano, Nigeria

ARTICLE INFO

Article history
Received: 03 April 2022
Revised: 16 September 2022
Accepted: 11 October 2022

Key words:
Irrigation performance; Irrigation scheme; Northern Nigeria; Sustainability pillars

ABSTRACT

Irrigation has been identified as a key to achieving food demand in the face of rapid increase in population and climate change impact. In northern Nigeria for example, irrigation practice has been adopted as an alternative to achieving in food production to meet the demand of the population. Nevertheless, the existing irrigation schemes encountered several challenges coming from the 5 basic sustainability pillars including social, environmental, economic, institutional and technological. This paper attempts to appraise the current state of irrigation schemes through revealing the underlined challenges confronting these schemes that cut across sustainability pillars. The findings discovered that irrigation schemes contributed immensely toward achieving food security and socio-economic development. However, the huge investment in irrigation sector have resulted in massive economic fatalities. This could be attributed to poor management, under-utilization, and abandonment even though few are performing remarkably well. Thus, there is a need to adopt new water sharing methods that can improve water-use efficiency, users-managers joint approach, building competent institutions with an improved monitoring, evaluation and surveillance systems. Others include frequent policy review, development of water conservation-base law enforcement agency as well as well-timed sensitization and awareness campaigns.

Cite this article as: Shanono NJ, Nasidi NM, Usman NY. Appraising the current state of irrigation schemes in northern Nigeria using sustainability pillars. Environ Res Tec 2022;5:4:305–314.

INTRODUCTION

The irrigation sector has undoubtedly contributed immensly toward economic development, poverty alleviation and food security in many countries including Nigeria [1]. The problem of food insecurity represents the biggest crisis of the 21st century worldwide. This is exacerbated due to additional changes posed by the ongoing challenges posed by the Corona Virus (COVID-19). The main point that require attention is that the harmfull effect of food insecurity is spreading from the developing to the developed countries of the world. According to the FAO report of 2018, about 821 million people do not have enough food, 2 billion people suffer from malnutrition and the numbers are rising at a high rate in both Africa and Asia [2]. Nigeria is not exceptional as its population is increasing at an alarming rate and this has glaringly highlighted the need for more food pro-

***Corresponding author.**
*E-mail address: njshanono.age@buk.edu.ng

duction to meet up and sustain the population demand. For example, the level of food insecurity in the rural areas of Nigeria is reportedly disturbing as it affected about 84% and 56% of the communities in northern and southern parts of the country respectively [3].

Nigeria relies mostly on the importation of agricultural products as about 31 and 23% of the total food demands were imported in 2011 and 2012 respectively [4]. For example, about 8 million metric tons of rice and 5.6 million tons of wheat were imported in 2019 to feed its growing population despite its production potential in agriculture [5]. Nigeria imported more than 10 million metric tons of rice between 2010 and 2014 [6]. It has been suggested that the only way out of food insecurity and poverty is to remarkably attain a sustainable crop production in the country [7]. To improve agricultural productivity in the country, irrigation farming along with the use of improved seeds, fertilizers, mechanized and smart farming as well as other relevant and modern farming technologies is the best alternative option. This will help in reducing the level of hunger, poverty and malnutrition [8]. Therefore, irrigation can be regarded as a powerful factor in increasing crop productivity, more stable incomes and providing employment and increasing prospects for multiple cropping and crop diversification [9]. In the specific context of agriculture, sustainable irrigation strategies need to allow for increased and sustainable crop production to meet the ever-increasing food demands, while preserving natural resources [10, 11]. Moreover, irrigation farming allows farmers to produce all year round thereby resulting in higher agricultural outputs and improved farmer's income. According to [12], the objective of irrigation practice is to achieve the economical use of available water and ensure equity for distribution over time and space. In addition, the success of any irrigation project depends on the proper functionality of water conveyance and distribution systems. Unfortunately, many irrigation schemes in northern Nigeria are performing far below their potentials due to poor management by both relevant governmental agencies and farmers [13]. Northern Nigeria was choosen as the case study because a larger proportion of irrigation is practiced in the northern part of the country. In addition, the northern part of Nigeria is characterized by low and erratic rainfall as well as a short rainy season. Mortherover, southern Nigeria depends largely on the northern for food production due to arable land in the northen part of Nigeria.

It was observed that improvement of the performance of the existing irrigation schemes is one of the possible approaches to water conservation, particularly in dryland areas like northern Nigeria [14]. The term sustainability in irrigation is often characterized through indicators that express the performance of an irrigation scheme not only in terms of its ability to deliver the required irrigation water but also on economic viability, social well-being, environmental health,

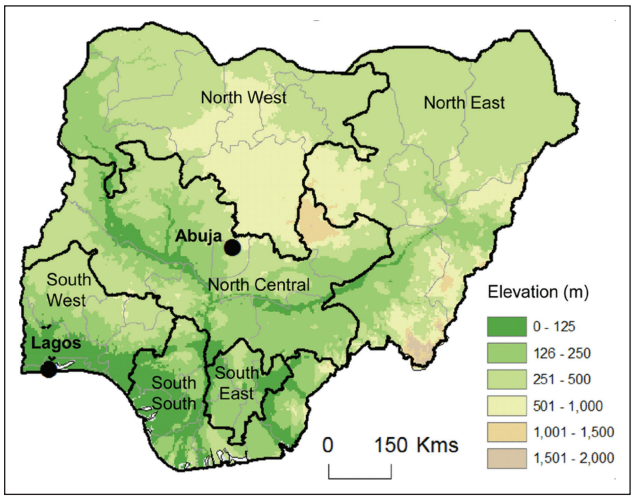

Figure 1. Map of Nigeria showing 3 northern and southern regions.

institution arrangement and technological advances. Thus, sustainable irrigated agriculture is said to be attained if irrigation practices do not lead to the depletion of either natural or human resources [11]. To meet the Nigerian population demands of food and fibre, there is a need to employ the concept of sustainability to further improve irrigated agriculture, thereby achieving sustainable food production, processing and value addition [15]. This can be achieved if all the causes and effects of many problems that have been lingering are diagnosed, propose solutions and the suggested solutions are implemented and put into practice. This review was therefore aimed to disclose the current status of the available irrigation schemes in northern Nigeria for their sustainability and functionality. The study will provide inside into what has been going on with regard to maintenance, utilization and level of crop productions in the irrigation schemes from sustainability point of view.

THE CURRENT STATE OF IRRIGATION SCHEMES IN NORTHERN NIGERIA

This section presents the review on the state of irrigation schemes in northern Nigeria and sustainability pillars were used to guide this review. The aim was to get more insight into the global irrigation scheme operations and maintenance practices with the main focus on northern Nigeria. This review yielded a schematic overview of irrigation scheme management using sustainability pillars. This is to evaluate the present state of functionality and the level of impact on the lives of people. Figure 1 shows the map of Nigeria showing the northern part, which constituted three regions (North West, North East and North Central), and southern part, which constituted three regions (South West, South East and South South). The irrigation scheme management sustainability-based review was conducted

and restricted to the northern part of the country. The history of irrigation practices in the northern Nigeria begun since when it was realized that the region is characterized with low rainfall and high rate of evaporation which make it either arid or semi-arid regions in addition to abandon arable lands. These made the previous governments of the regions to construct several water storage infrastructures (dams and canals) for irrigation practices. These resulted to several major irrigation schemes available in northern Nigeria most of which are intended to stimulate and facilitate the sustainable food production in the country.

Economic Aspect of Sustainable Irrigation Schemes

The economic productivity of several human endeavours depends largely on access to water resources [16]. Although about 24% of the global land area suffering from severe water scarcity [17] and 35% of the global population living in areas affected by water shortages [18], the economic development often occurs at the cost of overexploitation of water resources [19]. Agriculture is a major performer in the human appropriation of the limited water resources as about 70% of the global freshwater is consumed by this sector. After abandonment for about four decades due to abundant petroleum resources, the agricultural sector in Nigeria is gradually occupying a dominant position in the development of the national and rural economy. The sector provides not only food but also serves as the major source of employment to the teeming population of Nigeria. The agricultural sector provides jobs to about three-quarters of the Nigerian working population [20]. Farmers are usually less busy on the farm during the dry season, putting into account the rainy (May to October) and the dry (November to April) seasons of Nigeria. Hence, the provision of irrigation facilities that offer the opportunity for all-year-round farming can serve as an alternative source of employment and an additional gain to the Nigerian economy [21].

Recently, drastic agricultural reforms (closure of land borders and banning of importation of major agricultural food products among others) have been made in Nigeria resulting in a sharp increase in crop production which significantly reduce food importation and jobs were created [22, 23]. Agriculture is one of the main economic sectors in Nigeria employing about 60% of the population of the country [23]. This scenario is in line with other developing countries that agriculture provides the leading source of employment. Thus, increasing agricultural productivity is critical to economic growth, development, and the nation's Gross Domestic Products (GDP). One important way to increase agricultural productivity is through the introduction of improved agricultural technologies and management systems.

In Nigeria, post-project evaluations of the majority of the irrigation schemes revealed that their economic performances are low compared to pre-project predictions [15]. Such undesirable outcomes are a result of the fact that social and environmental concerns of these schemes were not incorporated in the analysis. The participation issue presents the usefulness of water users' involvement in the maintenance and sustainability of the irrigation schemes which further improve economic benefit [24]. One of the possible causes of the decline in food production is an inefficient allocation of resources in the agricultural production potentials [25]. For example, land, labour, capital and water resources are inefficiently allocated thereby leading to a decrease in their productivity. To further improve the economic status of the rural dwellers as well as to attain food security and national growth, irrigation schemes need to be revitalized to increase food and cash crops production [26].

The economic welfare of a country and its ecosystem health is directly linked to water stress and the rate of water depletion [24]. Evidently, the Kano River Irrigation Project (KRIP) has played an important role in discouraging migration from rural to urban centers and alleviating the employment problems of its immediate community [20]. Similarly, there has been a sharp difference from the dry season farmers' income in Bauchi State when compared with rain-fed farmers for the same kind of farm produce. The dry season (irrigation) farmers get more profit than rain-fed farmers counterparts. This is not unconnected with the high demand for fresh irrigated crops during the dry season [27]. Moreover, a study on the Socio-economic impact of an irrigation project in Taraba State reported similar findings among the farmers in respect of economic gain. Project on the beneficiary of the Fadama II project in Kaduna State indicates an increase in the net farm income of the beneficiary farmers [28]. Hence, creating a more efficient irrigation water management approach has the potential to substantially increase agricultural production, farmers' incomes, and create employment opportunities.

Social Aspect of Sustainable Irrigation Schemes

Inherently, human beings are aiming to achive their need and these needs describe in-born requirements for an individual to be satisfied [29]. The management of open-access resources such as irrigation water involved numerous stakeholders with diverse interests which posed a unique challenge to the managers. These interests are the factors that affect individuals' ethical practices including propensity to compliant or unlawful activities. Ethical awareness is the ability of an individual to identify his deliberate action and understand what consequences that action might cause to others. Thus, for an individual to make an ethically accepted action depends on a person's moral awareness, motives and the benefits that individual is expected to gain. This depends largely on value-related factors such as culture, knowledge, and social well-being [30]. One of the problems that devastate irrigation water users' well-being is water scarcity which leads to poor crop production. Water scarcity represents a multidimensional state of human so-

cial deprivation characterized by a lack of access to affordable and safe water to satisfy societal needs or a condition in which these needs are met at the expense of the environment [10]. The mission for sustainable natural resource utilization is an essential part of the ongoing 2030 agenda for sustainable development goals (SDGs). It is one of the 169 agreed targets being aimed at monitoring and assessing the level of sustainability with which resources, such as irrigation water are being managed and utilized [31].

This creates a challenge of ensuring societal well-being through the supply of human basic needs including food security, income to the rural dwellers and national GDP of which water (through irrigation) plays an essential role [32, 33]. Thus, irrigation contributed immensely to the provision of a wide range of socio-economic benefits on which the well-being of society is based [34]. However, irrigation water is subjected to several challenges including climate change, poor management, chemical, wastage, overexploitation and other human-related influences [35–38].

The social setting can be a social group, a community, town, region or a nation, thus, any change that occur either as ideas, norms, values, roles and social habits can be referred to as social change. When alteration occurs in the rural social system, it is termed as rural social change, and such a change could be in all attributes of a societal unit such as number, quality and importance. Different changes come to the notice of the rural population of the developing countries, including Nigeria. For example, the introduction of large scale irrigation projects, use of the machine in farming practices, application of agrochemicals to control weeds, pests, diseases and increase and sustain the fertility of the soil lead to the transformation of sustainable agriculture and hence, the well-being of that society [20]. The attainment of a sustainable agricultural production system is becoming a major concern of agricultural researchers and policymakers all over the world [39]. Implementation of sustainable development, therefore, requires integrated policy, planning and social learning process. Irrigation practices provide employment and stabilization to the rural population and undoubtedly provide major social benefits. A typical example is how the Kano River Irrigation Project (KRIP) played an important role in limiting rural-urban migration by creating jobs for the rural dwellers [20].

Environmental Aspect of Sustainable Irrigation Schemes

Environmental impact refers to any change in the environment or in its components that may affect human health, flora, fauna, natural and cultural heritage as well as other physical structures, social, economic or cultural conditions [40]. For example, the challenges facing the irrigation sector in Nigeria is not only to attain food security and eradicate poverty among rural dwellers but also to ensure a healthy environment. Inappropriate management of irrigation schemes might lead to environmental problems such as high-water tables, poor drainage, salinization and pollution [13]. The majority of irrigation schemes in northern Nigeria are characterized by environmental degradation such as salinity, waterlogging and declining groundwater resources which could adversely affect future demand for water [41]. Both quantity and quality aspects of water are important as these jointly affect the success of irrigation schemes and environmental sustainability [42]. Thus, in the process to establish any socio-economic projects such as irrigation schemes, there is a need to ensure long-term maintenance of valued environmental resources in an evolving human influence [43]. Studies revealed that the majority of the economic development of the developing countries often occur at the expense of overexploitation of water resources which ultimately leads to ecosystem degradation [19].

Even though the extent is different, several environmental-related problems including soil erosion, aquatic weeds infestation, sedimentation, infrastructural deterioration and overgrazing are observed in many irrigation schemes in Nigeria [43]. For example, despite the functioning of the Kano River Irrigation Project (KRIP), there was a serious decline in hectares of land due to environmental-related issues such as waterlogging, salt accumulation (salinity, sodicity, saline-sodic) and reduced fertility [20]. There is a gradually building up of salinity problems in KRIP, even though the threat from salinity is not alarming yet. This problem of salinity has been reportedly alleged to continue to increase as long as irrigation is practiced unless preventive and corrective measures are put in place [44]. Generally, irrigation schemes design, operation and management should seek to maximize not only crop productivity and economic and social gains but also to ensure environmental stability and health as shown on Figure 2 [45]. Thus, irrigation scheme designs should consider using new technologies that ensure water allocation and application efficiencies such as micro irrigation methods (sprinklers and drip). In addition, in situ soil and water conservation methods such as mulch practices and deficit irrigation can significantly improve the overall ecosystem health.

The quality of surface and ground water in Nigeria was generally poor due to oil and gas exploration, agricultural production, landfill leachate, and poor sewage disposal. In addition to discharging untreated and/or poorly treated wastewater by the manufacturing industries which is reportedly linked to the corrupt socio-political circumstances of the country [46]. Another major issue of concern that has to do with the groundwater quality is the hydro-geological interactions of the groundwater with the base-rock. Such hydro-geological interactions commonly led to the Lead and Barium in groundwater in many locations across the country. Rainwater in Nigeria was observed to be fairly clean however, low pH is the only major issue affecting rainwater. Bottled and sachet water are currently the best and safer source of drinking water for the country's popu-

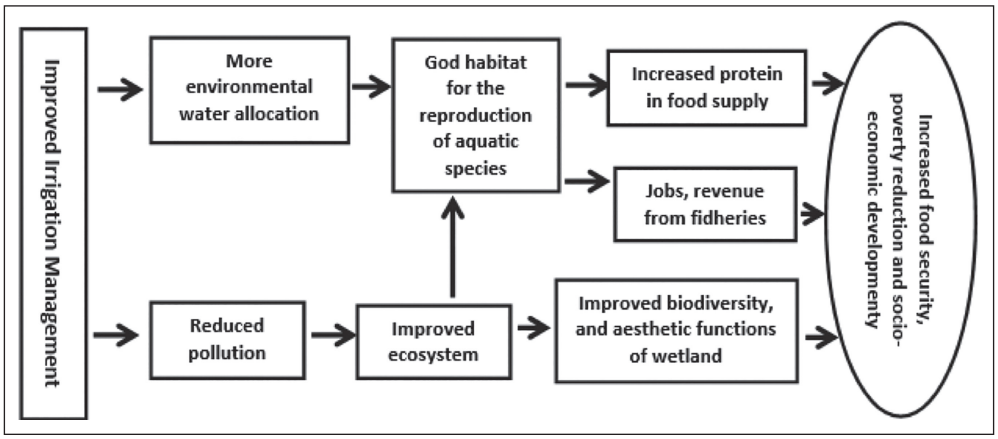

Figure 2. Framework for sustainable irrigation scheme design, operation and management [45].

lace. Generally, there are few wastewater treatment plants in the country, thus, there is a need to strengthen the water quality monitoring, and evaluation agencies.

Technological Aspect of Sustainable Irrigation Schemes

The development and improvement achieved so far in irrigation technologies are key to addressing the challenges of low agricultural productivity [47]. Availability and access to irrigation water and smart agricultural technologies were considered essential for crop production [48]. For instance, the success of the green revolution in Asia was achieved through the rapid expansion of irrigation areas with availability and access to new technologies including the development of high yielding varieties, fertilizers, micro irrigation techniques, tube-wells and water extraction mechanisms [49]. For example, technological advance provides irrigation sector with methods of optimizing water usage using variety of solutions based on sensor networks, microcontrollers and machine learning or fuzzy logic [50]. These methods have been in use to evaluate and predict optimum water required for irrigation. Such a smart irrigation is a systems made up of solar power station, networking infrastructure and water management and control stations (water storage, sprinkle or drip lines, water pumps, soil moisture sensors and micro-controller unit). In smart irrigation systems, the system components are commonly coupled using the Internet of Everything (IoE) approach as schematically summarized and shown in Figure 3. The use of such irrigation technology exerted a positive and significant impact on sustainable crop production and food security in Nigeria specifically [48].

Agricultural activities in Jibia Irrigation Project (JIP), Katsina State, depends mainly on power supply from diesel generators and electricity from the national grid to supply water to the farmlands. This has slowed down the pace of irrigation development in the area. The full exploitation of the agricultural potential of JIP and that of Nigeria in general, requires the exploitation of our vast renewable energy sources to provide the needed power [51]. Also, an alternative way to the high power demand of the operation of JIP and the likes is water conservation practices using different types of mulch. KRIP being one of the major irrigated agriculture in the northern Nigeria reported that, the majority of the farmers lack the technical know-how on water conservation and it is based on this that the researchers recommended the need to create awareness to the farmers where major irrigation is taking place. This will assist in achieving water conservation and management strategies in order to effectively and efficiently utilize the limited available water resources.

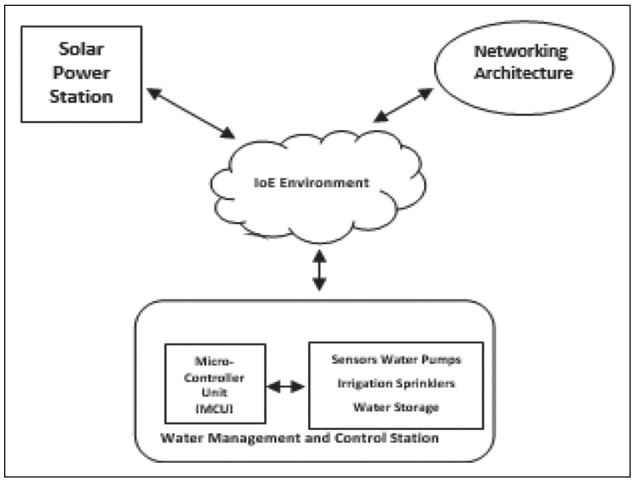

Figure 3. Technological advances for coupling smart irrigation components using IoE [50].

Irrigation schemes in Nigeria such as Watari Irrigation Project (WIP), Barwa-Minjibir Irrigation Scheme (BMIS), Tomas Irrigation Project (TIP) and Kpong Irrigation Project (KIP) in Niger Delta Basin Development Authority (NDBDA), had to abandon farming activities due to poor water-sharing techniques [51]. Thus, farmers should be fully conversant with irrigation technologies through agricultural machinery and credit facilities. Moreover, farm inputs such as fertilizer, seed, chemical and other materials

needed by farmers should be made available to the farmers. Infrastructural decay is also another problem that has been affecting the success of irrigated agriculture in northern Nigeria. About 30% of water structures at WIP were found to be damaged and malfunctioning [52]. Similarly, the conveyance structures were silted and infested by weeds which significantly reduced the carrying capacity of the canal. Also, about 8% of the irrigable area downstream was abandoned due to inadequate supply of water. There is an increased occurrence in soil salinity and sodicity issues within the WIP due to a poor drainage system [53].

In this regard, the majority of the irrigation schemes in northern Nigeria such as Sokoto Rima, Watari, Jibiya and Tomas are operated far below their design capacity due to lack of adoption of improved equipment and poor maintenance [54]. In addition, a larger proportion of the currently used irrigation equipment was purchased during the inception of the projects (the 1970s to 1980s) without replacement. Thus, there is a need to conduct empirical studies in Nigerian irrigation schemes to assess the following;

a. How farmers demand irrigation technologies.
b. How their zeal and willingness to adopt improved irrigation technologies are affected by specific agro-ecological and socio-economic characteristics.
c. How their adoption of such improved irrigation technologies may be hampered by poorly functioning markets.

Institutional Aspect of Sustainable Irrigation Schemes

Institutions are the political, social or business organisations (public or private) that are involved in policy-making and implementation. While institutional sustainability is the continuation of the benefit flows to the users/clients/owners/employees or the general public with or without the programmes or organisations that stimulated them in the first place [54]. Institutional performance is considered as one of the yardsticks with which the performance of developmental institutions such as irrigation schemes can be evaluated. At the end of the 20th century, the increasing role and relevance of social and institutional structures in connection with the whole field of contemporary environmental management are gaining prominence. Currently, institutional mandates constituted social well-being, economic gain as well as environmental health. Such a sustainability-based management strategy has gained more attention all over the world as this form an important developmental strategy as enclosed in the ongoing sustainable development goals (SDGs). The main aim of such a strategy was to effectively and sustainably manage and utilize the limited available natural resources [55]. For example, in the irrigation management sector, this approach has in recent years been employed to shift irrigation management toward a community-based by sharing power with multiple sets of other institutions stakeholders [56]. This requires every stakeholder involved in all levels of irrigation management to collectively take responsibility for managing the affairs of the schemes.

The small-scale private irrigation schemes (SPRI) sector in Nigeria is supported by a range of private agents, including irrigation technology service providers, NGOs, water user associations (WUAs) as well as public institutions such as the National Fadama Development Project (NFDP), the Agricultural Development Project (ADP), the State Irrigation Department (SID), river basin development authorities and state and federal government ministries [56]. A study carried in 1972 led to the institution of three models of public irrigation schemes; namely the Bakolori Scheme, the Chad Basin scheme, and Kano River Irrigation Project, subsequently additional eleven more River Basin Development Authorities (RBDAs) were added across the country after the success of the pilot schemes in 1976 [57].

The Nigerian government does not only own, operate and maintain irrigation schemes, but provides agro-support services such as land preparation, seeds, fertilizers, chemicals, and assists in marketing the produce. The reforms in water institutions such as Participatory Irrigation Management (PIM) systems were formulated and implemented to achieve effective operation of the schemes, equitable distribution of irrigation water among farmers, high crop productivity and food security among others [58].

In the Hadeja-Jama'are river irrigation project, the utilization of the project is just 50% while the Zobe dam in Dutsin-Ma, Katsina which was constructed 40 years ago, currently has few irrigation activities as the scheme is not formally developed. Also, at the Bakolori irrigation dam in Zamfara State, under the Sokoto Rima Water Project, the area cultivated is not commensurate with the amount of water in the dam [59]. For instance, at the end of the 1999/2000 irrigation season, out of the 100,300 ha developed only 35,000 ha were irrigated giving a pathetic 35% capacity utilization. Most of the irrigation schemes that the government has invested in are either under-utilized for irrigation or abandoned irrigation schemes like the Hadeja-Jama'are river project, the utilization is 50% while the Zobe dam in Dutsin-Ma in Katsina, which was constructed 40 years ago, currently has little irrigation activities [52]. Cases in points that highlighted the danger of poor irrigation management institutional performance are the findings by [53]. More than 29% of the farmers of Tomas Irrigation Project (TIP) expressed unhappiness with the water allocation method currently used and about 55% of water users hold the opinion that irrigation scheme management, operation and maintenance is an exclusive responsibility of the government. In addition to poor water management, infrastructural decay and stakeholders' conflict as the major problems affecting the scheme.

CONCLUSION

This chapter presented a review of the operation and management of irrigation schemes in the northern part of Nigeria. The main aim of this study was to identify and relate key values operating in the northern Nigerian irrigation sector from a sustainability point. This includes identifying the causes and effects of impending problems and hence, suggesting ways forward to achieve sustainable food security at the face of the ever-increasing population in the country. The major motivation factor for this review was the fact that studies on assessing the performance of systems such as irrigation schemes using the concept of sustainability are gradually gaining popularity and growing at a high rate in recent years. The appraisal revealed that several impediments have been hindering the performance of irrigation practice in Nigeria which includes inconsistent government policies, low awareness and lack of technical know-how among the farmers on irrigation farming system, and untimely financial intervention.

Another insight of interest gained from the work was that the huge investment in both large- and medium-scale irrigation schemes in the northern part of Nigeria have been resulted in irrecoverable losses due to quite several issues. Some of these problems comprise of under-utilization of water resources, poor management, infrastructural decay and abandonment. Generally, studies revealed that irrigation schemes in northern Nigeria performed far below expectations with approximately 65% capacity utilization. About half (50%) of the farmers express unhappiness, dismay and loss confidence with the way irrigation schemes are operated. Water managers blame farmers to lack enthusiasm toward abiding by the set rule and regulations governing irrigation schemes. In addition, study by [54] revealed that about 45% of the farmers do not participate in the maintenance of the irrigation schemes which further exacerbate the problems. However, some irrigation projects are performing relatively very well. The income and the standard of living of the farmers around well-performing irrigation projects were observed to improve significantly compared to poor performing ones.

Thus, there is a need to holistically improve the general operational performance of the existing irrigation schemes in northern Nigeria through the following.

Some of the suggestions that should be done in Nigeria to improve the current situation including encouraging participatory irrigation management, ensuring effective and competent institutions with a strong monitoring and evaluation mechanisms, frequent policy review and alterations to suit the situation, and timely sensitization and awareness campaigns. Functions of water regulatory institutions should be streamlined with each institution given specific and defined roles to enhance efficiency in irrigation water resource management and this should be organised using the sustainability pillars. A research effort using a sustainability-based approach is also required to further identify the causes and effects of problems that have been hampering the performance of irrigation schemes in northern Nigeria. There is also a need to adopt new water allocation and application methods that can improve water use efficiency.

ACKNOWLEDGMENTS

On behalf of the entire authors, I would like to thank the management of Bayero University Kano, Nigeria for the opportunity to conduct this study though Directorate of Research, Innovation and Partnerships (DRIP), Institution Based Research (IBR), a component of the Tertiary Education Trust Fund (TETFund).

DATA AVAILABILITY STATEMENT

The authors confirm that the data that supports the findings of this study are available within the article. Raw data that support the finding of this study are available from the corresponding author, upon reasonable request.

CONFLICT OF INTEREST

The authors declared no potential conflicts of interest with respect to the research, authorship, and/or publication of this article.

ETHICS

There are no ethical issues with the publication of this manuscript.

REFERENCES

[1] I. Y. A. M. B. Hassan, and R. Yahaya, "Economic analysis of micro-drip irrigation using integrated Agricultural Research for Development (Iar4d) approach: The case of vegetable innovation platform in rural Nigeria," Agricultural Transformation in a Deregulated Economy: Prospects and Challanges, pp. 103–106, 2012.

[2] M. T. Bayero, "Assessing the sustainability of drainage system in irrigated agricultural land: A case study of Kano River irrigation scheme in Nigeria defended," [Master Thesis], Pan-African University Institute for Water and Energy Sciences, pp. 1–133, 2019.

[3] I. O. Akinyele, "Ensuring food and nutrition security in rural Nigeria: An assessment of the challenges, information needs, and analytical capacity," International Food Policy Research Institute, Washington D.C. 2009.

[4] D. Astou, "Food imports as a hindrance to food security and sustainable development: The cases of Nigeria and Senegal," [Master Thesis], City University of New York, 2015.

[5] M. J. Beillard, U. M. Nzeka, and A. M. Specialist, "Nigeria grain and feed annual 2019 Nigeria's imports of wheat and rice to rise," [Rep. No: NG-19002]. Global Agricultural Information Network, 2019.

[6] W. A. Yusuf, S. A. Yusuf, A. Adesope, and O. Aadebayo, "Determinants of rice import demand in Nigeria," Journal of Applied Sciences and Environmental Management, Vol. 24(5), pp. 923–931, 2020. [CrossRef]

[7] T. H. Xiea, and H. L. Youa, "Invest in small-scale irrigated agriculture: A national assessment on potential to expand small-scale irrigation in Nigeria," Agricultural Water Management, Vol. 193, pp. 251–264, 2017. [CrossRef]

[8] T. O. Dauda, O. E. Asiribo S. O. Akinbode, J. O. Saka, and B. F. Salahu, "An assessment of the roles of irrigation farming in the millennium development goals," African Journal of Agricultural Research, Vol. 4(5), pp. 445–450, 2009.

[9] M. Joseph, D. C. Maurice, and J. N. Jatbong, "Profitability assessment of irrigated crop production among small-scale farmers in Gombe state, Nigeria," Direct Research Journal of Agriculture and Food Science, Vol. 7(7), pp. 166–172, 2019.

[10] L. Rosa, D. D. Chiarelli, M. C. Rulli, J. D. Angelo, and P. D. Odorico, "Global agricultural economic water scarcity," Science Advances, Vol. 6(18), pp. 6031–6060. [CrossRef]

[11] E. Borsato, L. Rosa, F. Marinello, and P. Tarolli, "Weak and strong sustainability of irrigation: A framework for irrigation practices under limited water availability," Frontiers in Sustainable Food Systems, Vol. 4, Article 17, 2020. [CrossRef]

[12] N. M. Nasidi, and N. J. Shanono, "Performance evaluation of water conveyance system at Watari Irrigation Project (WIP)," iSTEAMS Multidisciplinary Cross-Border Conference At: Accra, Ghana, Vol. 3, pp. 105–110, 2016.

[13] G. Jibril, M. Saidu, and A. A. Yabagi, "Performance evaluation of Badeggi irrigation scheme, Niger State Nigeria, using efficiency techniques," Scholarly Journal of Science Research and Essay, Vol. 6(2), pp. 42–47, 2017.

[14] N. J. Shanono, N. M. Nasidi, M. D. Zakari, and M. Bello, "Assessment of field channels performance at Watari Irrigation Project Kano, Nigeria," Proceedings of the 1st International Conference on Drylands, Bayero University, Kano, pp. 144–150, 2012.

[15] U. Mohammed, and M. S. Ali, "Socio economic challenges of irrigation farming along River Yobe (A case study of Yobe State)," IOSR Journal of Environmental Science, Toxicology and Food Technology, Vol. 15(4), pp. 1–7, 2021.

[16] P. D'Odorico, K. F. Davis, L. Rosa, J. A. Carr, D. Chiarell, J. Dell'Angelo, J. Gephart, G. K. MacDonald, D. A. Seekell, S. Suweis, and M. C. Rull. "Reviews of geophysics the global food-energy-water nexus," Advancing Earth Space Science, pp. 456–531, 2018. [CrossRef]

[17] J. Alcamo, P. Döll, T. Henrichs, F. Kaspar, B. Lehner, T. Rösch, and S. Siebert "Global estimates of water withdrawals and availability under current and future 'business-as- usual' conditions," Hydrological Sciences Journal, Vol. 48(3), pp. 339–348, 2010. [CrossRef]

[18] J. Rockström, M. Falkenmark, T. Allan, C. Folke, L. Gordon, A. Jägerskog, M. Kummu, M. Lannerstad, M. Meybeck, D. Molden, S. Postel, H. H. G. Savenije, U. Svedin, A. Turton, and O. Varis. The unfolding water drama in the Anthropocene: Towards a resilience-based perspective on water for global sustainability," Ecohydrology Bearings, Vol. 1261(7), pp. 1249–1261, 2014. [CrossRef]

[19] H. Savenije, P. Van Der Zaag, and I. H. E. Delft, "Water as an economic good and demand management paradigms with pitfalls," International Water Resources Association, Vol. 27(1), pp. 98–104, 2002. [CrossRef]

[20] S. K. Haruna, "Impact of participatory irrigation management (PIM) on the livelihood of water users in Kano River Irrigation Project (KRIP), Nigeria," [Doctorial Thesis], Ahmadu Bello University, 2015.

[21] A. Hassan, M. O. Adewumi, and A. Falola, "An assessment of the irrigation scheme on registered rice farmers of the upper benue rice basin development authority in Dadin Kowa, Gombe State, Nigeria," Vol. 4(1), pp. 1–24, 2015. [CrossRef]

[22] A. O. Kolawole, F. M. Oluwatusin, A. Ajiboye, O. A. Aturamu, K. A. Abdu-Raheem, and F. E. Akokoh, "Poverty status analysis of irrigation farming households in Nigeria," Multidisplinary Academic Journal Publisher, Vol. 12(2), pp. 15–26, 2018.

[23] Food and Agriculture Organization of the United Nation Database. [Policy Text] "National irrigation and drainage policy and strategy," Abuja-Nigeria, 2015. https://www.fao.org/faolex/results/details/en/c/LEX-FAOC181432/

[24] E. Borsato, M. Martello, and F. Marinello, "Environmental and economic sustainability assessment for two different sprinkler and a drip irrigation systems: A case study on maize cropping," Agriculture, Vol. 9(9), pp. 1–15, 2019. [CrossRef]

[25] A. J. Z. Ohikere, and A. F. Ejeh, "Impact of small scale irrigation technologies on crop production by fadama users in Kogi State, Nigeria," Advances in Applied Science Research, Vol. 3(2), pp. 854–861, 2012.

[26] A. Ahmed, M. A., Oyebode, H. E. Igbadun, and E. Oiganji, "Assessment of tomato farmers' irrigation practice in Pampaida Millennium Village, Ikara local government area, Kaduna State, Nigeria," FUDMA Journal of Sciences, Vol. 4(2), pp. 499–509, 2020. [CrossRef]

[27] G. J. Adama, D. O. Jimoh, and M. Y. Otache, "Optimization of irrigation water allocation framework based on genetic algorithm approach," Journal of Water Resource and Protection, Vol. 12, pp. 316–329, 2020. [CrossRef]

[28] A. S. Abdullahi, B. G. Jahun, and M. U. Sabo, "Impact of irrigation project on fadama community of Bauchi state Nigeria," International Journal of Advanced Engineering and Science, Vol. 5(1), pp. 20–30, 2016.

[29] M. Missimer, K-H. Robèrt, and G. Broman, "Postprint a strategic approach to social sustainability - Part 1: Exploring the social system," Journal of Cleaner Production, Vol. 140(1), pp. 32–41, 2017. [CrossRef]

[30] L. K. Treviño, G. R. Weaver, and S. J. Reynolds, "Behavioral ethics in organizations: A review," Journal of Management, Vol. 32(6), pp. 951–990, 2006. [CrossRef]

[31] N. J. Shanono, "Towards a more human-centered irrigation water management- A review," International Journal of Water Management Diploma, Vol. 1(3), pp. 5–16, 2021.

[32] S. Manju, and N. Sagar, "Renewable energy integrated desalination: A sustainable solution to overcome future fresh-water scarcity in India," Renewable and Sustainable Energy Reviews, Vol. 73, pp. 594–609, 2017. [CrossRef]

[33] S. Hossain, S. J. Pogue, L. Trenchard, A. P. E. Van Oudenhoven, C-L. Washbourne, and E. W. Muiruri, "Identifying future research directions for biodiversity, ecosystem services and sustainability: Perspectives from early-career researchers," International Journal of Sustainable Development & World Ecology, Vol. 25(3), pp. 249–261, 2018. [CrossRef]

[34] M. Wang, J. Li, and Y. Ho, "Research articles published in water resources journals: A bibliometric analysis," Desalination and Water Treatment, Vol. 28(4), pp. 353–365, 2011. [CrossRef]

[35] Y. Zhang, H. Chen, J. Lu, and G. Zhang, "Detecting and predicting the topic change of knowledge-based systems: A topic-based bibliometric analysis from 1991 to 2016," Knowledge-Based Systems, Vol. 133, pp. 255–268, 2017. [CrossRef]

[36] N. J. Shanono, and J. Ndiritu, "A conceptual framework for assessing the impact of human behaviour on water resource systems performance," Algerian Journal of Engineering and Technology, Vol. 2, pp. 35–44, 2020.

[37] N. J. Shanono, "Co-evolutionary dynamics ofhuman behaviour and water resource systems performance: A socio-hydrological framework," Academia Letters, Vol. 1191, pp. 1–6, 2021. [CrossRef]

[38] N. M. Nasidi, N. J. Shanono, M. D. Zakari, A. Ibrahim, and M. M. Bello, "Reclaiming salt-affected soil for the production of tomato at barwa-minjibir irrigation scheme, Kano," in International Conference on Green Engineering for Sustainable Development, IC-GESD 2015. Held at Bayero University, Kano Nigeria, 2015.

[39] N. Medugu, "Achieving sustainable agriculture in Nigeria: A land-use policy perspective," Tokyo Academic, Industry & Cultural Integration Tour 2006, 10-19 December, Shibaura Institute of Technology, Japan, pp. 10–19, 2006.

[40] M. D. Ulsido, E. A. Demisse, M. A. Gebul, and A. E. Bekelle, "Environmental impacts of small scale irrigation schemes: Evidence from Ethiopian rift valley lake basins environmental impacts of small scale irrigation schemes: Evidence from Ethiopian rift valley lake basins," Environmental Research, Engineering and Management, Vol. 1(63), pp. 17–29, 2013. [CrossRef]

[41] A. Sobowale, M. N. Tijani, A. E. Obayelu, A. S. Olatunji, and T. Shah, "Livelihood analysis of smallholder irrigation farmers in Nigeria," Journal of Agriculture and Environmental Sciences, Vol. 14, pp. 1–17, 2014.

[42] A. A. Mohamme, and D. H. A. Ibrahim, "Variabilty of irrigation water quality in Kano River Irrigation Project," JORİND, Vol. 13(2), pp. 1–7, 2015.

[43] N. Purity, and E. E. Adaeze, "Environmental sustainability and sustainable development in Nigeria: Environmental sustainability and sustainable development in Nigeria: Problems and prospects," International Journal of Academic Accounting, Finance & Management Research, Vol(1), pp. 6–11, 2020.

[44] M. M. Maina, M. S. M. Amin, W. Aimrun, and I. Sani, "Soil salinity assessment of Kadawa Irrigation of the Kano River Irrigation Project (KRIP)," Journal of Food, Agriculture and Environment, Vol. 10(3&4), pp. 132–138, 2012.

[45] M. F. Fonteh, "Guidelines for sustainable irrigation system design and management in sub-Saharan Africa," African Journal of Agricultural Research, Vol. 12, 1747–1755, 2017. [CrossRef]

[46] J. O. Ighalo, and A. G. Adeniyi "A comprehensive review of water quality monitoring and assessment in Nigeria," Vol. 260, Article 127569, 2020. [CrossRef]

[47] J. Ngango, and S. Hong, "Adoption of small-scale irrigation technologies and its impact on land productivity: Evidence from Rwanda," Journal of Integrative Agriculture, Vol. 20(8), pp. 2302–2312, 2021. [CrossRef]

[48] O. Adebayo, O. Bolarin, A. Oyewale, and O. Kehinde, "Impact of irrigation technology use on crop yield, crop income and household food security in Nigeria: A treatment effect approach," AIMS Agriculture and Food, Vol. 3(2), pp. 154–171, 2018. [CrossRef]

[49] M. Bhattarai, and A. Narayanamoorthy, "Impact of irrigation on agricultural growth and poverty alleviation: Macro level analyses in India," [Conference Paper], IWMI-Tata Workshop Water Policy Research, Water Policy Program, January 27-29, 2004.

[50] A. Favour, S. Misra, R. Maskeliunas, R. Damasevicius, and E. Kazanavicius, "Smart irrigation system for environment sustainability in Africa: An internated of everything (IoE) approach," Mathematical Biosciences and Engineering, Vol. 16(5), pp. 5490–5503, 2019. [CrossRef]

[51] N. J. Shanono, M. Bello, I. Muntaqa, and T. Usman, "Stakeholders conflict and infrastructural decay ın Nigerian irrigation schemes: A review," Nigerian Journal of Engineering Science and Technology Research, Vol. 6(1), pp. 78–90, 2020.

[52] N. J. Shanono A. A. Sabo, N. M. Nasidi, M. D. Zakari, M. Mohammed, H. Ismail, and A. G. Halilu, "Hydraulic Infrastructures and Asseeement of Watari Irrigation Project, Kano," Journal of Engineering Technology, Vol. 10(2), pp. 44–51, 2015.

[53] A. Y. Bashir, A. M. Samndi, M. A. Adam, K. T. Moji, and M. Auwal, "Appraisal and mapping of soil salinity and sodicity problems in sector one of watari irrigation scheme, Kano State," Nigeria Institute of Soil Science, Vol. 29(2), pp. 54–60, 2020. [CrossRef]

[54] N. J. Shanono, N. M. Nasidi, M. Maina, M. Bello, A. Ibrahim, S. I. Umar, I. M. Tijani Usman, and M. D. Zakari, "Socio-hydrological study of water users' perceptions on the management of irrigation schemes at tomas irrigation project, Kano, Nigeria," Nigeria Journal of Engineering and Technology, Vol. 5(2), pp. 139–145, 2019.

[55] S. Kayaga, J. Mugabi, and W. Kingdom. "Evaluating the institutional sustainability of an urban water utility: A conceptual framework and research directions," Utilities Policy, Vol. 27, pp. 15–27, 2013. [CrossRef]

[56] V. S. Saravanan, and P. Bhawan, "Institutionalising community-based watershed management in India: Elements of institutional sustainability," Water Science and Technology, Vol. 45(11), pp. 113–124, 1990. [CrossRef]

[57] H. Takeshima, S. S. Okoli, Silas, and V. Rhoe, "Demand characteristics for small-scale private irrigation technologies: Knowledge gaps in Nigeria," The Nigeria Strategy Support Program NSSP, 2010.

[58] B. Adelodun, and K. Choi, "A review of the evaluation of irrigation practice in Nigeria: Past, present and future prospects," African Journal of Agricultural Research, Vol. 13(40), pp. 2087–2097, 2018. [CrossRef]

[59] B. Ahmad, H. Duy Pham, M. Ashfaq, J. Alam Memon, R. Bano, Z. H. Dahri, R. Naveed Mustafa, I. A. Baig, and M. A. Rehman Naseer, "Impact of institutional features on the overall performance assessment of participatory irrigation management: Farmers' response from Pakistan," MDPI, Vol. 12(497), pp. 1–13, 2020. [CrossRef]

Environ Res Tec, Vol. 5, Issue. 4, pp. 315–324, December 2022

Environmental Research and Technology
https://ert.yildiz.edu.tr - https://dergipark.org.tr/tr/pub/ert
DOI: https://doi.org/10.35208/ert.1150943

Environmental Research & Technology

Research Article

Construction and demolition waste in Tungurahua: A case study from Ecuador

Juan Daniel CABRERA GÓMEZ*, Paola Cristina VELASCO ESPÍN

Independent Researcher, Convergentelab, Ambato, Ecuador

ARTICLE INFO

Article history
Received: 29 July 2022
Revised: 21 September 2022
Accepted: 02 November 2022

Key words:
Building material stock; Construction and demolition waste; Six "s" of brand; Tungurahua; Urban mining

ABSTRACT

This research will make an analysis of the material stock in Tungurahua-Ecuador from 2013 to 2019 using the general purpose of six "s" of Brand (1994) for site, structure, skin and space plan layers, data was taken from the Instituto Nacional de Estadisticas y Censos (INEC), from 2013 to 2019; and for the stuff layer the research applied online forms, the results show that reinforced concrete is the predominantly material used in foundation, structure and skin layers, then bricks and blocks are most common used in space plan layer and timber elements are the most used in the stuff layer, finally the paper proposes some ways to deal with this type of materials and future information to be addressed in new research.

Cite this article as: Cabrera Gómez JD, Velasco Espín PC. Construction and demolition waste in Tungurahua: A case study from Ecuador. Environ Res Tec 2022;5:4:315–324.

INTRODUCTION

While the construction sector is often a very important driver for the economy in many countries, it is also the main global consumer of raw materials and is accountable for large amounts of waste and 25% to 40% of global emissions [1]. And yet less than a third of construction and demolition waste (CDW) is recovered in United States., see Figure 1.

In 2014, 541 000 tonnes of urban waste per day were produced in Latin America, this is expected to increase by 25% for the year 2050. In the region, 90% of urban waste is not repurposed [2]. However, when it comes to CDW there is no consistent data in the region and often each country manages information differently.

In Ecuador the production of urban waste is directly related to population density and to territories with higher business development which now have collapsed disposal systems [3]. The latest National Plan for Managing waste (PNGIDS) aimed at promoting the national recycling and energy industries and extending the responsibility to the producer and importer in the management of hazardous and special waste [4]. This is to be done by involving the local governments, base recyclers and the private sector and assigning about USD$27M to the project for 12 years, meaning that by 2021 solid waste in the country would be efficiently managed [4]. However by 2020 Ecuador still buried 94% of its waste and every municipality deals with it according to their capacity in the absence of national guidelines [3].

***Corresponding author.**
*E-mail address: info@convergentelab.com

This paper has been presented at Sixth Symposium on Circular Economy and Urban Mining (SUM 2022)/Capri, Italy / 18–20 May 2022.

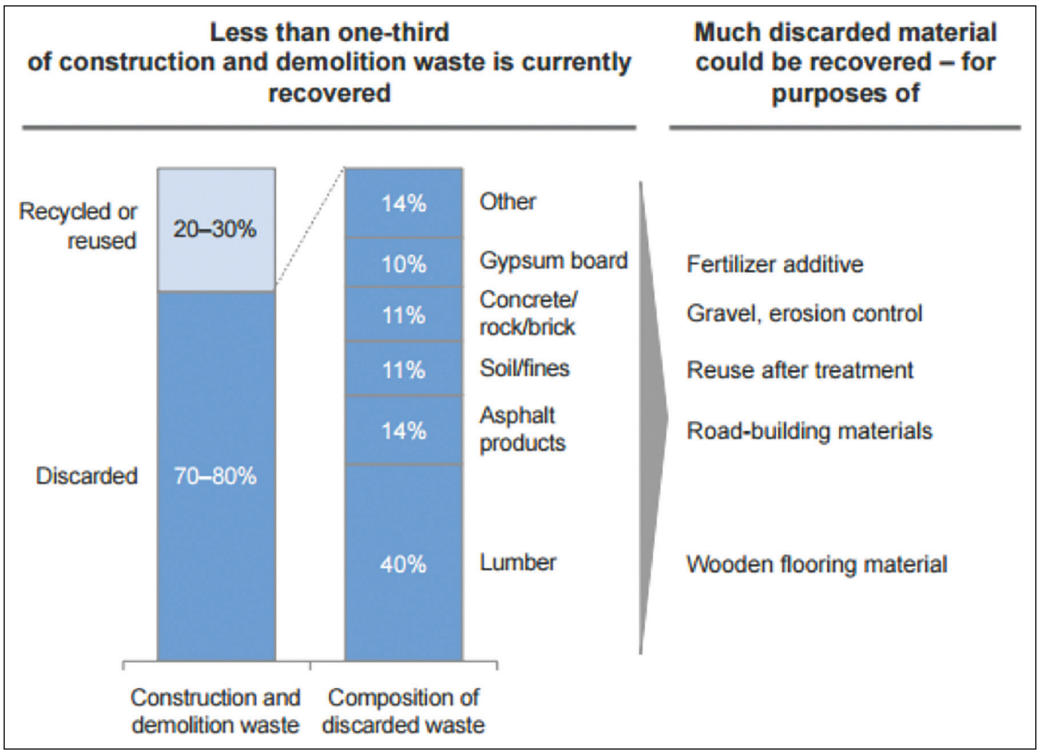

Figure 1. Amount of construction and demolition waste in the United States [1].

In Ecuador, 10 cities account for 70% of the national waste production, ranked according to the relation between population density and per capita waste production, Ambato ranked in third place with 1.29 kg/hab/day [3].

During 2019, Tungurahua construction industry contributed 2.1% to national incomes, where Guayas and Pichincha were the major contributors, 30.2% and 19.8% respectively, Ambato was the first state in Tungurahua contributing 82.8%, then, second Píllaro 7.5%, after, third Pelileo 3.8% and, fourth, Baños 2.3%. See Table 1.

Table 1. Construction industry aggregated value from Tungurahua in Ecuador [5]

States	Agregated value	Province contribution	National contribution
Ambato	205,347	82.8%	1.7%
Baños	5,725	2.3%	0.0%
Cevallos	310	0.1%	0.0%
Mocha	797	0.3%	0.0%
Patate	1,680	0.7%	0.0%
Quero	1,614	0.7%	0.0%
San Pedro De Pelileo	9,446	3.8%	0.1%
Tisaleo	4,313	1.7%	0.0%
Santiago De Píllaro	18,658	7.5%	0.2%

Literature Review: Circular Economy, Urban Mining, CDW Management and Research Framework

Circular Economy in Construction and Demolition Waste

Economic, organizational, technical, financial and cultural challenges have to be addressed to enable the circularity in the construction sector, in the economic field, material value and its uncertain prices into future and low prices at their end of life make uneconomically to reuse them. After, in the organizational aspect, lack of client awareness and unclear actors´ roles across building´s life cycle depending on circumstances of projects. Another challenge is related to the technical issues such as considering adaptability, flexibility and deconstruction [6]. Moreover, there are financial obstacles, such as the business approach that collaborate to the supply chain and circular business cases that reaffirm its feasibility [7]. Finally, there are cultural barriers depending on how solutions are well received and correctly utilized by users [8].

Circular economy in the construction context has little research [6] and its emerge is essential [9], short term and medium lived consumer goods have been targeted by the circular economy (CE) concepts forgetting long-lived products such as buildings, which are conformed by a variety of elements and materials that possess their own lifecycle, functions and characteristics are interacting each other at the same time in the entire building system [10], other sectors have explored business models about long-life structures but in the industry sector is lacking because of their value as material assets [6].

Urban Mining

Urban mining considers buildings as mines where stock and flow resources are important [11], annual stocks held in buildings may not vary over time nevertheless annual flows of materials may change considerably year to year depending on circumstances [12]. Materials are organized into buildings components and elements that determine an ease extraction or an availability for collection [11].

Materials lifespan makes complicated to decipher when a material will be available, detailed information such as bills of materials in combination with construction types would help to know quantities and material types, also, building information modelling (BIM) with waste management improves precisely waste predictions [11].

Stephan and Athanassiadis [13] proposes in their work an estimation, spatialization and quantification manner for inflows and outflows associated with replacement of construction materials in order to maintain urban building stocks. Their study is based on archetypes of possible assemblies, datasets, census of land use and employment that includes floor areas, year of construction and number of stories for around 14385 buildings.

Construction and Demolition Waste Management

Countries have tried to improve the construction and demolition waste (CDW) management by encouraging behaviours, implementing laws, motivating plans or creating taxes, eg., in Australia, deconstruct old timber houses is a common practice, the country has an estimated 80% of materials recovered and reused for renovation and remodeling of existing homes or in the construction of new replica housing. In the Netherlands, a strict government regulation states that dumping reusable waste is prohibited, this regulation generates an 80% of CDW reused in other construction generally in creating materials for road base. In Norway, a plan for design for deconstruction that dismantle building systems, relies on local building materials and simple traditional technology, the components are easily assembled and have the capability of easily changed or reconfigured. In United Kingdom, a landfill tax introduced in 1996 that incur rates depends on separated or mixed waste, £2 or £11/tonne respectively, this tax has contributed to a big increase of fixed and mobile crushing and recycling sites [7].

Research Framework for Construction and Demolition Waste

Three framed levels for CE research in the built environment are proposed consisting on macro (cities and neighbourhoods), meso (buildings) and micro (assemblies and components), and six fundamental dimensions are considered to achieve more circular buildings, there are environmental, technological, economic, societal, governmental and behavioural dimensions [9].

Materials are uncapable to be recovered because its replacement is always linked to demolish, this happens because, they are often part of an integrate fixed assembly, so most of the parts when a building ends its life cycle they are demolished and wasted with the entirely building, moreover, material's 'technical life cycle' is longer than their 'use life cycle' [14], so, some materials could be still used but the difficulties to be separated from other parts makes it complicated.

Various authors have developed guidelines for Design for Deconstruction DfD, for example Scot Fletcher classifies a total of 37 guidelines into three levels: systems, product and material level. Berge describes three principles: separate layers, possibilities for disassembly within each layer and use of standardized monomaterial components. Thormark postulates 18 design guidelines into three groups: choice of materials, design of construction and choice and connections. Sassi gives two main areas: the process of removal of building elements and materials from building structure and the requirements for reprocessing of building elements and materials to enable reintegration in a new building. Crowther proposes five generative fields: industrial design, architectural technology, buildability, maintenance and research. Addis and Schouten presents 19 principles into these outcomes: component reuse, component manufacture and material recycling. Durmisevic lists 37 guidelines relate to three levels: building, system and material level in a scenario between use life cycle and technical life cycle [15]. Overall aim is material resource efficiency through facilitating reuse and recycling.

As we have shown, fields studied about construction components are dispersed, there are many principles from different authors nevertheless Nordby et al. [15] characterise and classify them in three groups: behavioural statements, performance standards and prescriptive guidelines. They create a multi-purpose system based on design guidelines in order to be an assessment tool to be used when selecting buildings components for a new design with respect to their potential at the stage of deconstruction and applied in two cases studies of wood components and bricks.

Sassi [9] also develops a criteria for establishing suitability for recycling, down cycling, reuse as new and as second hand item, and apply it into floor finishes. The study shows different types of floor coveries and determined that solid wooden floor nailed have the highest score into the recycling category, rubber interlocking floor tiles loose laid have the best score to be down cycled, steel covered HDF raised floors screwed to plinths with loose laid carpet tiles have a high value for being reused as new, and, finally, carpet tiles loose laid and rubber interlocking floor tiles loose laid possess a high score for being reused as second hand item.

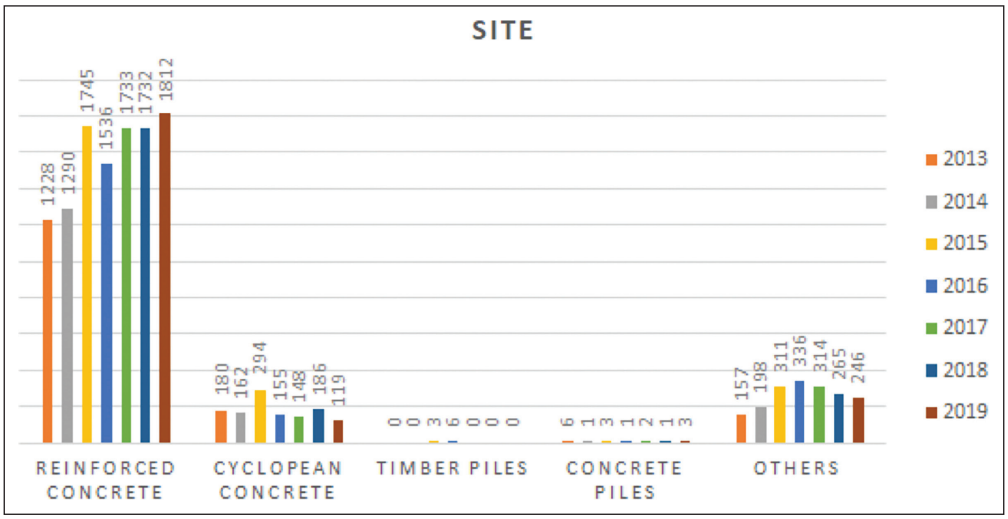

Figure 2. Site layer in Tungurahua from 2013 to 2019 [16].

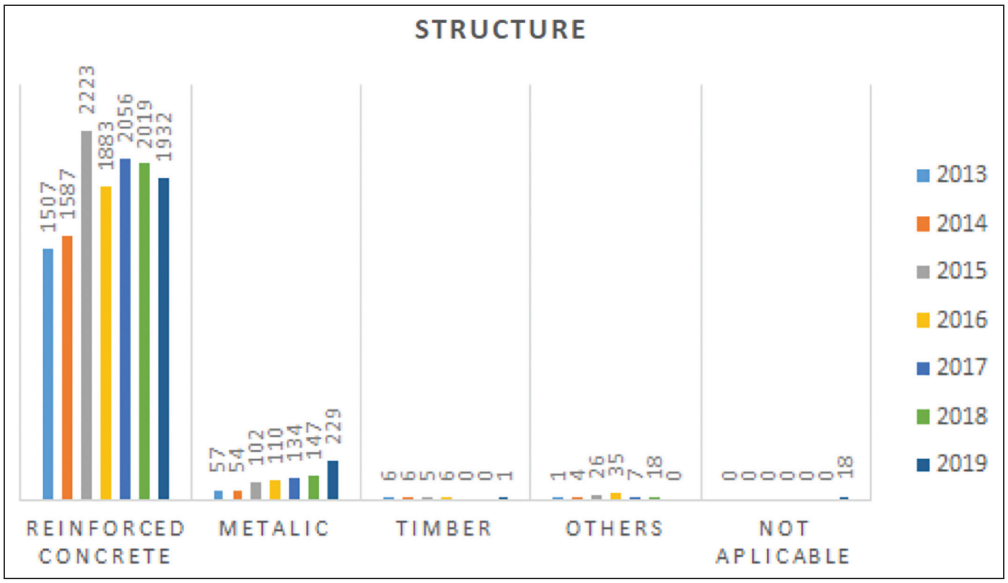

Figure 3. Structure layer in Tungurahua from 2013 to 2019 [16].

MATERIALS AND METHODS

This study is a descriptive quantitative research. The research uses public data from Instituto Nacional de Estadísticas y censos (INEC), specially related to the building survey done from the years 2013, 2014, 2015, 2016, 2017, 2018 and 2019. In the website there is no more data available about years 2020 and 2021 [16]. Also the project collect data from 104 people mainly from Ambato, they were asked to fulfill an online form by a massive message sent through whatsapp.

In overall the research took the general purpose of six "s" of Brand (1995): site, structure, skin, services, space plan and stuff [17]. For the site, structure, skin and space plan layers, data was taken from the Instituto Nacional de Estadísticas y censos (INEC). Data was compressed into four graphics divided by site, structure, space plan and skin layer. For the stuff layer the research applied an online form in order to discover the materials used in floor finishes, dinning furniture, doors and windows.

RESULTS

In the site layer most buildings have used reinforced concrete, others materials and cyclopean concrete, is not so common the use of timber and concrete piles as can be seen in Figure 2. The structure layer is made of reinforced concrete in most buildings, also the use of metallic structures have increased and the use of timber is not so common as can be seen in Figure 3. The space plan layer is constituted

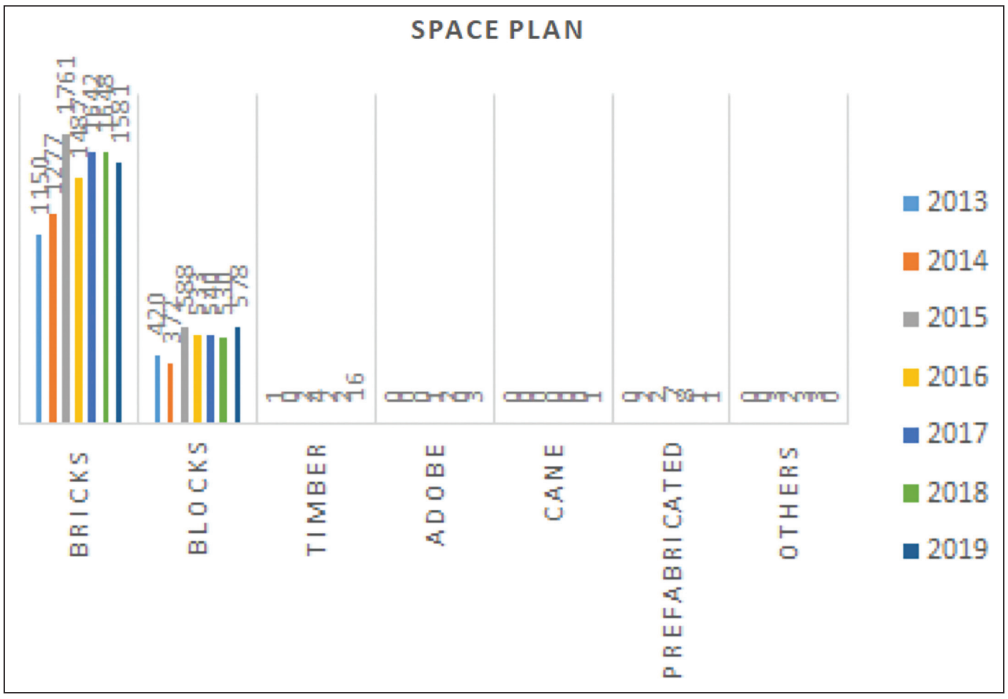

Figure 4. Space plan layer in Tungurahua from 2013 to 2019 [16].

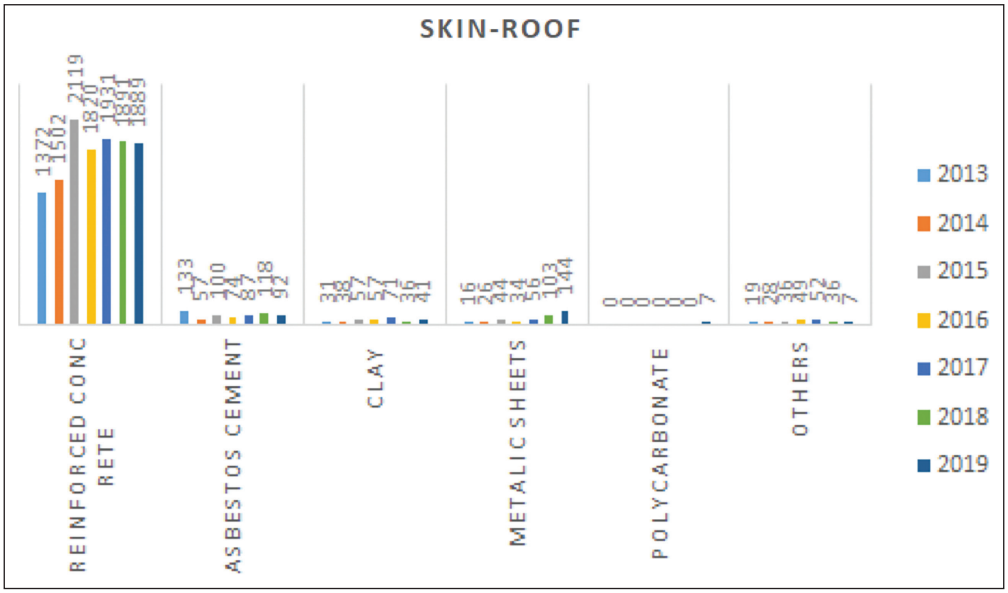

Figure 5. Skin layer in Tungurahua from 2013 to 2019 [16].

by bricks and blocks in most buildings, the use of timber, adobe, cane and prefabricated is not so common, as can be seen in Figure 4. The skin layer is conformed by reinforced concrete in most buildings, the use of asbestos cement, clay, metallic sheets and polycarbonate are not so common, as can be seen in Figure 5.

According to the report of predominant materials from INEC (2019) Tungurahua province has a total of 2180 buildings, from this total, reinforced concrete is the most common material used in foundation, structure and roofs, 1812 buildings used reinforced concrete in foundation, as can be seen in Figure 2; 1932 buildings used reinforced concrete in structure, as can be seen in Figure 3 and 1889 buildings used reinforced concrete in roofs, as can be seen in Figure 5. In the case of walls, 1581 buildings used bricks (apparently clay), then 578 buildings used blocks (apparently concrete), 16 buildings used wood, 3 earth, 1 used cane and 1 prefabricated components, as can be seen in Figure 4.

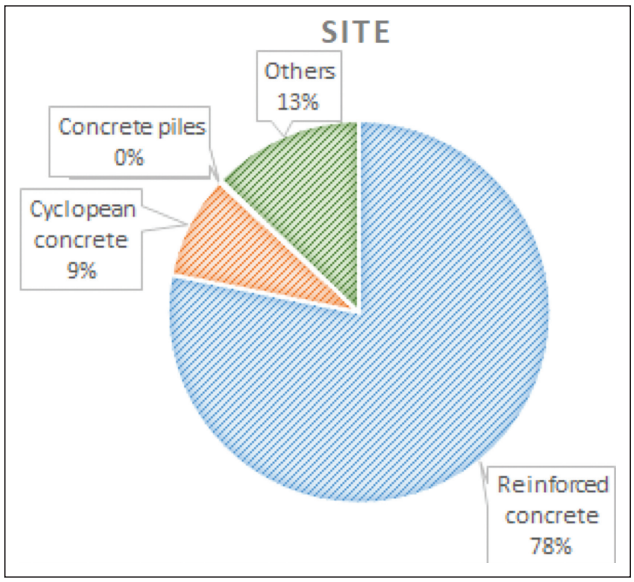

Figure 6. Percentage of buildings in Tungurahua according to the materials used in site layer from 2013 to 2019 [16].

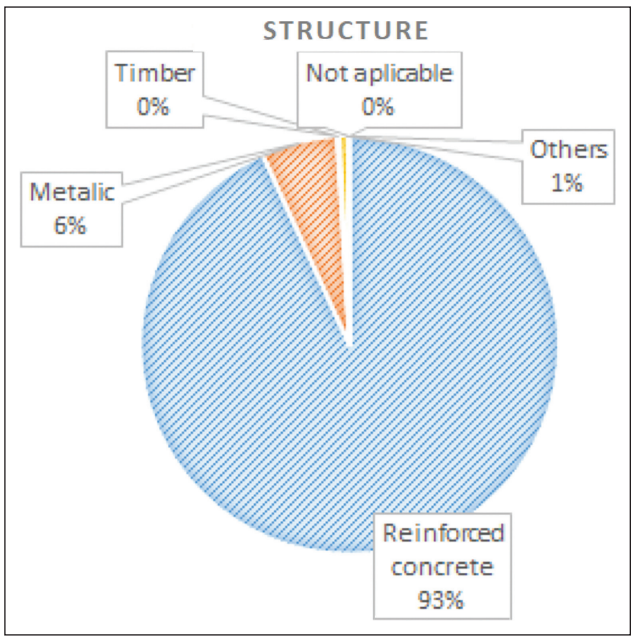

Figure 7. Percentage of buildings in Tungurahua according to the materials used in structure layer from 2013 to 2019 [16].

From 2013 to 2019, 14173 buildings have been created, in the site layer, 11076 buildings used reinforced concrete that represents 78%, just 1244 used cyclopean concrete representing 9% and other materials not specified represent 13%, as can be seen in Figure 6. In the structure layer, 13207 buildings were built using reinforced concrete, representing 93% and just 833 buildings used metallic structure representing 6%, as can be seen in Figure 7. In the space plan layer, 10546 buildings used bricks, representing 75% and 3561 buildings used blocks representing 25%, as

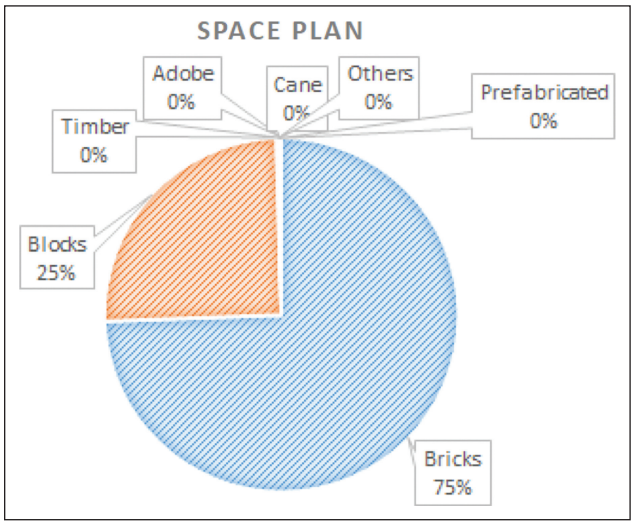

Figure 8. Percentage of buildings in Tungurahua according to the materials used in space plan layer from 2013 to 2019 [16].

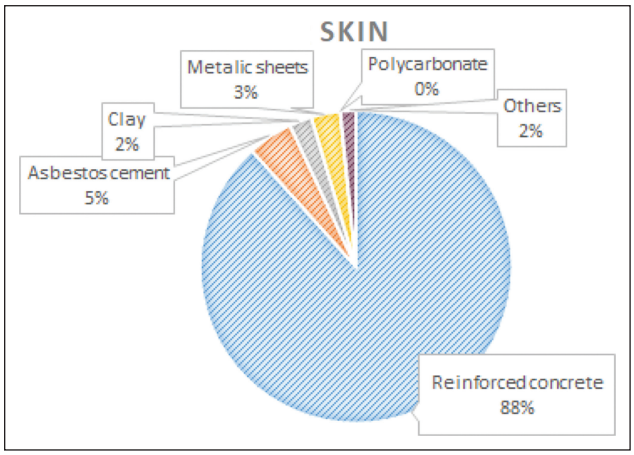

Figure 9. Percentage of buildings in Tungurahua according to the materials used in skin layer from 2013 to 2019 [16].

can be seen in Figure 8. Finally in the skin layer, 12524 buildings were built using reinforced concrete, represents 88% and just 661 buildings used asbestos cement, representing 5% and 423 metallic sheets, representing 3%. Clay and others materials represent 2% correspondingly, as can be seen in Figure 9.

For the stuff layer, 104 people contributed with the analysis, as can be seen in Figure 10. Figure 11 shows that 50% of floor recoverings are made of wood, then 21.2% has floating floor, 15.4% ceramics, 10.6% porcelain, 6.7% cement, 1.9% vinil and carpet 1%. Figure 12 shows that 99% of doors are made of wood, 1.9% metal and 1% glass. Figure 13 determines that 98.1% of furniture is made of wood, 1.9% metal and 1.9% plastic. Windows frames are mostly made of aluminium (58.7%), 26% are made of iron, 18.3% are made of wood and 1% of plastic, as can be seen in Figure 14.

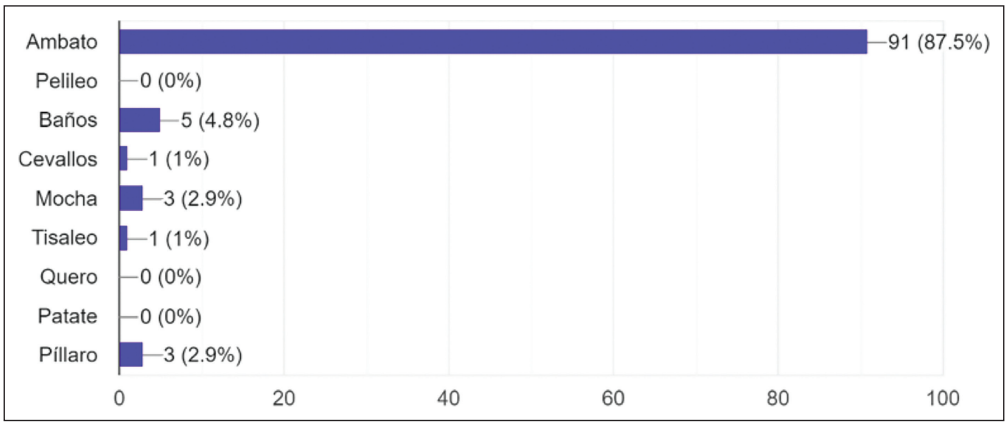

Figure 10. People in Tungurahua. Source: Online survey.

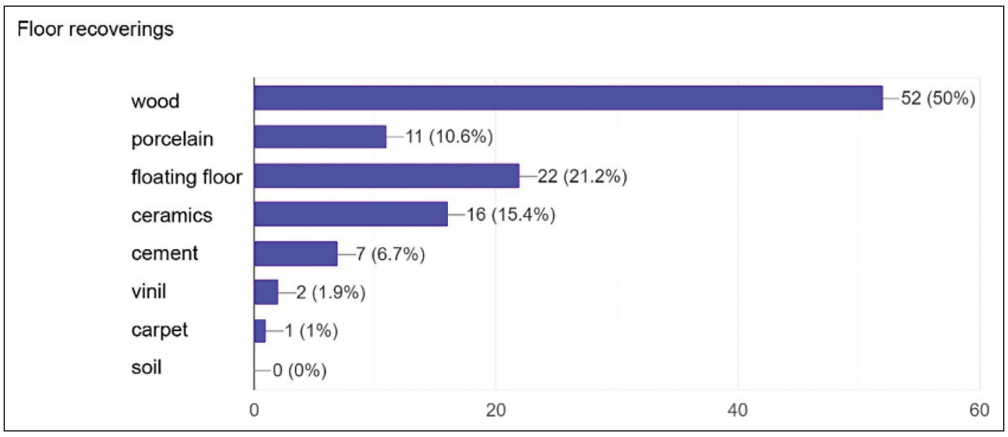

Figure 11. Floor covering in Tungurahua. Source: Online survey.

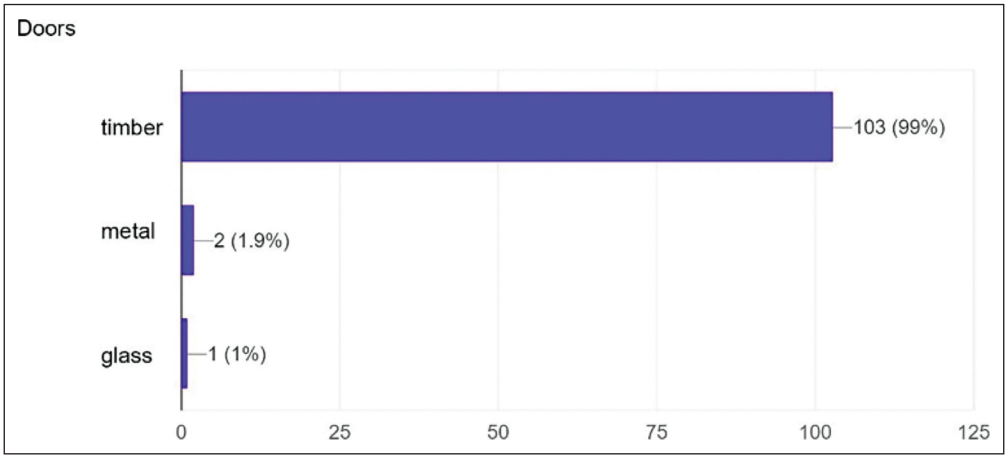

Figure 12. Doors in Tungurahua. Source: Online survey.

For behaviour tendencies the graphics show that most people do not waste any material from their homes, 51.9% do not throw away any element, 22.1% have wasted floor coverings, 15.4% furniture, 13.5% windows, 5.8% doors and 4.8 ceilings, as can be seen in Figure 15. Figure 16 shows that 38.5% would include second hand furniture, 37.5% prefer to not include any item, 19.2% doors, 11.5% windows, 10.6% floor covering, and 5.8% ceilings. Figure 17 shows that 49% of people would donate items, 41.3% will recycle, 20.2% sell and 15.4% will prefer interchanging.

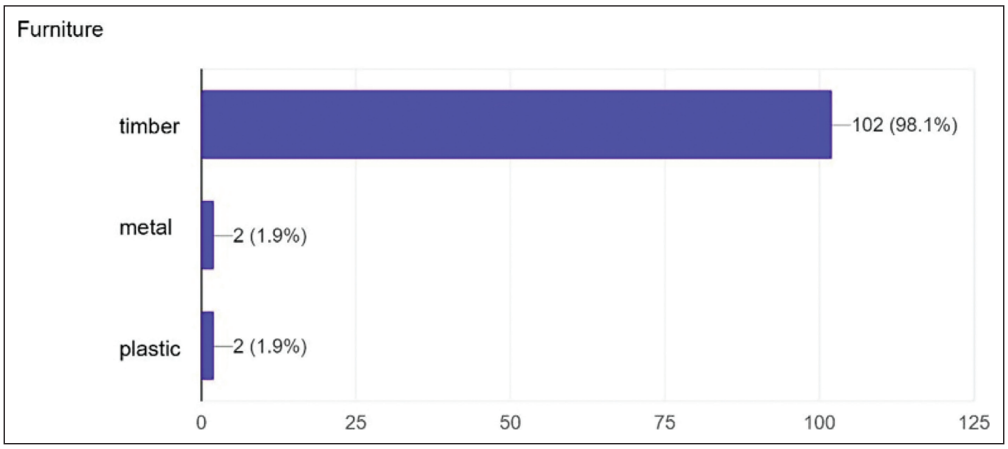

Figure 13. Furniture in dinning rooms in Tungurahua. Source: Online survey.

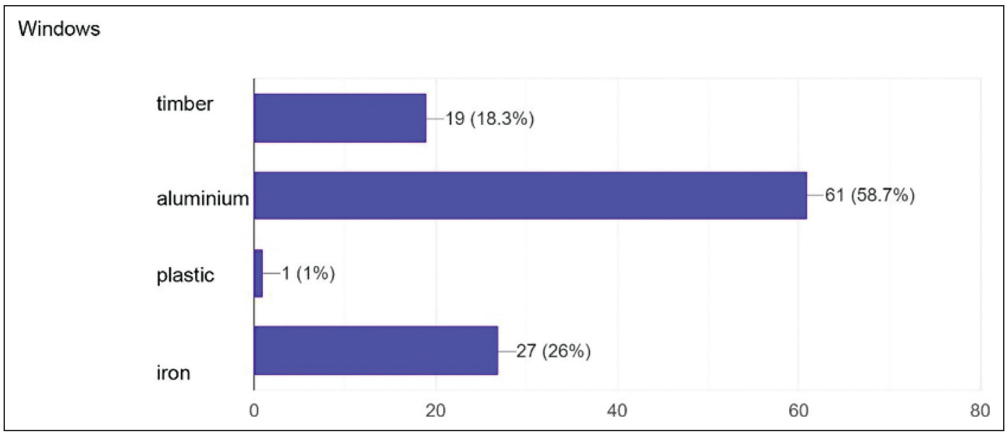

Figure 14. Frame windows in Tungurahua. Source: Online survey.

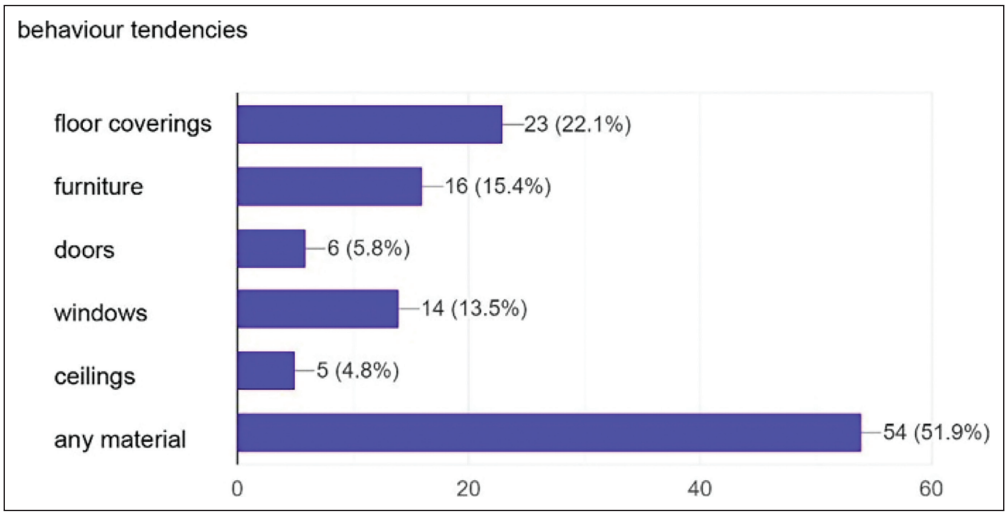

Figure 15. Elements wasted in Tungurahua. Source: Online survey.

DISCUSSION

There is no data related to the quantity of materials wasted, local government must know how much waste is being produced in order to size the capacity of any new disposal center. Nevertheless, the way that buildings are created could give a general background of what type of materials could be wasted in future, the construction sector defi-

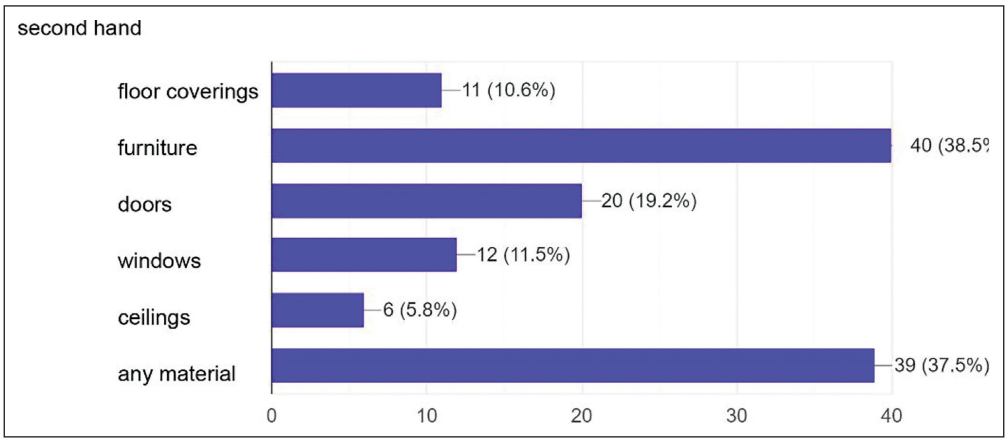

Figure 16. Elements that will be included in buildings in Tungurahua. Source: Online survey.

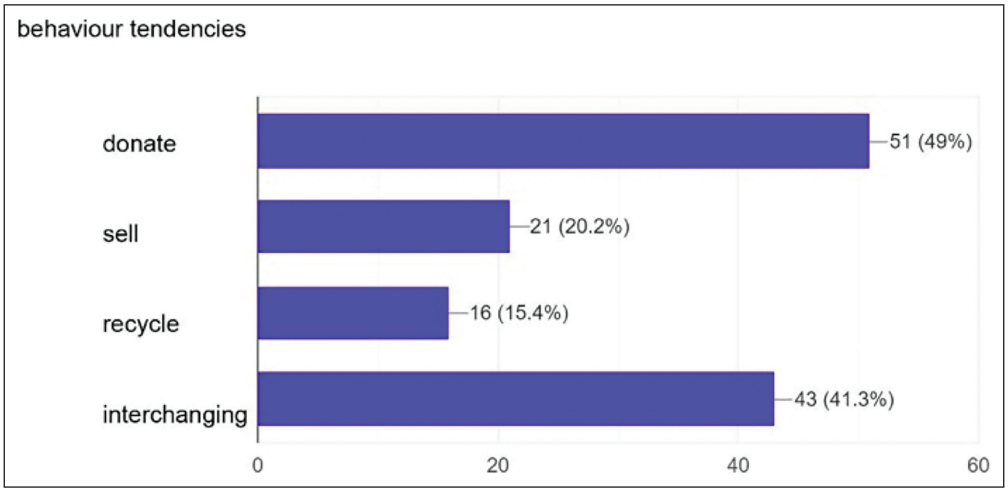

Figure 17. Actions instead waste in Tungurahua. Source: Online survey.

nitely has some re-usable and re-manufacturable materials such as timber elements from the stuff layer and some recyclable materials from site, structure and skin layers, the main goal will be to decipher when they are going to be available to the market.

The use of reinforced concrete as main material in foundation, structure and skin, and the use of bricks in space plan creates the possibility to introduce some centers for re-cycling into other elements such road bases [11]. Also, the use of timber elements as main element in the stuff layer in doors, furniture and floor coverings could allow implementing spaces for re-manufacturing and re-using.

CONCLUSIONS

From 2013 to 2019 the buildings in the Tungurahua province have as main material the reinforced concrete specially in the foundation (78%), structure (93%) and skin layers (88%), in the space plan layer the bricks (75%) and blocks (25%) are the principal materials used last years.

Timber floors (50%), doors (99%) and dinning furniture (98.1%) are the main elements inside households, in the case of windows frames there are made of aluminium in most buildings (58.7%). These elements could be considered as archetypes [13] in order to maintain building stocks.

On one hand, the fixed assembly of the reinforced concrete [14] founded in foundation, structure and skin layers makes uncapable to be easy recovered. On the other hand, timber floors, doors and furniture can generate a market for re-use of timber elements that include flexible and deconstruction strategies [6]. In the behavioural dimension [9], second hand furniture or donations could be promoted by implementing laws [7, 8].

More studies are needed to understand the design process of existing buildings and the possibilities for disassembly elements especially for the predominant timber elements in household. Moreover, another way to determine quantity of wasted materials and illegal debris disposals could be by addressing local recyclers. Finally, the stuff layer definition and behavioural dimension could include more people from other parts of the province.

DATA AVAILABILITY STATEMENT

The authors confirm that the data that supports the findings of this study are available within the article. Raw data that support the finding of this study are available from the corresponding author, upon reasonable request.

CONFLICT OF INTEREST

The authors declared no potential conflicts of interest with respect to the research, authorship, and/or publication of this article.

ETHICS

There are no ethical issues with the publication of this manuscript.

REFERENCES

[1] World Economic Forum, "Shaping the future of and technology a breakthrough in mindset construction," American Society of Civil Engineers, 1997. [CrossRef]

[2] Organizacion de las Naciones Unidas - Medio Am-biente (ONU Medio Ambiente), "Perspectiva de la Gestión de Residuos en América Latina y el Caribe Perspectiva de la Gestión de Residuos en Améri-ca Latina y el Caribe," 2018. https://www.unep. org/es/resources/informe/perspectiva-de-la-ges-tion-de-residuos-en-america-latina-y-el-caribe Ac-cessed on Nov 8, 2022.

[3] M. F. S. Torres, J. S. D. Cordero, J. L. S. Peláez, and M. A. Y. Fuentes, "Cartografía de los residuos sólidos en Ecuador 2020," Universidad Andina Simón Bolívar / GAIA / Acción Ecológica / Alianza Basura Cero Ecuador / VLIR-UOS / INEC, 2020.

[4] Ministerio del Ambiente, "Programa Nacional para la Gestión Integral de Desechos Sólidos (PNGIDS)," [En línea]. https://www.ambiente.gob.ec/wp-content/uploads/downloads/2020/07/5.PROYECTO-PNGIDS.pdf Accessed on Nov 8, 2022.

[5] Banco Central del Ecuador, "Cuentas Nacionales Regionales," https://contenido.bce.fin.ec/documentos/Estadisticas/SectorReal/CuentasCantonales/Indice.htm Accessed on Nov 4, 2022.

[6] K. T. Adams, M. Osmani, T. Thorpe, and J. Thornback, "Circular economy in construction: current awareness, challenges and enablers," Waste and Resource Management, Vol. 170(1), pp. 15–24, 2017. [CrossRef]

[7] C. J. Kibert, A. R. Chini, y L. Jennifer, "Deconstruction As an Essential Component of Sustainable Construction", CIB World Build. Congr., núm. April, pp. 1–11, 2001, [En línea]. https://www.irbnet.de/daten/iconda/CIB3122.pdf Accessed on Nov 8, 2022.

[8] F. Pomponi, and A. Moncaster, "Circular economy for the built environment: A research framework," Journal of Cleaner Production, Vol. 143, pp. 710–718, 2017. [CrossRef]

[9] P. Sassi, "Study of current building methods that enable the dismantling of building structures and their classifications according to their ability to be reused, recycled or downcycled," 2002. https://www.iisbe.org/iisbe/gbpn/documents/policies/research/products%20for%20re-use-sassi.pdf Accessed on Nov 8, 2022.

[10] L. C. M. Eberhardt, M. Birkved, and H. Birgisdottir, "Building design and construction strategies for a circular economy," Architectural Engineering and Design Management, Vol. 18(2), pp. 93–113, 2022. [CrossRef]

[11] A. Koutamanis, B. van Reijn, and E. van Bueren, "Urban mining and buildings: A review of possibilities and limitations," Resources, Conservation and Recycling, Vol. 138, pp. 32–39, 2018. [CrossRef]

[12] R. Cossu, and I. D. Williams, "Urban mining: Concepts, terminology, challenges," Waste Management, Vol. 45, pp. 1–3, 2015. [CrossRef]

[13] A. Stephan, and A. Athanassiadis, "Towards a more circular construction sector: Estimating and spatialising current and future non-structural material replacement flows to maintain urban building stocks," Resources, Conservation and Recycling, Vol. 129, pp. 248–262, 2018. [CrossRef]

[14] E. Durmisevic, "Transformable building structures: Design for dissassembly as a way to introduce sustainable engineering to building design & construction," [Doctoral Thesis], TU Delft, 2006.

[15] A. S. Nordby, "Salvageability of building materials: Reasons, criteria and consequences regarding architectural design that facilitate reuse and recycling," [Unpublished Doctoral Thesis], Norwegian University of Science and Technology, 2009.

[16] Instituto Nacional de Estadísticas y Censos, "Información de años anteriores – Edificaciones", https://www.ecuadorencifras.gob.ec/informacion-de-anos-anteriores-edificaciones/ Accessed on Nov 5,2022.

[17] S. Brand, "How Buildings Learn: What Happens After They're Built," Penguin Books, 1995.

Environ Res Tec, Vol. 5, Issue. 4, pp. 325–339, December 2022

Environmental Research and Technology
https://ert.yildiz.edu.tr - https://dergipark.org.tr/tr/pub/ert
DOI: https://doi.org/10.35208/ert.1070624

Environmental Research & Technology

Research Article

Characterization of high fluoride resistant *Pseudomonas aeruginosa* species isolated from water samples

Chellaiah EDWARD RAJA*, Ravi PANDEESWARI, Uthandakalaipandian RAMESH

Department of Molecular Biology, Madurai Kamaraj University School of Biological Sciences, Madurai, Tamil Nadu, India

ARTICLE INFO

Article history
Received: 10 February 2022
Revised: 28 September 2022
Accepted: 02 November 2022

Key words:
Antibiotic resistance; Fluoride resistant bacteria; Virulence genes

ABSTRACT

Groundwater fluoride contamination is one of the most serious toxicological environmental issues in India and around the world. Water samples were taken from Natham taluk and screened for fluoride resistant bacteria. Initially, twenty-four fluoride resistant colonies were selected from 50 mM NaF supplemented LB agar plates. On blood agar plates, all isolates showed β-haemolysis, confirming their status as pathogens. Virulence factors (*algD*, *plcH*, *toxA*, *gyrB*, *rhlC*, *lasB*) and biofilm-forming genes (*ppyR*, *pelA*, *pslA*) were identified in these isolates by PCR analysis. The fluoride ion transporter '*crcB*' was successfully amplified from these isolates by gene-specific PCR. Genus *Pseudomonas* and *P. aeruginosa* species-specific PCR analysis identified that all strains as belonging to the *P. aeruginosa* species. Besides, three high fluoride resistance strains were selected based on high fluoride resistance and confirmed as *P. aeruginosa* species by 16S rRNA sequencing and NCBI blast analysis.

Cite this article as: Edward Raja C, Pandeeswari R, Ramesh U. Characterization of high fluoride resistant *Pseudomonas aeruginosa* species isolated from water samples. Environ Res Tec 2022;5:4:325–339.

INTRODUCTION

Fluorine is the first element in the halogen group with the symbol 'F' [1]. Fluoride (F^-) exists in the groundwater due to natural or anthropogenic sources [2]. Fluorine occurs in nature as fluoride anion (F^-) in water. The natural sources of F^- are clay minerals, fluoride-bearing minerals and F^- replacing OH^- in the ferromagnesium silicates [3]. The industrial causes of F^- arise from phosphate-based fertilizer plants, mining operations and iron, glass, ceramics and oil refineries [4]. In drinking water, the allowable limit of fluoride is 1.5 mg/L fixed by the World Health Organization [5] and the Bureau of Indian Standards [6]. The F^- concentration in drinking water exceeds the permissible limit, it can lead to various health issues [7]. Pseudomonads are highly versatile and adapt to survive various environments [8, 9]. *P. aeruginosa* is ubiquitous, isolated from various water sources for example treated effluent wastewater [10], healthcare facilities [11, 12], municipal drinking water systems [13], and accommodation facilities [14], swimming pools [15] recreational water [16] and groundwater [17]. Several authors have investigated the F^- concentration in the Dindigul district's groundwater [18–22].

***Corresponding author.**
*E-mail address: edwardrajac@gmail.com

Table 1. The various oligonucleotide sequences used in the present study

Genes	Primer sequences (5'-3')	Anneal at °C	Size (bp)	References
PA-GS-F	GACGGGTGAGTAATGCCTA			[25]
PA-GS-R	CACTGGTGTTCCTTCCTATA	54	618	"
PA-SS-F	GGGGGATCTTCGGACCTCA			"
PA-SS-R	TCCTTAGAGTGCCCACCCG	58	956	"
GyrPA-398	CCTGACCATCCGTCGCCACAAC			[26]
GyrPA-620	CGCAGCAGGATGCCGACGCC	66	222	"
ETA1	GACAACGCCCTCAGCATCACCAGC			"
ETA2	CGCTGGCCCATTCGCTCCAGCGCT	66	397	"
algDF	ATGCGAATCAGCATCTTTGGT			[27]
algDR	CTACCAGCAGATGCCCTCGGC	55	1311	"
lasBF	GGAATGAACGAAGCGTTCTC			"
lasBR	GGTCCAGTAGTAGCGGTTGG	55	300	"
plcHF	GAAGCCATGGGCTACTTCAA			"
plcHR	AGAGTGACGAGGAGCGGTAG	55	307	"
rhlCF	ACCGGATAGACATGGGCGT			[28]
rhlCR	GCAGGCTGTATTCGGTGTC	61	570	"
pslA	TCCCTACCTCAGCAGCAAGC			[24]
pslAR	TGTTGTAGCCGTAGCGTTTCTG	65	656	"
pelAF	CATACCTTCAGCCATCCGTTCTTC			"
pelAR	CGCATTCGCCGCACTCAG	65	786	"
ppyF	CGTGATCGCCGCCTATTTCC			"
ppyR	ACAGCAGACCTCCCAACCG	65	160	"
FlucPF	AAGCTTATGTGGAAATCCATTCTCG			Present study
FlucPR	CTGCAGCTATTTGCCCAGCATCCA	66	384	"

In this work, water samples were taken from Natham taluk and isolate the F^- resistant bacteria, determine their F^- resistance, and assess the antibiotic susceptibility, investigate the presence of virulence genes profile and identify the F^- resistant gene '*crcB*' by gene specific PCR analysis.

MATERIALS AND METHODS

Isolation and Characterization of F^- Resistant Bacteria

Groundwater samples from borehole, handpump were taken from Natham Taluk, Tamilnadu, India. All the water samples were serially diluted and plated on LB agar (g/L): peptone 10, yeast extract 5, NaCl 10, agar 15 (HiMedia, Mumbai, India) plates added with 50 mM Sodium Fluoride (NaF). All the plates were incubated at 37 °C for 48 h incubation. After the duration, the selected resistant colonies transferred to selective chromogenic media like EMB (Eosin Methylene Blue) agar, MacConkey agar, and *Pseudomonas* isolation agar (HiMedia, Mumbai, India). All the plates were incubated at 37 °C for 24 h to check their growth. For this purpose, *P. aeruginosa* MTCC 2453 was used as the reference strain. Besides, F^- resistant isolates were identified with different characteristics.

Haemolysis

To determine the haemolytic activity, the selected F^- resistant isolates were streaked on blood agar plates (HiMedia, Mumbai, India) and kept at 37 °C for 24 h. After incubation, results were observed based on their haemolytic property.

Casein and Starch Hydrolysis

The selected F^- resistant isolates were streaked on Skim milk agar plates (HiMedia, Mumbai, India) and incubated at 37 °C for 24 h. The presence of a clear zone surrounding the colony indicated the proteolysis of casein. In this test *P. aeruginosa* MTCC 2453 was used as the reference strain. Starch hydrolysis was carried out with LB agar plates containing 1% starch and incubated at 37 °C for 24 h. Iodine crystals was used to confirm the starch hydrolysis test.

Determination of F– Resistance
The minimum inhibitory concentration (MIC) was determined on LB agar plates containing different concentrations of NaF. The concentration of NaF was used starting from 50 to 300 mM. MIC was evaluated until the selected isolates were unable to grow on F^- containing media. Based on this analysis, MIC was found at 37 °C in five days.

Antibiotic Resistance
Antibiotic resistance of F^- tolerant isolates was determined by the disc diffusion method. A sterile swab used for culture swabbing and 24 h broth culture was prepared as inoculum. The sterile antibiotic discs (HiMedia, Mumbai, India) were placed on the surface of MH (Muller Hinton) agar plates and incubated at 37 °C for 24 h. Twenty-Six antibiotics were used in this study is mentioned in Table 4 and 5. Antibiotic sensitivity was classified as resistant, intermediate or sensitive. The zone of inhibition (mm) was measured from each disc as suggested by Clinical & Laboratory Standards Institute (CLSI) and The European Union Committee on Antimicrobial Susceptibility Testing (EUCAST) guidelines.

Salt Tolerance
The salt tolerance of F^- resistant isolates was determined on LB agar plates supplemented with different concentrations of NaCl (Sodium Chloride). Based on an earlier report [23], the working concentration of NaCl selected from 0 to 18% (V/V) was prepared from 20% NaCl stock solution (W/V). The growth was monitored at 37 °C for 120 h.

Biofilm Production and Screening of Biofilm Forming Genes
Microtiter plate assay was used to check the biofilm production. The 1% inoculum was transferred to 96-well plate and incubated for 24 h at 37 °C. The biofilm formation is assessed into four ways 1. Non-adherent (0), 2. Weak (+), 3. Moderate (++) and 4. Strong (+++) production [24]. Tests were performed in 3 times. Besides, biofilm forming genes are identified by PCR using specific primers [24]. The primers detail is shown in Table 1. PCR was performed in Veriti 96 well thermal cycler and amplified products were separated on 2% agarose gel.

Virulence Genes Profile
The identification of virulence genes in fluoride resistant *Pseudomonas* was evaluated by PCR using gene-specific primers. The virulent factors 1) alginate (*algD*), 2) elastase (*lasB*), 3) haemolytic phospholipase (*plcH*), 4) rhamnolipid C (*rhlC*), 5) DNA gyrase (*gyrB*), and 6) exotoxin A (*toxA*) were used in this study. For this purpose, *P. aeruginosa* MTCC 2453 acted as the positive control. The priming details and annealing conditions are shown in Table 1.

Fluoride Resistant Gene Amplification
F^- resistant gene '*crcB*' was amplified using gene-specific primers, and genomic DNA was used as a template. The primers were designed to contain *Bam*HI and *Nco*I restriction sites used for the amplification of *crcB* gene. PCR was performed on a Veriti 96 well thermal cycler (Applied Biosystems, Foster City, CA, USA). The amplified PCR products were separated on 1.5% agarose gel electrophoresis.

Molecular Identification of *Pseudomonas* by PCR
In this study, PCR based assay was used for the identification and differentiation of *P. aeruginosa* from other *Pseudomonas* species [25]. The primer details are mentioned in Table 1. PCR was carried out in Veriti 96 well thermal cycler. The amplified PCR products were separated on 1.5% agarose gel electrophoresis.

PCR Amplification and 16S rRNA Sequencing
The 16S rRNA gene amplification was carried out Using the universal bacterial 16S rRNA primers, 27 F 5'-AGA GTT TGA TCM TGG CTC AG-3' and 1429 R 5'-CGGT TACC TTG TTA CGA CTT-3' in thermal cycler under the following cyclic conditions as follows: 95 °C for 5 min, 35 cycles of denaturation at 94 °C for 30 sec, annealing at 58 °C for 30 sec, extension at 72 °C for 1.5 min and final extension at 72 °C for 5 min. The polymerase chain reaction was performed in Veriti 96 well thermal cycler Applied Biosystems. Genomic DNA was used as template for PCR and products were separated on 1% agarose gel electrophoresis. The amplified PCR products were eluted by GeneJET gel extraction kit (ThermoScientific, USA) and then carried out for sequencing. The sequences obtained were compiled and compared to the sequences in the GenBank databases using BLAST analysis [29].

RESULTS AND DISCUSSION

Isolation and Characterization of F– Resistant Bacteria
Twenty-four colonies were selected from 50 mM NaF containing LB agar plates used for further studies. The selected isolates were grown on EMB and MacConkey agar plates, which may belong to Gram-negative bacteria. The biochemical characteristics and carbon utilization are listed in Tables 2 and 3. F– resistant isolates tested positive for the phenylalanine deamination test. All isolates utilized citrate and malonate and were involved in casein hydrolysis and production of glucose, xylose, and oxidase. Based on haemolysis, all strains exhibited a clear colourless zone surrounding the growing colonies and were found to have beta (β)- haemolytic activity. Based on morphological characteristics, the selected isolates were grown on specific selective media for *Pseudomonas*.

Table 2. Biochemical characteristics of F^- resistant isolates

Tests/ isolates	Blood agar	ONPG	Lysine utilization	Ornithine utilization	Urease	Phenylalanine deamination	Nitrate reduction	H_2S production	Citrate	VP test	Methyl red	Indole	Malonate utilization	Esculin hydrolysis	Oxidase	Starch hydrolysis	Casein hydrolysis
S6-2	β	N^-	N^-	N^-	N^-	P^+	N^-	N^-	P^+	N^-	N^-	N^-	P^+	N^-	P^+	N^-	P^+
S6-4	β	N^-	N^-	N^-	N^-	P^+	N^-	N^-	P^+	N^-	N^-	N^-	P^+	N^-	P^+	N^-	P^+
S15-6	β	N^-	N^-	N^-	N^-	P^+	N^-	N^-	P^+	N^-	N^-	N^-	P^+	N^-	P^+	N^-	P^+
S18	β	N^-	N^-	N^-	N^-	P^+	N^-	N^-	P^+	N^-	N^-	N^-	P^+	N^-	P^+	N^-	P^+
S6-6	β	N^-	N^-	N^-	N^-	P^+	N^-	N^-	P^+	N^-	N^-	N^-	P^+	N^-	P^+	N^-	P^+
S6-7	β	N^-	N^-	N^-	N^-	P^+	N^-	N^-	P^+	N^-	N^-	N^-	P^+	N^-	P^+	N^-	P^+
S29	β	N^-	N^-	N^-	N^-	P^+	N^-	N^-	P^+	N^-	N^-	N^-	P^+	N^-	P^+	N^-	P^+
S28-25	β	N^-	N^-	N^-	N^-	P^+	N^-	N^-	P^+	N^-	N^-	N^-	P^+	N^-	P^+	N^-	P^+
S6-1	β	N^-	N^-	N^-	N^-	P^+	N^-	N^-	P^+	N^-	N^-	N^-	P^+	N^-	P^+	N^-	P^+
S6-3	β	N^-	N^-	N^-	N^-	P^+	N^-	N^-	P^+	N^-	N^-	N^-	N^-	N^-	P^+	N^-	P^+
S6-5	β	N^-	N^-	N^-	N^-	P^+	N^-	N^-	P^+	N^-	N^-	N^-	P^+	N^-	P^+	N^-	P^+
S9-1	β	N^-	N^-	N^-	N^-	P^+	N^-	N^-	P^+	N^-	N^-	N^-	P^+	N^-	P^+	N^-	P^+
S9-2	β	N^-	N^-	N^-	N^-	P^+	N^-	N^-	P^+	N^-	N^-	N^-	P^+	N^-	P^+	N^-	P^+
S15	β	N^-	N^-	N^-	N^-	P^+	N^-	N^-	P^+	N^-	N^-	N^-	P^+	N^-	P^+	N^-	P^+
S15-1	β	N^-	N^-	N^-	N^-	P^+	N^-	N^-	P^+	N^-	N^-	N^-	P^+	N^-	P^+	N^-	P^+
S15-2	β	N^-	N^-	N^-	N^-	P^+	N^-	N^-	P^+	N^-	N^-	N^-	P^+	N^-	P^+	N^-	P^+
S15-3	β	N^-	N^-	N^-	N^-	P^+	N^-	N^-	P^+	N^-	N^-	N^-	P^+	N^-	P^+	N^-	P^+
S15-4	β	N^-	N^-	N^-	N^-	P^+	N^-	N^-	P^+	N^-	N^-	N^-	N^-	N^-	P^+	N^-	P^+
S15-5	β	N^-	N^-	N^-	N^-	P^+	N^-	N^-	P^+	N^-	N^-	N^-	N^-	N^-	P^+	N^-	P^+
S15'	β	N^-	N^-	N^-	N^-	P^+	N^-	N^-	P^+	N^-	N^-	N^-	P^+	N^-	P^+	N^-	P^+
S18-18	β	N^-	N^-	N^-	N^-	P^+	N^-	N^-	P^+	N^-	N^-	N^-	P^+	N^-	P^+	N^-	P^+
S19	β	N^-	N^-	N^-	N^-	P^+	N^-	N^-	P^+	N^-	N^-	N^-	P^+	N^-	P^+	N^-	P^+
S28-12	β	N^-	N^-	N^-	N^-	P^+	N^-	N^-	P^+	N^-	N^-	N^-	P^+	N^-	P^+	N^-	P^+
S28-27	β	N^-	N^-	N^-	N^-	P^+	N^-	N^-	P^+	N^-	N^-	N^-	P^+	N^-	P^+	N^-	P^+
MTCC	β	N^-	N^-	P^+	N^-	P^+	N^-	N^-	P^+	N^-	N^-	N^-	P^+	P^+	P^+	N^-	P^+

Table 3. Utilization of carbon sources by F^- resistant isolates

Tests/ isolates	Xyl.	Ado.	Rha.	Cell.	Mel.	Sacc.	Raff.	Tre.	Glu.	Lac.	Inu.	Sodium gluconate	Gly.	Sal.	Dul.	Ino.	Sor.	Mann.	Ado.	Ara.	Ery.	α Methyl D- Glucoside
S6-2	P^+	N^-	N^-	N^-	N^-	N^-	N^-	N^-	P^+	N^-	N^-	N^-	N^-	N^-	N^-	N^-	N^-	N^-	N^-	N^-	N^-	N^-
S6-4	P^+	N^-	N^-	N^-	N^-	N^-	N^-	N^-	P^+	N^-	N^-	N^-	N^-	N^-	N^-	N^-	N^-	N^-	N^-	N^-	N^-	N^-
S15-6	P^+	N^-	N^-	N^-	N^-	N^-	N^-	N^-	P^+	N^-	N^-	N^-	N^-	N^-	N^-	N^-	N^-	N^-	N^-	N^-	N^-	N^-
S18	P^+	N^-	N^-	N^-	N^-	N^-	N^-	N^-	P^+	N^-	N^-	N^-	N^-	N^-	N^-	N^-	N^-	N^-	N^-	N^-	N^-	N^-
S6-6	P^+	N^-	N^-	N^-	N^-	N^-	N^-	N^-	P^+	N^-	N^-	N^-	N^-	N^-	N^-	N^-	N^-	N^-	N^-	N^-	N^-	N^-
S6-7	P^+	N^-	N^-	N^-	N^-	N^-	N^-	N^-	P^+	N^-	N^-	N^-	N^-	N^-	N^-	N^-	N^-	N^-	N^-	N^-	N^-	N^-
S29	P^+	N^-	N^-	N^-	N^-	N^-	N^-	N^-	P^+	N^-	N^-	N^-	N^-	N^-	N^-	N^-	N^-	N^-	N^-	N^-	N^-	N^-
S28-25	P^+	N^-	N^-	N^-	N^-	N^-	N^-	N^-	P^+	N^-	N^-	N^-	N^-	N^-	N^-	N^-	N^-	N^-	N^-	N^-	N^-	N^-
S6-1	P^+	N^-	N^-	N^-	N^-	N^-	N^-	N^-	P^+	N^-	N^-	N^-	N^-	N^-	N^-	N^-	N^-	N^-	N^-	N^-	N^-	N^-
S6-3	P^+	N^-	N^-	N^-	N^-	N^-	N^-	N^-	P^+	N^-	N^-	N^-	N^-	N^-	N^-	N^-	N^-	N^-	N^-	N^-	N^-	N^-
S6-5	P^+	N^-	N^-	N^-	N^-	N^-	N^-	N^-	P^+	N^-	N^-	N^-	N^-	N^-	N^-	N^-	N^-	N^-	N^-	N^-	N^-	N^-
S9-1	P^+	N^-	N^-	N^-	N^-	N^-	N^-	N^-	P^+	N^-	N^-	N^-	N^-	N^-	N^-	N^-	N^-	N^-	N^-	N^-	N^-	N^-
S9-2	P^+	N^-	N^-	N^-	N^-	N^-	N^-	N^-	P^+	N^-	N^-	N^-	N^-	N^-	N^-	N^-	N^-	N^-	N^-	N^-	N^-	N^-
S15	P^+	N^-	N^-	N^-	N^-	N^-	N^-	N^-	P^+	N^-	N^-	N^-	N^-	N^-	N^-	N^-	N^-	N^-	N^-	N^-	N^-	N^-
S15-1	P^+	N^-	N^-	N^-	N^-	N^-	N^-	N^-	P^+	N^-	N^-	N^-	N^-	N^-	N^-	N^-	N^-	N^-	N^-	N^-	N^-	N^-
S15-2	P^+	N^-	N^-	N^-	N^-	N^-	N^-	N^-	P^+	N^-	N^-	N^-	N^-	N^-	N^-	N^-	N^-	N^-	N^-	N^-	N^-	N^-
S15-3	P^+	N^-	N^-	N^-	N^-	N^-	N^-	N^-	P^+	N^-	N^-	N^-	N^-	N^-	N^-	N^-	N^-	N^-	N^-	N^-	N^-	N^-
S15-4	P^+	N^-	N^-	N^-	N^-	N^-	N^-	N^-	P^+	N^-	N^-	N^-	N^-	N^-	N^-	N^-	N^-	N^-	N^-	N^-	N^-	N^-
S15-5	P^+	N^-	N^-	N^-	N^-	N^-	N^-	N^-	P^+	N^-	N^-	N^-	N^-	N^-	N^-	N^-	N^-	N^-	N^-	N^-	N^-	N^-
S15'	P^+	N^-	N^-	N^-	N^-	N^-	N^-	N^-	P^+	N^-	N^-	N^-	N^-	N^-	N^-	N^-	N^-	N^-	N^-	N^-	N^-	N^-
S18-18	P^+	N^-	N^-	N^-	N^-	N^-	N^-	N^-	P^+	N^-	N^-	N^-	N^-	N^-	N^-	N^-	N^-	N^-	N^-	N^-	N^-	N^-
S19	P^+	N^-	N^-	N^-	N^-	N^-	N^-	N^-	P^+	N^-	N^-	N^-	N^-	N^-	N^-	N^-	N^-	N^-	N^-	N^-	N^-	N^-
S28-12	P^+	N^-	N^-	N^-	N^-	N^-	N^-	N^-	P^+	N^-	N^-	N^-	N^-	N^-	N^-	N^-	N^-	N^-	N^-	N^-	N^-	N^-
S28-27	P^+	N^-	N^-	N^-	N^-	N^-	N^-	N^-	P^+	N^-	N^-	N^-	N^-	N^-	N^-	N^-	N^-	N^-	N^-	N^-	N^-	N^-
MTCC	P^+	N^-	N^-	N^-	N^-	N^-	N^-	N^-	P^+	N^-	N^-	N^-	N^-	N^-	N^-	N^-	N^-	N^-	N^-	N^-	N^-	N^-

Xyl: Xylose; Ado: Adonitol; Rha: Rhamnose; Cell: Cellobiose; Mel: Melibiose; Sacc: Saccharose; Raff: Raffinose; Tre: Trehalose; Glu: Glucose; Lac: Lactose; Inu: Inulin; Gly: Glycerol; Sal: Salicin; Dul: Dulcitol; Ino: Inositol; Sor: Sorbitol; Mann: Mannitol; Ara: Arabitol; Ery: Erythritol.

Table 4. Antibiotic sensitivity of F^- resistant isolates

DISC	mcg	S15-1	S15-2	S15-3	S15-4	S15-5	S15'	S9-1	S9-2	S18-18	S19	S28-27	S28-12	MTCC
Amikacin (AK)	30	28(S)	27(S)	23(S)	23(S)	29(S)	22(S)	23(S)	23(S)	22(S)	29(S)	23(S)	23(S)	18(S)
Amoxyclav (AMC)	30	NZ	NZ	NZ	NZ	NZ	NZ	NZ	NZ	NZ	NZ	NZ	NZ	NZ
Ampicillin (AMP)	10	NZ	NZ	NZ	NZ	NZ	NZ	NZ	NZ	NZ	NZ	NZ	NZ	NZ
Chloramphenicol (C)	30	13(I)	10(S)	10(S)	12(S)	14(I)	10(S)	10(S)	10(S)	13(I)	12(R)	9(R)	15(I)	13(I)
Ciprofloxacin (CIP)	5	35(S)	32(S)	31(S)	36(S)	37(S)	35(S)	36(S)	33(S)	33(S)	37(S)	36(S)	35(S)	32(S)
Cefoperazone (CPZ)	75	19(I)	22(S)	18(I)	20(I)	22(S)	20(I)	19(I)	18(I)	17(I)	15(R)	22(S)	22(S)	19(I)
Cefotaxime (CTX)	30	20(I)	20(I)	18(R)	18(R)	18(R)	18(R)	17(R)	19(R)	18(R)	19(R)	20(I)	21(I)	20(I)
Doxycycline-Hcl(DO)	30	NZ	NZ	NZ	NZ	16(S)	NZ	NZ	NZ	NZ	15(S)	NZ	NZ	NZ
Fosfomycin (FO)	200	NZ	NZ	NZ	NZ	NZ	NZ	NZ	NZ	NZ	NZ	NZ	NZ	NZ
Gentamycin (G)	10	33(S)	31(S)	24(S)	23(S)	31(S)	24(S)	25(S)	25(S)	27(S)	32(S)	26(S)	28(S)	19(S)
Imipenem (IPM)	10	32(S)	31(S)	29(S)	30(S)	30(S)	29(S)	30(S)	29(S)	29(S)	30(S)	31(S)	30(S)	25(S)
Kanamycin (K)	30	15(I)	17(I)	9(R)	8(R)	17(I)	9(R)	11(R)	12(R)	10(R)	18(R)	10(R)	12(R)	15(I)
Minocycline (MI)	30	16(S)	13(I)	11(R)	14(I)	16(S)	10(R)	11(R)	12(R)	11(R)	17(S)	12(R)	11(R)	NZ
Meropenem (MRP)	10	33(S)	29(S)	35(S)	35(S)	30(S)	35(S)	33(S)	34(S)	34(S)	33(S)	33(S)	34(S)	30(S)
Nalidixic Acid (NA)	30	NZ	NZ	NZ	NZ	NZ	NZ	NZ	NZ	NZ	NZ	NZ	NZ	NZ
Netillin (NET)	30	34(S)	31(S)	26(S)	26(S)	33(S)	26(S)	24(S)	25(S)	25(S)	34(S)	26(S)	24(S)	19(S)
Nitrofurantoin (NIT)	300	NZ	NZ	NZ	NZ	NZ	NZ	NZ	NZ	NZ	NZ	NZ	NZ	NZ
Norfloxacin (NX)	10	30	30(S)	30(S)	30(S)	32(S)	30(S)	31(S)	31(S)	29(S)	33(S)	31(S)	31(S)	27(S)
Piperacillin (PI)	100	25(S)	25(S)	22(S)	25(S)	25(S)	25(S)	24(S)	22(S)	21(S)	23(S)	22(S)	25(S)	23(S)
Streptomycin (S)	10	24(S)	25(S)	22(S)	13(S)	26(S)	14(S)	17(S)	15(S)	15(S)	28(S)	14(S)	18(S)	17(S)
Tetracycline (TE)	30	15(S)	15(S)	12(I)	16(S)	18(S)	15(S)	20(S)	18(S)	15(S)	19(S)	14(I)	15(S)	9(R)
Trimethoprim (TR)	10	NZ	NZ	NZ	NZ	NZ	NZ	NZ	NZ	NZ	NZ	NZ	NZ	NZ
Methicillin (MET)	5	NZ	NZ	NZ	NZ	NZ	NZ	NZ	NZ	NZ	NZ	NZ	NZ	NZ
Penicillin (P)	2	NZ	NZ	NZ	NZ	NZ	NZ	NZ	NZ	NZ	NZ	NZ	NZ	NZ
Rifampicin (RIF)	2	NZ	NZ	NZ	NZ	NZ	NZ	NZ	NZ	NZ	NZ	NZ	NZ	NZ
Vancomycin (VA)	10	NZ	NZ	NZ	NZ	NZ	NZ	NZ	NZ	NZ	NZ	NZ	NZ	NZ

NZ: No zone; R: Resistance; I: Intermediate; S: Sensitive.

Table 5. Antibiotic sensitivity of F^- resistant isolates

DISC	mcg	S6-2	S6-4	S6-6	S6-7	S15-6	S18	S29	S28-25	S6-1	S6-3	S6-5	S15	MTCC
Amikacin (AK)	30	17 (S)	16(I)	17(S)	17(S)	17(S)	24(S)	21(S)	18(S)	16(S)	18(S)	18(S)	22(S)	18(S)
Amoxyclav (AMC)	30	NZ	NZ	NZ	NZ	NZ	NZ	NZ	NZ	NZ	NZ	NZ	NZ	NZ
Ampicillin (AMP)	10	NZ	NZ	NZ	NZ	NZ	NZ	NZ	NZ	NZ	NZ	NZ	NZ	NZ
Chloramphenicol (C)	30	11(R)	14(I)	15(I)	12(I)	15(I)	12(I)	13(I)	13(I)	12(I)	14(I)	13(I)	14(I)	13(I)
Ciprofloxacin (CIP)	5	30(S)	30(S)	30(S)	29(S)	34(S)	35(S)	30(S)	30(S)	28(S)	31(S)	31(S)	34(S)	32(S)
Cefoperazone (CPZ)	75	20(I)	18(I)	19(I)	20(I)	20(I)	23(S)	21(S)	21(S)	18(I)	18(I)	18(I)	19(I)	19(I)
Cefotaxime (CTX)	30	19(R)	18(R)	19(R)	18(R)	18(R)	20(R)	14(R)	18(R)	19(R)	18(R)	19(R)	17(R)	20(R)
Doxycycline-Hcl (DO)	30	NZ	NZ	NZ	NZ	NZ	NZ	NZ	NZ	NZ	NZ	NZ	NZ	NZ
Fosfomycin (FO)	200	NZ	NZ	NZ	NZ	NZ	NZ	NZ	NZ	NZ	NZ	NZ	NZ	NZ
Gentamycin (G)	10	18(S)	18(S)	18(S)	18(S)	20(S)	27(S)	21(S)	18(S)	18(S)	18(S)	18(S)	23(S)	19(S)
Imipenem (IPM)	10	27(S)	26(S)	26(S)	28(S)	25(S)	30(S)	27(S)	26(S)	27(S)	26(S))	26(S)	28(S)	25(S)
Kanamycin (K)	30	9(R)	9(R)	9(R)	9(R)	8(R)	15(I)	13(S)	8(R)	9(R)	9(R)	9(R)	13(R)	15(I)
Minocycline (MI)	30	NZ	NZ	NZ	NZ	NZ	NZ	NZ	NZ	NZ	NZ	NZ	NZ	NZ
Meropenem (MRP)	10	34(S)	33(S)	33(S)	33(S)	33(S)	33(S)	33(S)	31(S)	35(S)	33(S)	34(S)	34(S)	30(S)
Nalidixic Acid (NA)	30	NZ	NZ	NZ	NZ	NZ	NZ	NZ	NZ	NZ	NZ	NZ	NZ	NZ
Netillin (NET)	30	18(S)	18(S)	18(S)	19(S)	19(S)	26(S)	23(S)	19(S)	19(S)	18(S)	18(S)	24(S)	19(S)
Nitrofurantoin (NIT)	300	NZ	NZ	NZ	NZ	NZ	NZ	NZ	NZ	NZ	NZ	NZ	NZ	NZ
Norfloxacin (NX)	10	27(S)	27(S)	27(S)	26(S)	27(S)	30(S)	26(S)	25(S)	27(S)	30(S)	27(S)	28(S)	27(S)
Piperacillin (PI)	100	23(S)	22(S)	21(S)	23(S)	22(S)	26(S)	22(S)	22(S)	23(S)	22(S)	23(S)	22(S)	23(S)
Streptomycin (S)	10	18(S)	17(S)	16(S)	16(S)	19(S)	22(S)	19(S)	14(S)	19(S)	19(S)	17(S)	22(S)	17(S)
Tetracycline (TE)	30	9(R)	NZ	9(R)	11(R)	10(R)	12(R)	10(R)	8(R)	8(R)	10(R)	10(R)	9(R)	9(R)
Trimethoprim (TR)	10	NZ	NZ	NZ	NZ	NZ	NZ	NZ	NZ	NZ	NZ	NZ	NZ	NZ
Methicillin (MET)	5	NZ	NZ	NZ	NZ	NZ	NZ	NZ	NZ	NZ	NZ	NZ	NZ	NZ
Penicillin (P)	2	NZ	NZ	NZ	NZ	NZ	NZ	NZ	NZ	NZ	NZ	NZ	NZ	NZ
Rifampicin (RIF)	2	NZ	NZ	NZ	NZ	NZ	NZ	NZ	NZ	NZ	NZ	NZ	NZ	NZ
Vancomycin (VA)	10	NZ	NZ	NZ	NZ	NZ	NZ	NZ	NZ	NZ	NZ	NZ	NZ	NZ

NZ: No zone; R: Resistance; I: Intermediate; S: Sensitive.

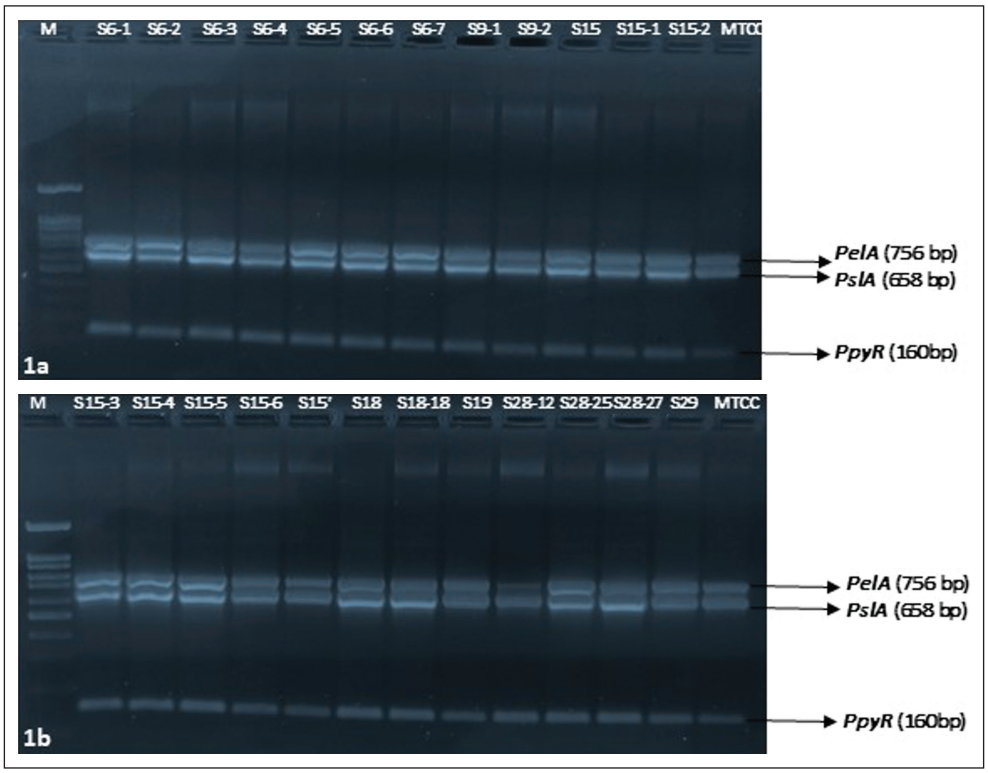

Figure 1. Detection of biofilm forming genes (*pslA*, *pelA*, *ppyR*) by PCR analysis. Lanes M: 100 bp DNA ladder RTU (Gene DireX); **(a)** Lanes (S6-1, S6-2, S6-3, S6-4, S6-5, S6-6, S6-7, S9-1, S9-2, S15, S15-1, S15-2) and **(b)** Lanes (S15-3, S15-4, S15-5, S15-6, S15, S18, S18-18, S28-12, S28-25, S28-2, S29) biofilm genes amplified by F– resistant isolates; Lanes MTCC: positive (+) control gene amplification by *P. aeruginosa* MTCC 2453.

Antibiotic Resistance

Fluoride tolerant isolates showed resistance to chloramphenicol, cefotaxime, doxycycline hydrochloride, fosfomycin, minocycline, nalidixic acid, nitrofurantoin, and trimethoprim (Tables 4, 5). In particularly, isolates S19, S15-5 was sensitive only to doxycycline hydrochloride. In other side, all isolates including positive controls were showed sensitive to gentamycin, imipenem, meropenem, netillin, and norfloxacin (Tables 4, 5). Similarly, many *Pseudomonas* species retrieved from water were resistant to various antimicrobial agents [30]. Moreover, *P. aeruginosa* showed resistance to amoxillin when isolated from sewage and sputum samples [31]. Recently, the WHO announced 12 species of waterborne antibiotic-resistant bacteria, including *Pseudomonas*, *Acinetobacter*, and various *Enterobacteriaceae*, which may cause a threat to human health [32]. According to the WHO report, we identified antibiotic-resistant *Pseudomonas* with fluoride tolerance that was isolated from water sources.

Salt Tolerance

The F^- resistant isolates were able to survive upto 5% NaCl (V/V) augmented LB agar plates. Similarly, Kirupa Sree et al. [33] reported that F^- resistant *Pseudomonas* strains THP6, THP41 and OPH5 grow upto 5% NaCl. In another study, F^- resistant isolates DWC1, DWC2 and DWC5 showed their tolerance only 2.5% and 4% NaCl [34]. But, F^- resistant *Bacillus flexus* NM25 showed upto 20% NaCl high salt tolerance was isolated from soil [23].

Biofilm Forming Genes

Tissue culture method is one of a standard method for biofilm detection [24]. Fluoride resistant isolates exhibited non-adherent, weak and moderate biofilm producer. The biofilm producing genes *ppyR*, *pslA* and *pelA* was present in these *Pseudomonas* isolates amplified by PCR analysis (Fig. 1a, b). Earlier these kinds of biofilm genes have been identified in the clinical isolates of *P. aeruginosa* [35]. Hou et al. [36] stated that no *P. aeruginosa* isolates were phenotypically positive for biofilm formation.

Virulence Profile of *Pseudomonas*

P. aeruginosa has secreted multiple virulence factors including EPS, lipopolysaccharides, elastases and proteases, lipases, exotoxin A, exoS, and type IV pili, rhamnolipids and pyocyanin production [37]. In this work, six different (*algD*, *gyrB*, *lasB*, *plcH*, *toxA*, *rhlC*) virulence factors were amplified by PCR (Fig. 2a–f). The gene "*gyrB*" gene PCR is one of the important target for the detection and identification of *P. aeruginosa* was isolated from water [38]. Under environmental stress conditions, *P. aeruginosa* able to secrete '*algD*' and '*lasB*' genes can influence

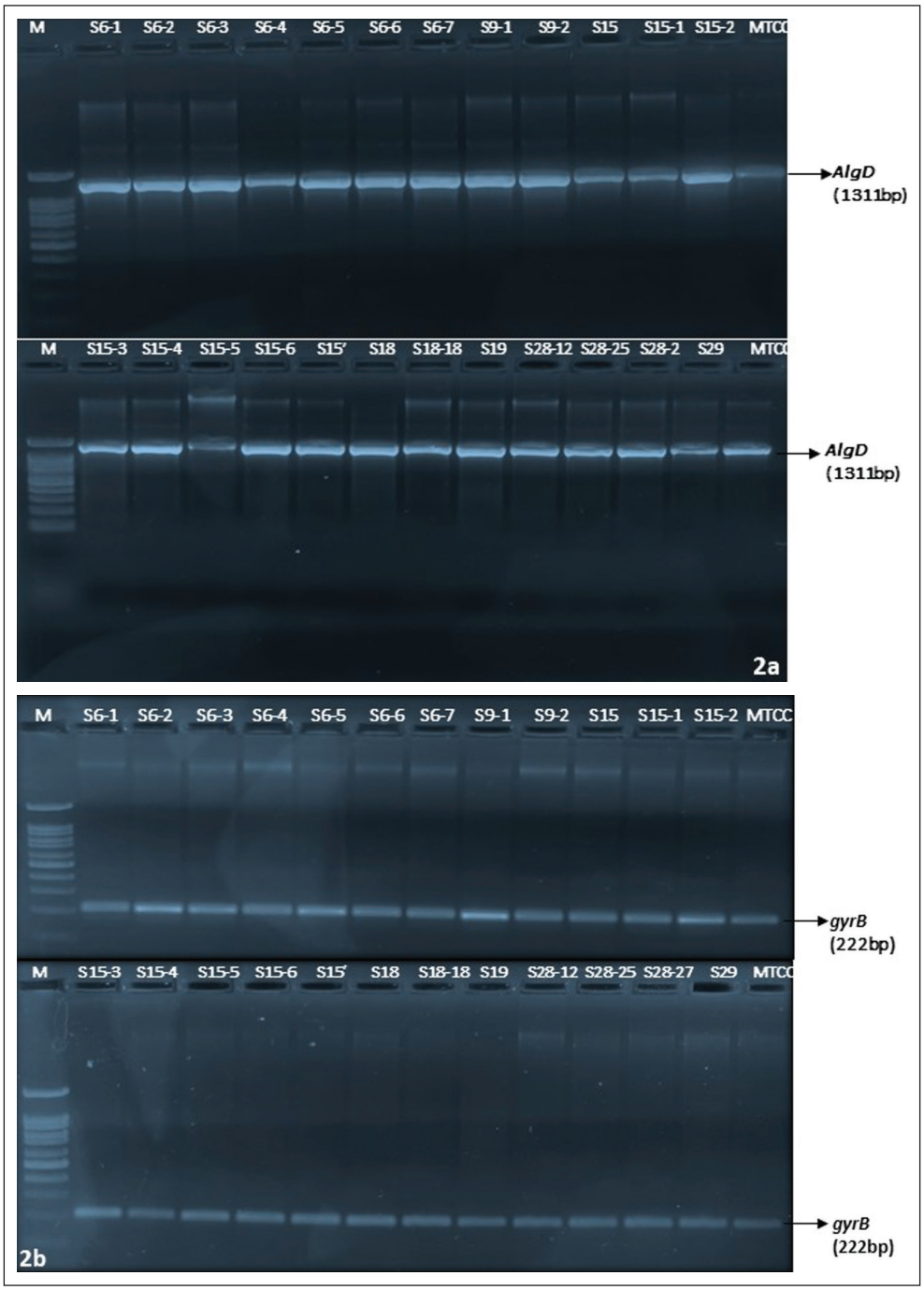

pathogenesis by enhancing adhesion, colonization, and invasion of tissues causing chronic pulmonary inflammation [27]. Likewise, Martins et al. [39] reported that the most common virulent genes (*algD*, *lasB*, and *plcH*) existing in *P. aeruginosa* were isolated from clinical and environmental origins.

Exotoxin A (*toxA*) was identified in this study. The '*toxA*' gene inhibits protein biosynthesis, and contributes to the colonization process [40]. In general, *rhlA*, *rhlB* and *rhlC* are key enzymes found in *Burkholderia* and *Pseudomonas* species responsible for rhamnolipid biosynthesis [41, 42]. In this study, we found only '*rhlC*' was amplified in these isolates by PCR (Fig. 2f).

Fluoride Resistant Gene Amplification

In *Pseudomonas* species, fluoride resistant gene was amplified using gene specific PCR. For this purpose, we designed the primers from the target sequence of *P. aeruginosa* AR_0111 was obtained from NCBI database. The 384 bp product was successfully amplified from *Pseudomonas* species (Fig. 3a, b).

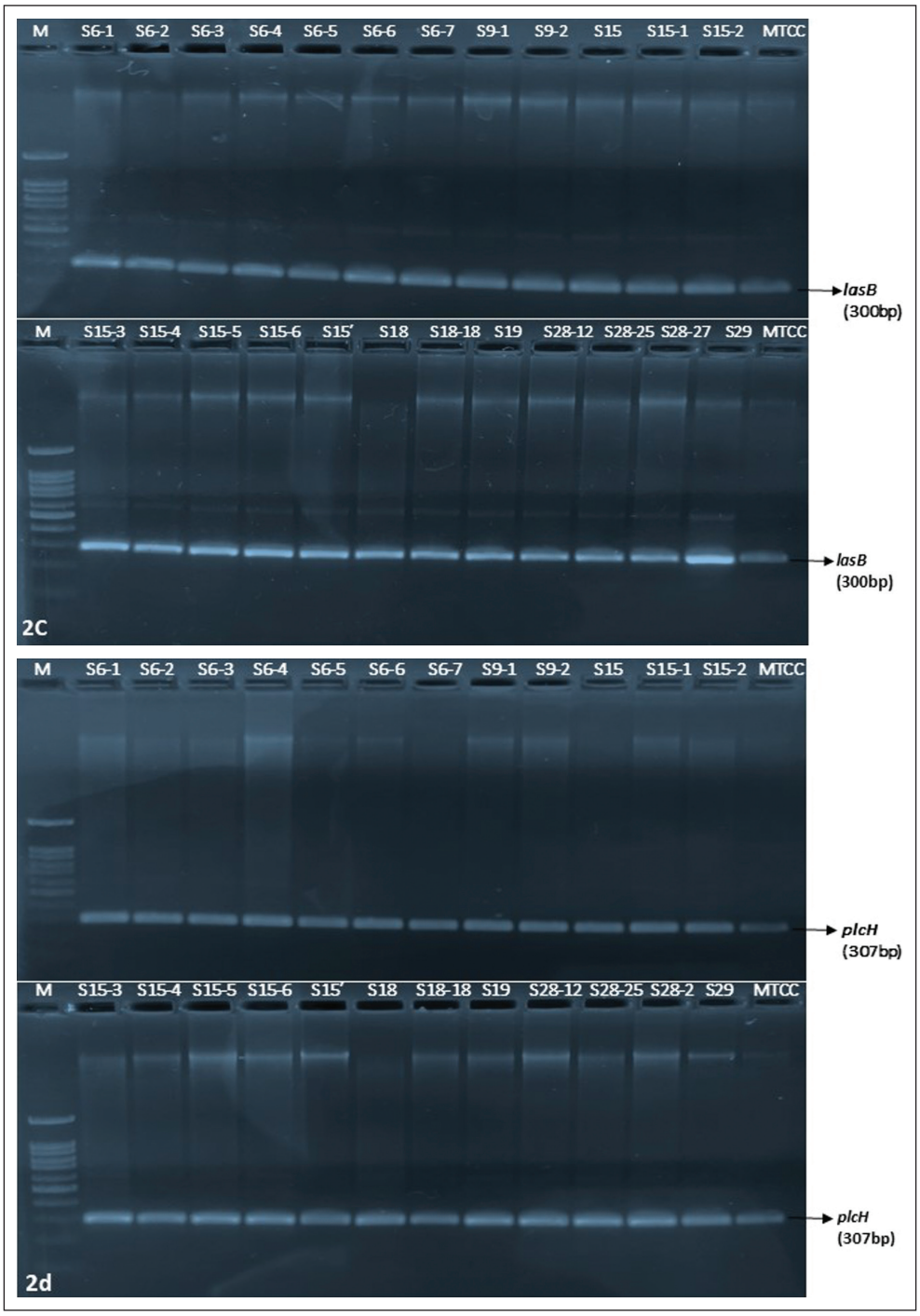

Confirmation of *Pseudomonas* by PCR

Two primers were used for the specific identification of genus *Pseudomonas* and *P. aeruginosa* species [25]. In this work, we amplified 618 bp fragment from fluoride resistant isolates and identified as *Pseudomonas* species (Fig. 4a). Besides, 956 bp fragment amplified from all isolates were further confirmed as *P. aeruginosa* (Fig. 4b). The 16S rDNA variable region and '*toxA*' coding gene PCR are simple, and rapid identification of environmental *P. aeruginosa* strains [43].

Selection of Potent Strains

In plate assay studies, all the *Pseudomonas* isolates were efficiently growing in 200 mM NaF containing LB agar plates. Further, three strains (S6-3, S15', and S28-25) were selected based on their growth performances on NaF-supplemented liquid media. The selected strains are able to tolerate 150 mM NaF in LB broth. Based on their growth performances in fluoride-containing liquid media, potent fluoride-resistant strains were selected for further identification.

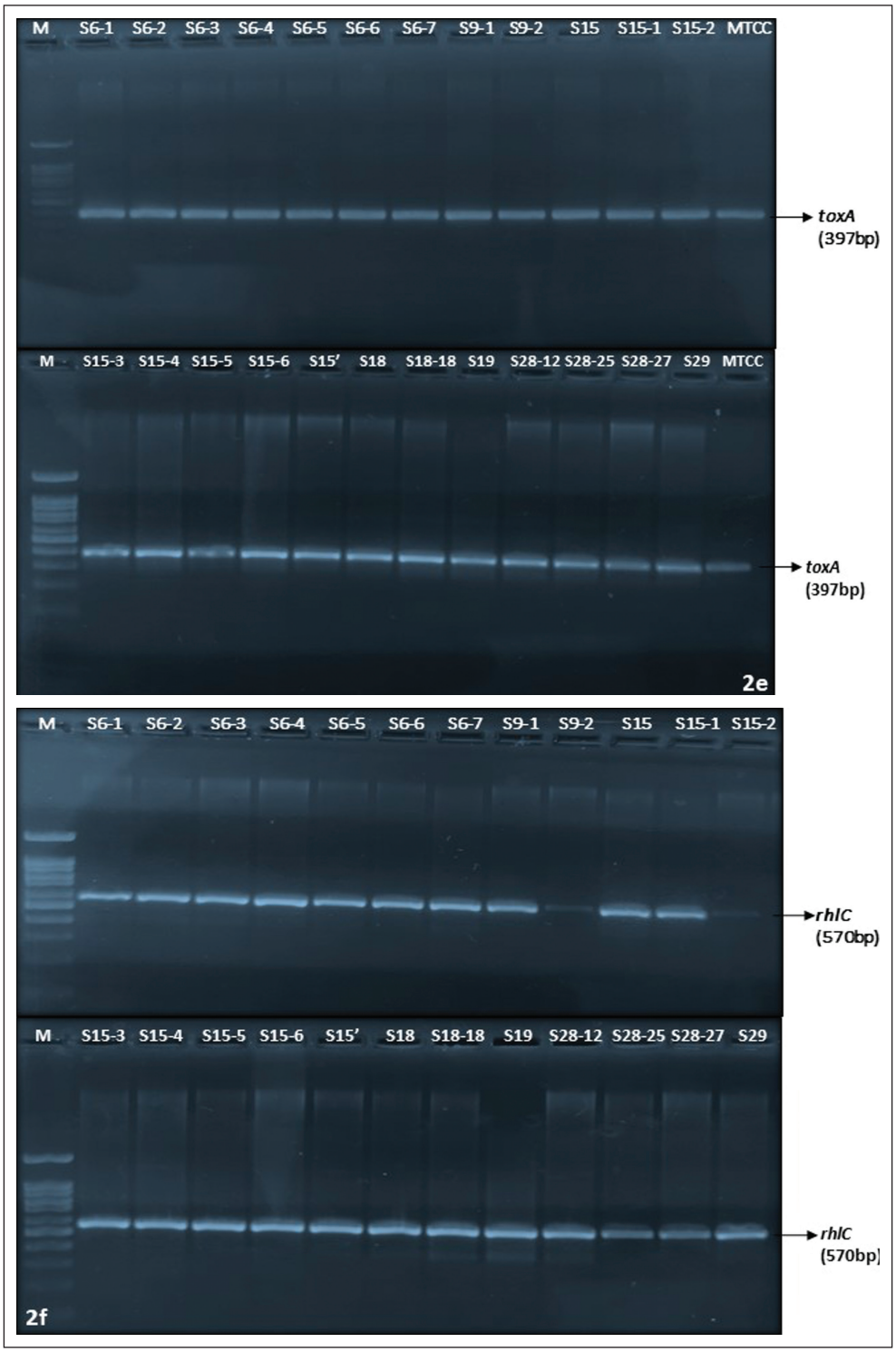

Figure 2. Virulence profile of F^- resistant *Pseudomonas* isolates. Lanes M: 100bp DNA ladder; lanes MTCC: (+) control *P. aeruginosa* 2453; The selected virulence genes **(a)** *algD* **(b)** *gyrB* **(c)** *lasB* **(d)** *plcH* **(e)** *toxA* **(f)** *rhlC* amplifications confirmed by gene specific primers.

16SrRNA Sequencing Analysis

Genomic DNA was extracted from these strains (S6-3, S15", S28-25) used as templates for PCR reactions. The 1.5 kb PCR products were successfully amplified from each isolate using 16S rRNA universal primers. The amplified products were gel excised and eluted by gel extraction kit (Thermofisher Scientific, USA). The purified PCR products was used as template for Sequencing process. The sequencing analysis was performed

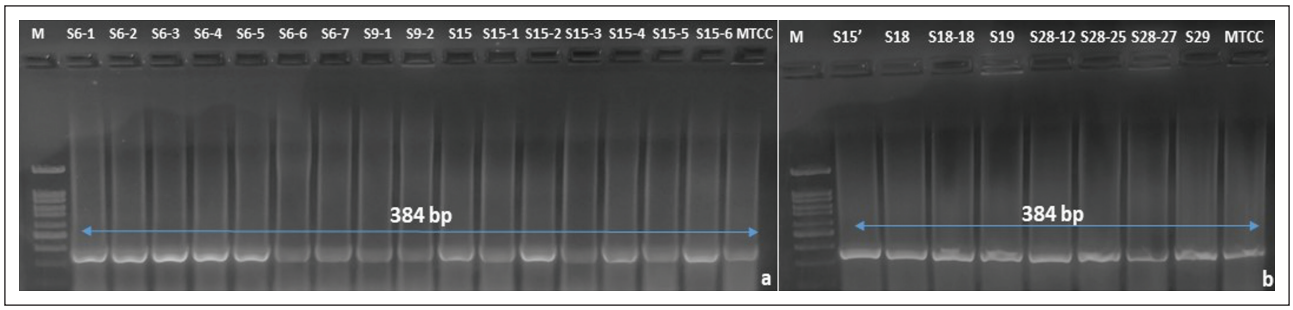

Figure 3. **(a, b)** The '*crcB*' gene amplification by F^- resistant *Pseudomonas* isolates. Lanes M: 100 bp DNA ladder; Lanes MTCC: (+) control *P. aeruginosa* 2453.

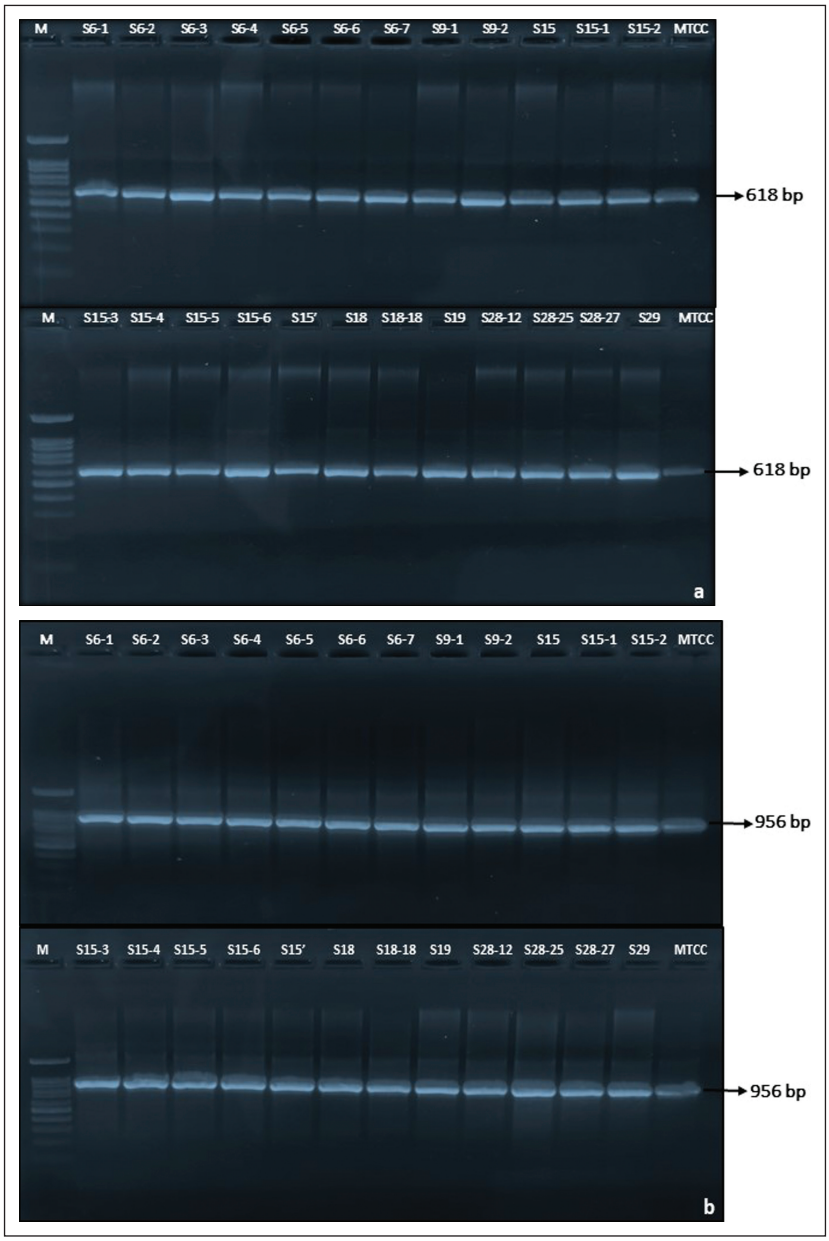

Figure 4. Genus and species-specific PCR analysis. **(a)** F^- resistant isolates amplified (618 bp) PCR products and identifying as genus *Pseudomonas*. **(b)** The PCR products (956 bp) shown by *Pseudomonas* isolates confirmed as *Pseudomonas aeruginosa* species. Lanes M: 100 bp DNA ladder; Lanes MTCC: (+) control *P. aeruginosa* 2453.

in AgriGenome Pvt Ltd, Cochin, Kerala. Comparative analysis of the 16S rRNA sequences with already available database showed that the selected isolates were closed to the family of Pseudomonadaceae. The present result also coincides with previous studies have shown that *Pseudomonas* was one of the bacterial species commonly found in groundwater [44].

Earlier studies shown that various F– resistant bacterial species isolated from various environment regimens [33, 34, 45–48]. In this study, *Pseudomonas* was recognized as F– resistant bacteria confirmed by genus, species-specific PCR and 16S rRNA sequencing analysis.

CONCLUSIONS

Genus, species-specific PCR, 16S rRNA sequencing and blast analysis concluded that twenty-two F– resistant strains were identified as *Pseudomonas* species. All the strains showed 200 mM NaF resistance determined in LB agar plates. They exhibited β-haemolytic activity on blood agar plates. Virulence genes and biofilm-forming genes were present in these isolates confirmed by Gene-specific PCR analysis. In addition, β-haemolytic *Pseudomonas* showed resistance to multiple antibiotics evidenced by a disc diffusion method. We identified the *crcB* domain in *Pseudomonas* using gene-specific primers. In near future, genetically modified fluoride resistant bacteria will be used in fluoride bioremediation studies.

FUNDING

This work was supported by grant from Science and Engineering Research Board (SERB), DST, New Delhi, India, Ramanujan Fellowship to C. Edward Raja (Award No:SB/S2/RJN-009/2016).

DATA AVAILABILITY STATEMENT

The authors confirm that the data that supports the findings of this study are available within the article. Raw data that support the finding of this study are available from the corresponding author, upon reasonable request.

CONFLICT OF INTEREST

The authors declared no potential conflicts of interest with respect to the research, authorship, and/or publication of this article.

ETHICS

There are no ethical issues with the publication of this manuscript.

REFERENCES

[1] W. M. Edmunds and P.L. Smedley, "Fluoride in natural waters," In O. Selinus (Eds.), Essentials of medical geology. Springer. pp. 311–336, 2001. [CrossRef]

[2] Meenakshi, and R. C. Maheshwari, "Fluoride in drinking water and its removal", Journal of Hazardous Materials, Vol.137(1), pp. 456–463, 2006. [CrossRef]

[3] R. K. Dey, S. K. Swain, S. Mishra, P. Sharma, T. Patnaik, V. K. Singh, B. N. Dehury, U. Jha, and R. K. Patel, "Hydrogeochemical processes controlling the high fluoride concentration in ground-water: A case study at the Boden block area, Orissa, India," Environmental Monitoring and Assessment, Vol. 184, pp. 3279–3291, 2012. [CrossRef]

[4] H. N. Bhattacharya, and S. Chakrabarti, "Incidence of fluoride in the groundwater of Purulia District, West Bengal: a geo-environmental appraisal," Current Science, Vol. 101(2), pp. 152–155, 2011.

[5] World Health Organization, "Guidelines for drinking-water Quality," (4th ed.), World Health Organization, 2011.

[6] (BIS) Bureau of Indian Standards. "Drinking Water-Specification, IS 10500 Second Revision," 2012. Accessed on Nov 15, 2022. http://cgwb.gov.in/Documents/WQ-standards.pdf

[7] H. Liu, S. Deng, L. Zhijian, G. Yu, and J. Huang, "Preparation of Al–Ce hybrid adsorbent and its application for defluoridation of drinking water," Journal of Hazardous Materials, Vol. 179(1-3), pp. 424–430, 2010. [CrossRef]

[8] K. D. Mena, and C. P. Gerba, "Risk assessment of *Pseudomonas aeruginosa* in water," Reviews in Environmental and Contamination Toxicology, Vol. 201, pp. 71–115, 2009. [CrossRef]

[9] C. Edward Raja, "Cadmium (heavy metals) bioremediation by *Pseudomonas aeruginosa*: a minireview," Applied Water Science, Vol. 8, Article 154, 2018. [CrossRef]

[10] C. Edward Raja, K. Anbazhagan and G. S. Selvam, "Isolation and characterization of a metal resistant *Pseudomonas aeruginosa* strain. World Journal of Microbiology & Biotechnology, Vol. 22, pp. 577–585, 2006. [CrossRef]

[11] A. Lefebvre, X. Bertrand, C. Quantine, P. Vanhems, J. C. Lucet, G. Nuemi, K. Astruc, P. Chavanet, and L. S. Aso-Glele, "Association between *Pseudomonas aeruginosa* positive water samples and healthcare-associated cases: nine-year study at one university hospital", The Journal of Hospital Infection, Vol. 96, pp. 238–243, 2017. [CrossRef]

[12] E. J. Anaissie, S. R. Penzak, M. C. Dignani, "The hospital water supply as a source of nosocomial infections: a plea for action," Achieves of Internal Medicine, Vol. 162, pp. 1483–1492, 2002. [CrossRef]

[13] T. Felföldi, T. Tarnóczai, and Z. G. Homonnay, "Presence of potential bacterial pathogens in a municipal drinking water supply system," Acta Microbiologica et Immunologica Hungarica, Vol. 57, pp.165–179, 2010. [CrossRef]

[14] S. Huhulescu, M. Simon, M. Lubnow, M. Kaase, G. Wewalka, A. T. Pietzka, A. Stoger, W. Ruppitsch, and F. Allerberger, "Fatal *Pseudomonas aeruginosa* pneumonia in a previously healthy woman was most likely associated with a contaminated hot tub," Infection, Vol. 39(3), pp. 265–269, 2011. [CrossRef]

[15] M. Guida, V. Di Onofrio, F. Gallè, R. Gesuele, F. Valeriani, R. Liguori, V. R. Spica, and G. Liguori, "*Pseudomonas aeruginosa* in swimming pool water: Evidences and perspectives for a new control strategy," International Journal of Environmental Research and Public Health, Vol. 13(9), Article 919, 2016. [CrossRef]

[16] G. Amagliani, M. L. Parlani, G. Brandi, G. Sebastianelli, V. Stocchi, and G. F. Schiavano, "Molecular detection of *Pseudomonas aeruginosa* in recreational water," International Journal of Environmental Health Research, Vol. 22(1), pp. 60–70, 2012. [CrossRef]

[17] E. R. Chellaiah, P. Ravi, and R. Uthandakalaipandian, "High fluoride resistance and virulence profile of environmental *Pseudomonas* isolated from water sources," Folia Microbiologica, Vol. 66, pp. 569–578, 2021. [CrossRef]

[18] G. Viswanathan, S. Gopalakrishnan, and S. Siva Ilango, "Assessment of water contribution on total fluoride intake of various age groups of people in fluoride endemic and non-endemic areas of Dindigul District, Tamil Nadu, South India", Water Research, Vol. 44, pp. 6186–6200, 2010. [CrossRef]

[19] S. Chidambaram, M. Bala Krishna Prasad, R. Manivannan, U. Karmegam, C. Singaraja, P. Anandhan, M.V. Prasanna, and S. Manikandan, "Environmental hydrogeochemistry and genesis of fluoride in groundwaters of Dindigul district, Tamilnadu (India)," Environmental Earth Sciences, Vol. 68, pp.333–342, 2013. [CrossRef]

[20] S. Selvam, S. Venkatramanan, S. Y. Chung, and C. Singaraja, "Identification of groundwater contamination sources in Dindugal district of Tamil Nadu, India using GIS and multivariate statistical analyses," Arabian Journal of Geosciences, Vol. 9, Article 407, 2016. [CrossRef]

[21] T. S. R. Umamageswari, D. Sarala, Thambavani, and M. Liviu, "Hydrogeochemical processes in the groundwater environment of Batlagundu block, Dindigul district, Tamil Nadu: conventional graphical and multivariate statistical approach," Applied Water Science, Vol. 9, Article 14, 2019. [CrossRef]

[22] C. Edward Raja, R. Pandeeswari, and U. Ramesh, "Isolation and identification of high fluoride resistant bacteria from water samples of Dindigul district, Tamil Nadu, South India," Current Research in Microbial Sciences, Vol. 2, pp. Article 100038, 2022. [CrossRef]

[23] K. C. Pal, N. K. Mondal, S. Chatterjee, T. H. Ghosh, and J. K. Datta, "Characterization of fluoride-tolerant halophilic *Bacillus flexus* NM25 (HQ875778) isolated from fluoride affected soil in Birbhum District, West Bengal, India," Environmental Monitoring Assessment, Vol. 186, pp. 699, 709, 2014. [CrossRef]

[24] A. Pournajaf, S. Razavi, G. Irajian, A. Ardebili, Y. Erfani, S. Solgi, S. Yaghoubi, A. Rasaeian, Y. Yahyapour, R. Kafshgari, S. Shoja, and R. Rajabnia, "Integron types, antimicrobial resistance genes, virulence gene profile, alginate production and biofilm formation in Iranian cystic fibrosis *Pseudomonas aeruginosa* isolates," Infezioni in Medicina, Vol. 26, pp. 226–236, 2018.

[25] T. Spilker, T. Coenye, P. Vandamme, and J. J. LiPuma, "PCR-based assay for differentiation of *Pseudomonas aeruginosa* from other *Pseudomonas* species recovered from cystic fibrosis patients," Journal of Clinical Microbiology, Vol. 42, pp. 2074–2079, 2004. [CrossRef]

[26] S. M. Mulamattathil, C. Bezuidenhout, M. Mbewe, and C. N. Ateba, "Isolation of environmental bacteria from surface and drinking water in Mafikeng, South Africa, and characterization using their antibiotic resistance profiles," Journal of Pathogens, Vol. 2014, Article 371208, 2014. [CrossRef]

[27] P. Lanotte, S. Watt, L. Mereghetti, N. Dartiguelongue, A. Rastegar-Lari, A. Goudeau, and R. Quentin, "Genetic features of *Pseudomonas aeruginosa* isolates from cystic fibrosis patients compared with those of isolates from other origins," Journal of Medical Microbiology, Vol. 53, pp. 73–81, 2004. [CrossRef]

[28] A. Perfumo, I. B. Banat, F. Canganella, and R. Marchant, "Rhamnolipid production by a novel thermophilic hydrocarbon-degrading *Pseudomonas aeruginosa* AP02-1", Applied Microbiology and Biotechnology, Vol. 32, pp. 132–138, 2006. [CrossRef]

[29] S. F. Altschul, T. L. Maddan, A. A. Schaffer, J. Zang, Z. Zang, W. Miller, and D. J. Lipman, "Gapped BLAST and PSI-BLAST: a new generation of protein database search programs," Nucleic Acids Research, Vol. 25, pp. 3389–3402, 1997. [CrossRef]

[30] H. Hernandez-Duquino, and F. A. Rosenberg, "Antibiotic resistant *Pseudomonas* in bottled drinking water," Canadian Journal of Microbiology, Vol. 33, pp. 286–289, 1987. [CrossRef]

[31] A. A. J. Aljanaby, "Antibiotics susceptibility pattern and virulence-associated genes in clinical and environment strains of *Pseudomonas aeruginosa* in Iraq," Asian Journal of Scientific Research, Vol. 11, pp. 401–408, 2018. [CrossRef]

[32] World Helath Organization, "Global priority of antibiotic-resistant bacteria to guide research, discovery, and development of new antibiotics," World Helath Organization. pp. 1–7, 2017.

[33] K. Kirupa Sree, C. Edward Raja, and U. Ramesh, "Isolation and characterization of fluoride resistant bacteria from ground waters in Dindigul, Tamil Nadu, India," Environmental Research and Technology, Vol. 1, pp. 69–74, 2018.

[34] S. Sharma, D. Upadhyay, B. Singh, D. Shrivastava, N.M. Kulshreshtha, "Defluoridation of water using autochthonous bacterial isolates," Environmental Monitoring Assessment, Vol. 191, pp. 781, 2019. [CrossRef]

[35] A. Ghadaksaz A.A.I. Fooladi H.M. Hosseini and M. Amin, "The prevalence of some *Pseudomonas* virulence genes related to biofilm formation and alginate production among clinical isolates", Journal of Applied Biomedicine, Vol. 13, pp. 61-68, 2015. [CrossRef]

[36] W. Hou, X. Sun, Z. Wang, and Y. Zhang, "Biofilm-forming capacity of Staphylococcus epidermidis, Staphylococcus aureus, and *Pseudomonas aeruginosa* from ocular infections biofilm-forming capacity of human flora bacteria. Investigative Ophthalmology & Visual Science, Vol. 53, pp. 5624–5631, 2012. [CrossRef]

[37] A. Pitondo-Silva, G.B. Goncalves, and E.G. Stehling, "Heavy metal resistance and virulence profile in *Pseudomonas aeruginosa* isolated from Brazilian soils," APMIS, Vol. 124, pp. 681–688, 2016. [CrossRef]

[38] C. S. Lee, K. Wetzel, T. Buckley, D. Wozniak, and J. Lee, "Rapid and sensitive detection of *Pseudomonas aeruginosa* in chlorinated water and aerosols targeting gyrB gene using real-time PCR," Journal of Applied Microbiology, Vol. 111, pp. 893–903, 2011. [CrossRef]

[39] V.V. Martins, A. Pitondo-Silva, M. Manco Lde, J. P. Falcao, S. S. Freitas, W. D. da Silveira, and E. G. Stehling, "Pathogenic potential and genetic diversity of environmental and clinical isolates of *Pseudomonas aeruginosa*," APMIS, Vol. 122, pp. 92–100, 2013. [CrossRef]

[40] M. Michalska, and P. Wolf, "*Pseudomonas* exotoxin A: optimized by evolution for effective killing," Frontiers in Microbiology, Vol. 6, pp. 963, 2015. [CrossRef]

[41] A. M. Abdel-Mawgoud, F. Lepine, and E. Deziel, "Rhamnolipids: diversity of structures, microbial origins and roles," Applied Microbiology and Biotechnology, Vol. 86, pp. 1323–1336, 2010. [CrossRef]

[42] R. Rahim, U. A. Ochsner, C. Olvera, M. Graninger, P. Messner, J. S. Lam, and G. Soberoan-Chaavez, "Cloning and functional characterization of the *Pseudomonas aeruginosa rhlC* gene that encodes rhamnosyltransferase 2, an enzyme responsible for di-rhamnolipid biosynthesis," Molecular Microbiology, Vol. 40, pp. 708–718, 2001. [CrossRef]

[43] B. Atze´l, S. Szoboszlaya, Z. Mikuskab, and B. Kriszta, "Comparison of phenotypic and genotypic methods for the detection of environmental isolates of *Pseudomonas aeruginosa*," International Journal of Hygiene and Environmental Health, Vol. 211, pp. 143–155, 2008.

[44] C. Griebler, and T. Lueders, "Microbial biodiversity in groundwater ecosystems," Freshwater Biology, Vol. 54, pp. 649–677, 2009. [CrossRef]

[45] S. Chouhan, U. Tuteja, and S. J. S. Flora, "Isolation, identification and characterization of fluoride resistant bacteria: possible role in bioremediation," Applied Biochemistry and Microbiology, Vol. 48, pp. 43–50, 2012. [CrossRef]

[46] S. Mukherjee, V. Yadav, M. Mondal, S. Banerjee, and G. Halder, "Characterization of a fluoride-resistant bacterium *Acinetobacter* sp. RH5 towards assessment of its defluoridation capability," Applied Water Science, Vol. 7, pp. 1923–1930, 2015. [CrossRef]

[47] S. Mukherjee, P. Sahu, and G. Halder, "Microbial remediation of fluoride-contaminated water via a novel bacterium *Providencia vermicola* (KX926492)", Journal of Environmental Management, Vol. 204, pp. 413–423, 2017. [CrossRef]

[48] S. Mukherjee, P. Sahu, and G. Halder, "Comparative assessment of the fluoride removal capability of immobilized and dead cells of *Staphylococcus lentus* (KX941098) isolated from contaminated groundwater," Environmental Progress & Sustainable Energy, Vol. 37, pp. 1573–1586, 2018. [CrossRef]

Environ Res Tec, Vol. 5, Issue. 4, pp. 340–348, December 2022

Environmental Research and Technology
https://ert.yildiz.edu.tr - https://dergipark.org.tr/tr/pub/ert
DOI: https://doi.org/10.35208/ert.1150743

Environmental Research & Technology

Research Article

A process "algorithm" for C&D materials reuse through file-to-factory processes

Marina RIGILLO[1], Sergio Russo ERMOLLI[1], Giuliano GALLUCCIO[*1], Sara PICCIRILLO[1], Sergio TORDO[1], Flavio GALDI[2], Michela MUSTO[3]

[1]Department of Architecture, Federico II University of Naples, Naples, Italy
[2]ETESIAS, Corso Nicolangelo Protopisani, Naples, Italy
[3]The Spark Creative Hub, Naples, Italy

ARTICLE INFO

Article history
Received: 29 July 2022
Revised: 31 October 2022
Accepted: 19 November 2022

Key words:
Circular economy; C&D waste; Urban regeneration project; 3D print technology

ABSTRACT

The paper illustrates some of the ongoing results of the interdepartmental research Prosit "PROgettare in SostenibilITà: qualification and digitalization in construction", analyzing the key steps aimed at testing, within the actual regulatory and technological framework, new possible applications of recycled materials from construction and demolition (C&D) in sustainable and innovative supply chains. In Italy, in particular, about 98% of the non-hazardous waste from C&D activities is recycled already in 2018, as documented by the Eurostat's "Recovery rate of construction and demolition waste" report. Nevertheless, C&D waste is mainly reused for the construction of embankments and road foundations. The research, therefore, identifies in the use of file-to-factory technologies a possible way to extend the scope of the reuse of these resources to realize diversified and non-standard manufactures and components, in the perspective of a greater spread of virtuous practices of circular economy in the construction sector. In this sense, a process "algorithm" is described, designed to be scaled and replicated in different contexts for similar purposes.

Cite this article as: Rigillo M, Ermolli SR, Galluccio G, Piccirillo S, Tordo S, Galdi F, Musto M. A process "algorithm" for C&D materials reuse through file-to-factory processes. Environ Res Tec 2022;5:4:340–348.

INTRODUCTION

The need to promote circular economy to reduce the consumption of renewable resources has long been identified in European policy as one of the key issues of the environmental challenge. Notably, the EC Report for the implementation of the Second Action Plan for the Circular Economy addresses the circular initiatives as «a backbone of the EU industrial strategy, enabling circularity in new areas and sectors, [so that] life-cycle assessments of products should become a norm and the eco-design framework should be broadened as much as possible» [1]. Similarly, the EU investments for the circular economy (2016–2020) reached almost 10 million euros, intercepting both the research programs (Horizon 2020 funds and other programs), and the economic and industrial pol-

***Corresponding author.**
*E-mail address: giuliano.galluccio@unina.it

This paper has been presented at Sixth Symposium on Circular Economy and Urban Mining (SUM 2022)/Capri, Italy / 18–20 May 2022.

icies (Cohesion Policy 2016–2020, European Fund for Strategic Investments and Innovfin). Despite these efforts, operational practices are struggling to reconvert the typical "take-make-dispose" process into widespread circular practices. The latter fails due to roughly three groups of reasons: economic interests, environmental concerns, and regulatory requirements [2]. In particular, limits to a more effective approach to waste management concern the difficulty in a exact quantification of waste due to illegal abandonment and the lack of an on-site monitoring system for non-dangerous waste. Also, circular processes are hindered in some UE country because of low prices for landfilling and for raw materials [3].

Especially for Construction and Demolition (C&D) waste, these factors affect the development of new production processes aimed at reducing the withdrawal of natural resources (especially land-take), and at extending the material life-span. The introduction of circular processes in the construction sector finds, in fact, its main barriers both in the technical background of experts and firms, both in the operational practices, and in the specific C&D waste regulation [4].

In the wake of the depicted scenario, the study aims at outlining a methodological process for shortening the C&D supply chains. The paper presents here the advances of the POR CAMPANIA FESR 2014/2020 research, titled "Prosit - Design in Sustainability: qualification and digitization in construction". The study concerns the application of the selective demolition process in the urban regeneration yard with the aim of testing the opportunities for recycling "in situ" the waste produced through BIM-based file-to-factory processes.

Circular Building Process in Italy: State of the Art

In Italy, the reuse, recovery and recycling of the outcomes of the complete or partial buildings demolition fails to enhance the development of supply chains consistent with the operational potential offered by the sector, nor is able to create a reference for a Secondary Raw Materials (SRM) market to be re-introduced in the construction sector [5]. The 2021 ISPRA Report on special waste highlights that of approximately 78% of inert material recovered, only a few parts are reintroduced into the construction sector, while the greater volumes are addressed to backfilling [6]. The Italian scenario is also characterized by great variability between Regions, due both to the differences in the degree of industrial development in the Country, and to the local regulations [7]. Further distinctions are recognizable in the technological and material specificity of the regional building heritage, which shows significant differences in terms of construction techniques, ages of construction, and the industrial capacity of the building sector.

In general terms, however, the difficulty in getting systemic procedures capable of integrating the various actors and contexts off the ground can be traced back to some factors characterizing the Italian system, as well as the lack of procedural tools for providing a guideline and protocols for the construction sector. In this regard, there is a certain delay in the introduction of innovative and circular processes within consolidated construction practices, as well as a weakness in the political direction. The latter, especially, seems to be unable to take fully advantages of the opportunities offered by the digital technologies, notably those aimed at Information Management, that allow to model the production of C&D flows and their traceability. Public policies seem unable to find the conceptual and legislative framework to reduce C&D production. This objective involves a combination of strategies aimed both at reducing C&D waste volumes and at enhancing SRM's performances so that the latter can be re-introduced into the construction cycle.

C&D Waste Criticalities in the Light of Enhancing the Concrete Supply Chain

The C&D waste recovery is a key issue for reducing the land-take, and the environmental impacts of the full construction chain. In particular, it should be emphasized that the concrete industry is one of the most polluting on the planet with 5% CO_2 emissions and 33% of the waste produced annually in Europe, as for a world production of about 4 billion tons for year.

The entire concrete life cycle (from extraction to production, to transport, and from use to disposal) strongly contributes to the global warming, acidification, photochemical smog, eutrophication. Several experiments carried out by research centers and private companies enhanced strategies and interventions to limit the impact of constructions by outlining new scenarios relating to the entire construction sector are inscribed within this framework.

File-to-Factory Computational Processes for Reusing the C&D Cementitious Waste

In this scenario, the PROSIT research investigated the opportunities coming from the implementation of construction processes based on digital manufacturing technologies. Specially, the focus is on the 3D printing techniques, and for the production of CDW cement mortars within the 3D printers constraints (Fig. 1).

The additive manufacturing sector has a specific research field active on producing printing materials, precisely with the aim of maximizing the content of recycled elements within cementitious mortars, and of improving the quality and performance of the final products. The implementation of additive manufacturing processes (3D printing) with cementitious materials is a key challenge featured by a strong industrial potential, as well as environmental benefits. The latter are mainly focused on the material performances with respect to the entire building process (optimization of material use, cost and construction time reduction, etc.; Fig. 2).

Figure 1. Automated work site with an on-site 3d printer. 3D Autonomous Robotic Construction System (ARCS).

Figure 2. Concrete walls 3d printing process, Winsun.

A further challenge is about the capacity of outlining a virtuous process that links the building dismantling, the recovery of materials and their reuse through digital manufacturing. Therefore, the research interest is to apply this methodology to the existing building stock, so that it bears a relevant significance in the Italian building panorama [8].

Starting from these assumptions, a procedural two-steps "algorithm" has been developed for taking together thematic areas and the issues involved in the recycle workflow.

MATERIALS AND METHODS

"Starting from the End": Site Management and on-Site Recycling

The first step in the "algorithm" concerns the aspects related to the construction site, its management and the demolition process of the building components. Looking this way, the first step is placed in the "end-of-life" phase of a building to start a new construction cycle. The first step in method is strongly influenced by the bunding context, and by the administrative and regulatory framework in which the latter is inserted. The selective demolition operations are a key secondary step in order to maximize the content of recycled materials as aggregates for the composition of cement mortars. This approach provides benefits in terms of saving time and costs, and for the C&D waste management in the design and demolition phases. According to the selective demolition protocols and guidelines [9–12], three scenarios might be addressed: up-cycling, off-site manufacturing, on-site recycle. The latter represents the preferential scenario for the development of the proposed workflow because it allows for a cost reduction in terms of material transport, and because it provides the possibility of direct recycling and reuse.

The regulatory framework governing the use of recycled aggregates for the production of building components is scattered in various documents relating to methods and quantities of C&D waste recovery.

Specifically, the UNI 8520-2 [13] identifies the different material categories that can be used as recycled aggregates according to the demolition methods. For each of these categories, the mass content is defined, and split into percentage ranges. This classification is taken from UNI 11104:2016 which defines the maximum percentages of replacement of the coarse aggregate with recycled coarse aggregate in relation to its type, exposure class and strength class of the concrete.

The exposure classes are defined within the same standard, and depend on the features related to the environment and the ways in which the product made from recycled concrete will be used. In this sense, informative examples of situations to which the exposure classes may correspond are given. The resistance classes of the concrete can be identified through the Ministerial Decree January 14, 2008.

The use of these three tools makes it possible to calculate the amount of recycled aggregates that can be used and is linked to the quality of the product and its final destination.

"Process Algorithm" Development: File-to-Factory Possibilities for on-Site Operations

The second step of the "algorithm" is aimed at identifying the most suitable process to involve in the transformation of demolition waste into construction materials. Specifically, the steps involved in using recycled aggregates for cement mortars suitable for 3D printing technology are analyzed.

Several parameters come into play within the process algorithm that frame a range of possible workflows assuming different scenarios. Great importance is attributed to information and context-related aspects (environmental characteristics, site accessibility, etc.) that contribute to the definition of the processes of demolition, recycling, and accessibility possibilities related to the activation of on-site operations. These processes are regulated by a framework of standards that provide the information related to the quantities and methods of use. Of paramount importance are the material aspects. On the one hand, parameters that derive from demolitions come into play (type of aggregates, grain size, etc.) on the other, issues that are related to the moldability of the cement mortar produced, which must possess certain physical and mechanical characteristics (rheology, hydration, etc.). These aspects directly inform the characteristics and technological choices that influence the digital manufacturing process. In this regard, two macrocategories are identified that are defined by the numerical control tool used: robotic arm and gantry system. A number of constraints related to the final products depend on these categories. The latter constitute the output of the process and consist of categories of products that can be realized in concrete through 3D printing.

The objective is to frame this type of construction process by breaking it down into steps that affect the different actors in the construction sector, with the aim of shaping itself as a decision-making tool that can be used by contracting stations to evaluate possible recovery scenarios through digital fabrication. The goal is to decline with respect to different contexts the succession of design and strategic choices leading to the workflow to be followed during the construction phase.

Expected Impact of the Proposed Methodology

The tool proposed in this research appears to be potentially useful; its implementation, however, requires the activation of a series of synergies related to the actors of the entire supply chain involved in the construction process from demolition to the creation of the printing material and 3D printing. Its operation, in fact, depends on the amount of input information in its possession that pertains to different domains. The point of the "algorithm", therefore, is precisely to seek a synthesis between different disciplines

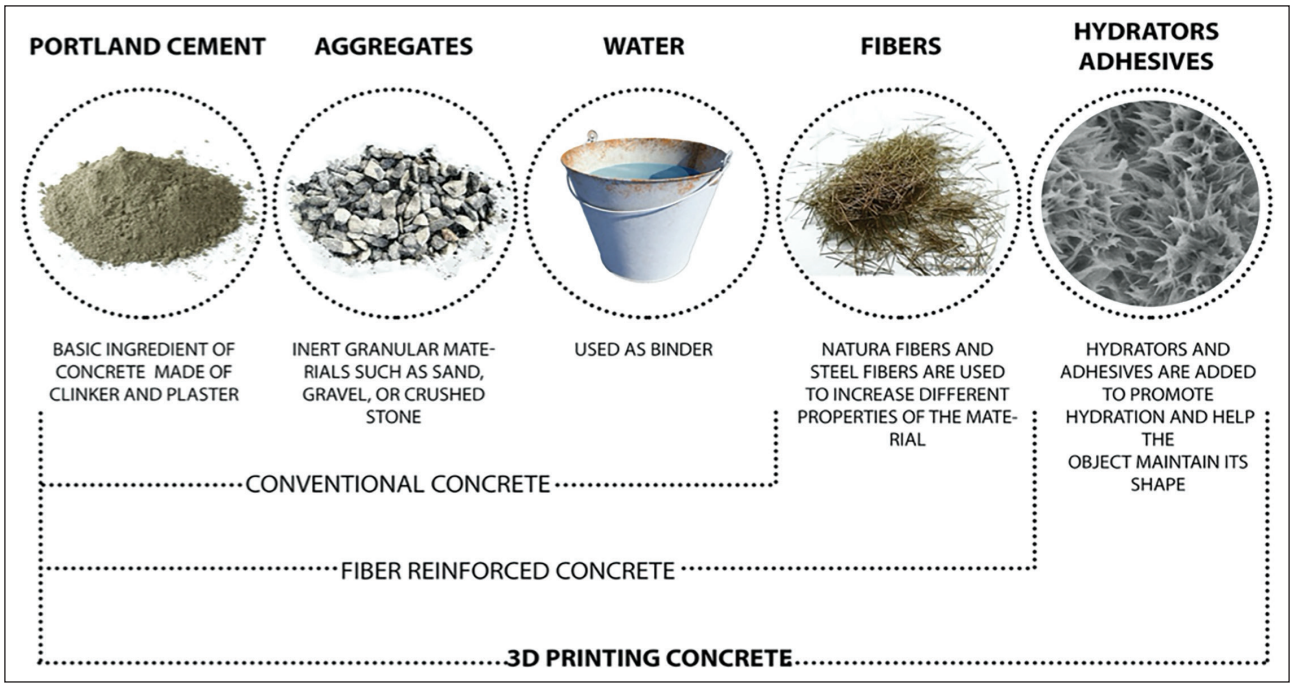

Figure 3. 3D printing concrete composition.

that are aimed at the same purpose and need mutual feedback as they inform each other. Another implication is the connection of the process algorithm to a BIM based system with the aim of recording and updating in real time aspects related to material (quantity of demolished materials) and site management (accessibility). The use of digital fabrication technologies within the construction site, moreover, implies significant changes from a socio-economic point of view within the construction site with the need, for example, to have specialized workers capable of planning and evaluating choices regarding the materials and machinery to be used. From a cultural perspective, the workflow from demolition to digital manufacturing represents a virtuous example of how technologies can change the entire construction industry by reducing economic and resource expenditures and limiting environmental impact. The case study examined considers, specifically, concrete, whose industrial supply chain is among the most polluting but is, theoretically, applicable and repeatable by referring to all materials derived from demolition and different production technologies related to digital manufacturing (subtractive manufacturing, 3D FDM printing).

RESULTS AND DISCUSSION

Quality Assessment of the Aggregates as 3D Printing Material

This part of the study analyzes the relationship between the product coming from the recycling chain, and its use as an inert for the compound used as a raw material in 3D printing.

The most evident feature of the aggregate is its granularity, which is relative to the form in which it is presented. Aggregates with a diameter of less than 5 mm are defined as "sand", aggregates with a larger diameter are defined as crushed stone or generally "large aggregates", and they are those actually affected by recycling. The C&D waste treatment and recovery process can be divided into the following phases:

- Crushing phase, that is aimed at reducing cement waste in the size to make it suitable for final use;
- Separation phase, that is aimed at eliminating undesirable materials in the final product;
- Classification phase by screening, that is aimed at separating the grains according to their size to obtain homogeneous particle size fractions.

With respect to this classification, it should be emphasized that the demolition method is crucial for improving the aggregate's quality, since it directly affects the capacity in differentiate C&D waste ab-origine. In the ordinary industrial practice, in order to contain the disposal costs, construction companies care for separating C&D waste in homogeneous flows as much as possible because the recovery plants generally require greater costs in the case of poorly selected materials and/ or great volumes of undesirable fractions.

In the procedural algorithm, three ranges of aggregate diameters have been identified to be reused:

- 4–8 mm,
- 8–16 mm,
- 15–25 mm.

Figure 4. 3D printing cycle industry Expo Park, Shangai.

The size of the aggregates directly influences the diameter of the extruder to be used for 3D printing. This is because to avoid obstructions, the cement compound must flow continuously. The parameter relating to the diameter of the extruder is divided into four scales of size: less than 8 mm, between 8 mm and 5 cm, between 5 cm and 30 cm and greater than 30 cm.

This choice does not involve the definition of a specific technology (for example, gantry system - multi-axis operating system with airlift - or robotic arm). It is because the use of extruders with a smaller diameter is often combined with robotic arms, larger extruders, which need greater stability, are generally mounted on machines that use gantry system technology.

As coming from literature [14–16], the optimal composition for a cement mortar suitable for 3D printing requires the use of large aggregates with a proportion of 0.63 with respect to the total mass of the compound. These quantities were calculated through various experiments in which the printability and characteristics of the extruded material were tested. Specifically, the control of the semi-fluid's ability to exit from the extremity of the extruder is fundamental, in order to maintain a continuous flow and retaining the shape once it is deposited (Fig. 3, 4).

Site Accessibility in off/on-Site Production Scenarios

A further aspect of the proposed process is related to dual operating options offered by 3D printing, that can be on-site or off-site mode. This option involves a number of differences in terms of operating costs, of the need of skilled operators, and of the quality of the final products. Generally speaking, the on-site mode provides benefits in containing economic and energy costs relating to the waste transport and with respect to construction times. On the contrary, a number of criticalities are in the need to manage of unexpected events arising from the context during the construction phase, such as greater risks for the workforce, resolution of problems deriving from printing errors, control of the quality of the material during the extrusion phase in relation to the atmospheric conditions.

On the other hand, the off-site mode allows a greater quality control during the production phase, and it offers the possibility of printing elements featured by a greater degree of complexity also reducing risks and errors during the construction phase. These advantages are balanced by the increasing of transport and assembly costs, and by the dimensional constraints coming from the site in which the elements are manufactured. Therefore, the choice between these two methods is done according to

Figure 5. Case study area: The former industrial area Corradini, Naples.

the conditions of the operational site and, in particular, to the following conditions: the accessibility of the construction site, the availability of economic resources, specialized work forces and technologies.

CONCLUSIONS

The "algorithm" presented in this study is configured as an operational tool through which to develop building process scenarios declined with respect to the context. Its use as a decision-making tool is linked to the quantity and quality of information in its possession that constitute its inputs. Specifically, different parameters come into play, belonging to separate domains, which have been grouped into five sets:

- Material;
- Information;
- Technology;
- Performance constraints;
- Regulatory constraints.

The result is the definition of a complex system whose reading and use are not deterministic but interpretable with respect to needs that may vary according to the project (maximizing the amount of recycled materials, obtaining a certain type of product, working in a specific context).

For this reason, links between the various process steps were differentiated by dividing them into deterministic type links and indicative links to be interpreted as preferential association. What emerges is the potential of the algorithm to be used to address choices regarding the technologies to be used based on the quality and quantity of materials from demolition. One of the strengths is the possibility of parametrically declining the same process to different situations depending on the repeatability of the process from demolition to recycling and 3D printing.

The “algorithm” presented in this study was developed assuming two different scenarios. These are both theoretically appropriate and feasible according to the presence of specific constraints (for example the accessibility of the construction site for as regards the possibility of operating with on-site technologies).

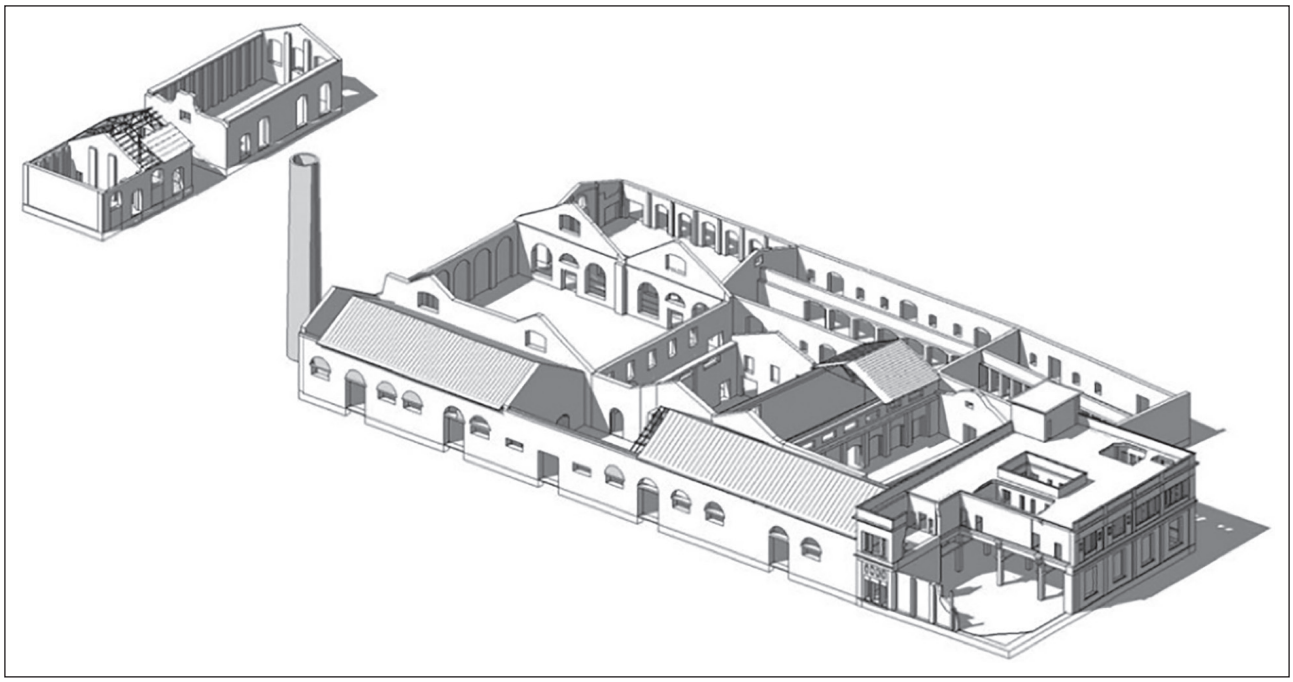

Figure 6. Former industrial area Corradini, Naples – As-is BIM Model.

Notably, the research focused on the possibility of applying the methodology to the follow, different cases:

- Urban furniture. This category has been tested with respect to 3D printing for which components are generally conceived and designed as closed elements, obtainable through a continuous printing path, realised off-site in a controlled environment;
- Façade elements. These are elements with a great level of detail aimed at maximizing the performance of the building façades;
- Interior elements. This group of elements is made up of highly customizable and site-specific components;
- Structural elements. This group consists of structural components in which issues relating to the optimization of the use of material and the quality of the recycled material are pivotal (also defined from a regulatory point of view).

The methodology is currently in the process of being tested with design case studies within the construction site of the ex-Corradini area of Naples [17], a heavily degraded site of great urban interest, which has long been off-limits to the public due to asbestos pollution (Fig. 5, 6).

ACKNOWLEDGMENTS

This research was funded by the CAMPANIA REGION, as part of the research project 'PROSIT - Projecting in Sustainability: qualification and digitization in construction', PO FESR 2014–2020 - Specific objectives 1.2.1 - expression of interest for the 'realization of technological platforms under the program agreement: High-tech districts, aggregations and private public laboratories for strengthening the scientific and technological potential of the Campania Region, awarded to STRESS scarl insert. The activity involves among the project partners the Department of Architecture and the Department of Structures for Engineering and Architecture of the Federico II University of Naples, the public-private consortium STRESS s.c.a.r.l. and the Municipality of Naples. Authors thank the all participants for the contribution to achieve the research findings.

DATA AVAILABILITY STATEMENT

The authors confirm that the data that supports the findings of this study are available within the article. Raw data that support the finding of this study are available from the corresponding author, upon reasonable request.

CONFLICT OF INTEREST

The authors declared no potential conflicts of interest with respect to the research, authorship, and/or publication of this article.

ETHICS

There are no ethical issues with the publication of this manuscript.

REFERENCES

[1] European Commission, "Communication from the Commission to the European Parliament, the Council, the European Economic and Social Committee and the Committee of the Regions on the Implementation of the Circular Economy Action Plan, COM2019", 2019.

[2] European Commission, "EU construction and demolition waste management protocol," 2016. https://single-market-economy.ec.europa.eu/news/eu-construction-and-demolition-waste-protocol-2018-09-18_en Accessed on Nov 30, 2022.
[3] P. Altamura, "Costruire a zero rifiuti. Strategie e strumenti per la prevenzione e l'upcycling dei materiali di scarto in edilizia, Franco Angeli, 2015. [Italian]
[4] E. Antonini, "Residui da costruzione e demolizione: una risorsa ambientalmente sostenibile," In E. Antonini (Ed.), Il progetto VAMP ed altre esperienze di valorizzazio-ne dei residui. Franco Angeli, 2001. [Italian]
[5] M. Rigillo, and M. T. Giammetti, "Management of the C&D waste in the urban regeneration Project," Journal of Technology and Environment, Vol. 22, pp. 240–-248, 2021. [CrossRef]
[6] ISPRA, "Rapporto Rifiuti Speciali", 2021. https://www.regione.puglia.it/web/ufficio-statistico/-/ispra.-rapporto-rifiuti-speciali.-edizione-2021 Accessed on Nov 30, 2022.
[7] J. Cárcel-Carrasco, E. Peñalvo-López, M. Pascual-Guillamón, and F. Salas-Vicente, "An overview about the current situation on C&D waste management in Italy: Achievements and challenges," Buildings, Vol. 11(7), Article 284, 2021.
[8] FAOLEX Database, "Art 205, Legislative Decree 152/2006," https://www.ecolex.org/details/legislation/legislative-decree-no-152-approving-the-code-on-the-environment-lex-faoc064213/ Accessed on Nov 30, 2022.
[9] PVC Forum, "UNI/PdR 75:2020: Selective deconstruction - Methodology for selective deconstruction and waste recovery from a circular economy perspective," https://www.pvcforum.it/pvc-hub/news/unipdr-752020-selective-deconstruction/ Accessed on Nov 30, 2022.
[10] R. Cossu, V. Saliebri, and V. Bisinella, "Urban mining: A global cycle approach to resource recovery from solid waste, CISA Publisher, 2012.
[11] M. Dri, P. Canfora, I. S. Antonopoulos, and P. Gaudillat, "Best envi-ronmental management practice for the waste management sector," JRC Science for Po-licy Report, EUR 29136 EN, Publications Office of the European Union, Luxembourg, 2018.
[12] K. Ghosh, "Urban mining and sustainable waste management," Springer, 2020. [CrossRef]
[13] Un Monda Fatto Bene, "UNI 8520-2 Aggregati per calcestruzzo - Istru-zioni complementari per l'applicazione della EN 12620 - Parte 2: Requisiti," 2016. https://store.uni.com/uni-8520-2-2016 Accessed on Nov 30, 2022.
[14] T. T. Le, S. A. Austin, S. Lim, R. A. Buswell, A. G. F. Gibb, and T. Thorpe, "Mix design and fresh properties for high-performance printing concrete," Ma-terials and Suctures, Vol. 45, pp. 1221–1232, 2012. [CrossRef]
[15] B. Gang, W. Li, M. Guowei, S. Jay, and B. Mingke, "3D printing eco-friendly concrete containing under-utilised and waste solids as aggregates," Cement and Concrete Composites, Vol. 134, Article 104742, 2021.
[16] J. Pasco, Z. Lei, and C. Aranas, "Additive manufacturing in off-site construction: Review and future directions," Buildings, Vol. 12(1), Article 53, 2022. [CrossRef]
[17] M. Rigillo, S. Russo Ermolli, and G. Galluccio, "Digital rule-based compliance processes. The urban regeneration of ex-Corradini, Naples (IT)," Agathon International Journal of Architecture, Art and Design, Vol. 10, pp. 120–131, 2021.

Environ Res Tec, Vol. 5, Issue. 4, pp. 349–356, December 2022

Environmental Research and Technology
https://ert.yildiz.edu.tr - https://dergipark.org.tr/tr/pub/ert
DOI: https://doi.org/10.35208/ert.1191003

Environmental Research & Technology

Research Article

Operation cost analysis of UV-based ballast water treatment system used on a bulk carrier ship

Veysi BAŞHAN*[1], Ahmet KAYA[2]

[1]*Department of Naval Architecture and Marine Engineering, Bursa Technical University, Faculty of Maritime, Bursa, Türkiye*
[2]*Department of Marine Engineering, Yıldız Technical University, Faculty of Naval Architecture and Maritime, İstanbul, Türkiye*

ARTICLE INFO

Article history
Received: 18 October 2022
Revised: 03 November 2022
Accepted: 19 November 2022

Key words:
Ballast water treatment; Bulk carrier, Cost analysis; Ship; UV

ABSTRACT

According to IMO rules, when a new machine system needs to be integrated into the ship, it is required to have low fuel consumption in terms of energy efficiency and emissions. The same is true for ballast treatment. Many different types of ballast water treatment systems (BWTS) are available on the marine market. Ship operators want to choose BWTS that will consume minimum fuel and operate at maximum efficiency. Therefore, in this study, fuel consumption under both IMO and USCG conditions, and hence the operational cost, is calculated if the UV-based BWTS system is integrated into a bulk carrier ship. As a result, the highest cost is $9773 when the most expensive fuel, MGO, is used and operation is performed with a single ballast pump. In USCG mode, the minimum cost is $6382 and the maximum cost is $18929 under the same conditions. It is seen that if the fuel price increases to 1.4 $/kg, the cost of using BWTS in IMO mode can increase to $11392, and if it drops to 0.3 $/kg, the cost of using BWTS in IMO mode can decrease to $1826. It is seen that the highest cost can go up to $22066 and the lowest cost can go down to $3983, with the change of fuel prices in the use of BWTS in USCG mode. With the resulting formulation, with the power consumption of the BWTS and the diesel generator shop trail test fuel consumption values, researchers or shipping companies can repeat the calculations for all kinds of different fuels and different amounts of ultraviolet (UV) chambers for variable ballast operations with different ballast tank capacities. Consequently, it is thought that this study is useful in determining the additional operational cost of UV-based BWTSs.

Cite this article as: Başhan V, Kaya A. Operation cost analysis of UV-based ballast water treatment system used on a bulk carrier ship. Environ Res Tec 2022;5:4:349–356.

INTRODUCTION

Ballast water is seawater carried by ships to provide stability, trim and structural integrity. When a ship loads cargo, it discharges the ballast water in its tanks. Likewise, when a ship is unloaded, it fills its ballast tanks with ballast water. In literature, it is stated that about 3 to 5 billion tons of ballast water are transferred worldwide every year [1]. When ballast water is transferred from one region to another, it creates direct and indirect effects on regional ecology, economy, and human health, due to species such as microorganisms, phytoplankton, and zooplankton [2].

***Corresponding author.**
*E-mail address: veysibashan@gmail.com

For all these reasons, the International Maritime Organization (IMO) put into effect the Ballast Water Management Convention (BWMC) on 8 September 2017. Thanks to this convention, all ships in international traffic are required to manage their ballast water and sediment to a certain standard according to a ship-specific ballast water management plan. From now on, new ships will need to meet the ballast water treatment standard, while existing ships will be required to replace mid-ocean ballast water but meet the ballast water treatment standard until a specified renewal survey date. As a result, most ships will need to install an onboard ballast water treatment system (BWTS) [3]. Therefore, maritime businesses and shipping companies have started to search for which type of BWTS would be more effective. It is known that in BWTSs, mechanical methods (filtration, hydro cyclone, and magnetic separation), physical methods (heat treatment, UV, ultrasound, and cavitation), and chemical methods (hydrogen peroxide, biocides, electro-chlorination, and ozone) are combined and used as hybrids methods. The initial investment cost of these systems, as well as the treatment efficiency and operating costs, can be different from each other because the equipment and energy amounts they need are different. There are studies on BWTS in many different aspects in the literature [4–8]. In this context, Gerhard et al. [9] investigated the impact of policy on the use of BWTSs by examining IMO Type Approval registries and country-level databases in the United States and Australia. The authors found that most ships with BWTS had either electrolytic or UV purification systems. Altug et al. [10] have taken samples from the ballast water of 21 ships coming to the Sea of Marmara, Türkiye from different parts of the world. Samples were tested and 38 bacterial species, 27 pathogenic bacteria belonging to 17 families, were identified. Vorkapić et al. [11] carried out the analysis and comparison of the economic feasibility of BWTS systems operating with UV irradiation and electrochlorination methods on merchant ships. The authors noted that systems using electrochlorination can be almost five times more cost-effective than those based on UV irradiation and almost eight times more cost-effective than ballast water exchange using the sequential method. It is known that different BWTSs are preferred in different regions. For example, Animah [12] examined 17 ballast water treatment technologies and features such as technological readiness, commercial readiness, operational readiness, seafarer skills readiness, biological efficiency readiness, and cost of ballast water treatment technologies, and stated that BWTS using membrane filters would be the best option for Ghana. Doğru et al. [13] emphasized the harmful effects of ballast water and analyzed the systems used in ballast water treatment. Vural and Yonsel [14] examined two ships with different ballast water capacities built in Türkiye and the most suitable systems for ships were proposed using the Key Performance Indicators method. Elçiçek et al. [15] evaluated the effect of ballast water on marine and coastal ecology and compiled IMO regulations on ballast water in this context. Ren [16] carried out a study with an evaluation criteria system consisting of eight criteria in four categories used to evaluate BWTS. An example case involving four technologies for ballast water treatment, namely Alfa Laval, Hyde, Unitor, and NaOH was studied with the proposed method and Hyde was considered the best choice. Jang et al. [17] conducted a ship ballast water test using extremely turbid seawater (>300 mg total suspended solids (TSS)/L) collected from the Shanghai Port and normal seawater (<100 mg TSS/L) collected from other ports. For ballast water retained for long storage periods, the results suggest the use of UV units or electrolysis-containing BWTSs during deballasting. This indicates the importance of using the UV unit. UV irradiation inactivates organisms by disrupting chemical bonds in DNA and RNA and cellular proteins [18]. Although the UV method is known to be very effective in the inactivation or destruction of microorganisms, it is recommended to be used after an efficient pre-treatment. UV-based BWTS technology creates acoustic cavitation by creating high-frequency radiation in the liquid and takes advantage of the disinfectant effect of the physical and chemical processes that take place during this time. When the microscopic gas bubbles formed during cavitation burst, very high local heat is released, and it also causes the formation of disinfectants such as hydroxyl radicals and hydrogen peroxide [19]. However, the cavitation created varies depending on the frequency, power density, duration of action, and properties of the water in question. On the other hand, high-intensity ultrasound energy is required to provide the desired standard in microbiological disinfection in large-scale waters [20]. Therefore, the cost of ultrasound technology per ballast water volume is considered to be relatively high [21, 22]. Before BWTS systems, only ballast pumps constituted the operating cost in ballast operations. Başhan et al. [23] calculated the operational cost of ballast operation for a case bulk carrier ship at different diesel generator loads and different fuel unit prices. In this study, apart from prior studies, it has been studied the additional operational cost of a UV-based BWTS is considered to be added to this bulk carrier ship.

MATERIALS AND METHODS

The capacities of all ballast tanks belonging to M/V İnce İnebolu (52376 DWT) and also technical specifications of the ballast pump are given in the previous study [23]. The vessel's technical particulars are provided in Table 1.

The simple system diagram of the UV-based BWTS that is planned to be integrated into the bulk carrier ship is shown in Figure 1. Developed by Optimarin [24], this system works in ballasting and deballasting modes. During ballast, ballast water first passes through a 20-micron

Table 1. M/V İnce İnebolu's ship particulars

IMO no	9254472
Call sign	TCPK7
Build	2002
DWT (summer)	52376 M/T
Length overall	189.99 m
Breadth	32.26 m
Ballast capacity	28930 m^3
Diesel genera-tors	Daihatsu 5DK-20

Table 2. Design conditions of the BWTS

Description	Specification
Water type	Ballast water
Flow range	Ballast: 155–1000 m^3/h
	Deballast: 60–1000 m^3/h
Filter Capacity	95–1040 m^3/h
Back flush pump capacity	100 m^3/h @ 2,5 bar
Design pressure	10 bar
Ballast water temperature range	-2 → +37 °C
Ambient temperature range	0 → +50 °C
System pressure loss	Filter: 0,3 bar
	UV system: 0,12 bar
	FPV: 0,2 bar
	Total: 0,62 bar
OBS power supply range	440 VAC, 60 Hz, 3 phase+E
Power requirement	6 × 40 kW
Average power consumption	6 × 17 kW (in IMO mode)
	6 × 35 kW (in United States Coast Guard (USCG) mode
Heat dissipation	Approx. 1,5 kW per UV Power Cabinet (6 pcs.)
	The rest of the system is negligible

filter. This filter removes larger particles, including the majority of zooplankton. After the filter, the water passes through the UV chamber(s), where the water is exposed to high doses of UV light. The number of UV chambers is related to the capacity of the ship's ballast tanks. In this study, BWTS with 6 UV chambers is considered. UV exposure kills/inactivates bacteria/viruses as well as the rest of the plankton. In the deballasting process, the filter is bypassed and the ballast water once again passes through the UV chamber(s). This ensures that plankton and bacteria/viruses are neutralized if any of them pass the initial treatment in the ballasting process. Detailed design conditions of the UV-based BWTS are provided in Table 2.

Table 3. Maximum flow rate correlation according to the number of UV chambers

Number of UV chambers	Max flow rate (m^3/h)
2	334
3	500
4	667
5	834
6	1000
7	1167
8	1334
9	1500
10	1667
11	1834
12	2000
13	2167
14	2334
15	2500
16	2667
17	2834
18	3000

Besides, the maximum flow rate correlation according to the number of UV Chambers is provided in Table 3. This is directly related to the ship's ballast water tank capacities. Considering M/V İnce İnebolu, the total capacity of the topside and ballast tanks is 15407.1 m^3 with the aft peak tank. No: 3 cargo ballast amount is 13522.9 m^3. The ship has a total ballast tank capacity of 28930 m^3.

The energy needs of almost all auxiliary machinery on ships, except propulsion, are provided by diesel generators. Thus, diesel generators provide the energy needs of ballast pumps and BWTS to be integrated into the system. The total load on the generators on ships is known, and the total fuel consumption is also known. However, it is not known how much energy each of the auxiliary machines fed by the generator consumes. Therefore, in order to determine the energy consumption (direct fuel consumption) of an auxiliary machine fed by the generator, a function is fitted by regression analysis from the fuel consumption values of the generator at different loads. Thanks to this function, it is determined by calculating how much fuel consumption has increased considering that the relevant auxiliary machine is activated and, on which load range the generator is operating.

The fuel consumption values of a DAIHATSU generator with the machine model of 6DC-17A x 500 kW belonging to the M/V İncebolu ship were used. Fuel consumption is 36.6 kg/h for 125 kW, 58.2 kg/h for 250 kW, 81.4 kg/h for

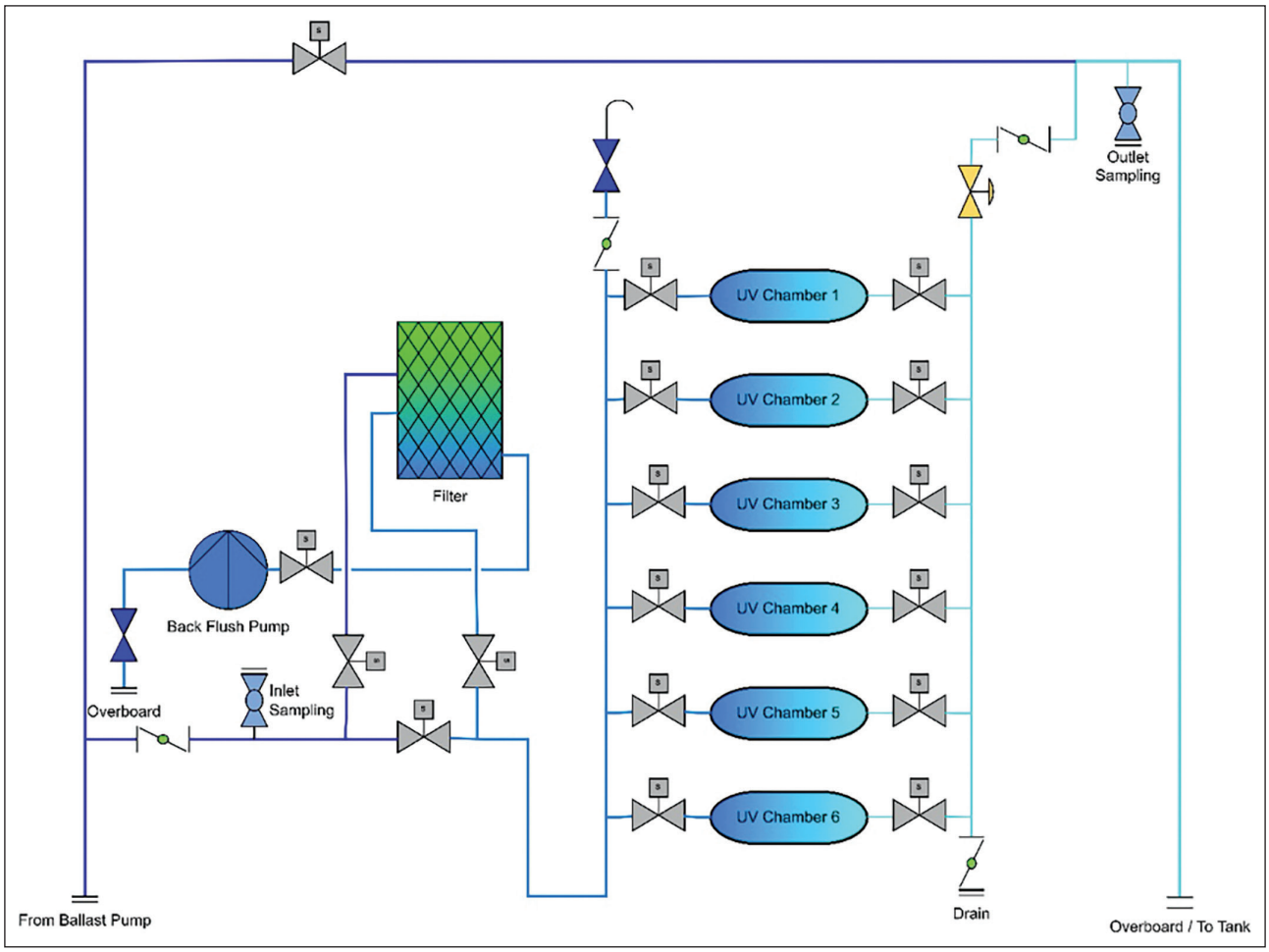

Figure 1. Basic schematic flow diagram of the BWTS.

375 kW, and 105.1 kg/h for 500 kW. A figure and function were obtained by using the fuel consumption values at different loads from the shop trail test information of the diesel generator and given in Figure 2. The new fuel consumption data is shown in Figure 2 when BWTS is started on the generator operating at 25%, 50%, and 75% loads. When the regression analysis is made from these consumption values, the fuel consumption of the BWTS can be found in Table 4. P denotes power, dg subscript is diesel generator and bwts is ballast water treatment system.

Global average bunker prices can be found at [25]. This average is from major global bunkering ports of Busan, Colombo, Durban, Fujairah, Gibraltar, Hong Kong, Houston, İstanbul, LA/Long Beach, Las Palmas, Mumbai, New York, Panama, Piraeus, Rotterdam, Santos, Shanghai, Singapore, St Petersburg, and Tokyo. The prices are $760.50, $1201 and $481 for Very Low Sulphur Fuel Oil (VLSFO), Marine Gas Oil (MGO), and Intermediate Fuel Oil, 380 cSt (IFO380), respectively. The three fuel types mentioned here are taken into account while making the calculations. For IFO180 and other types of fuel, additional calculations can be made with price and fuel consumption data.

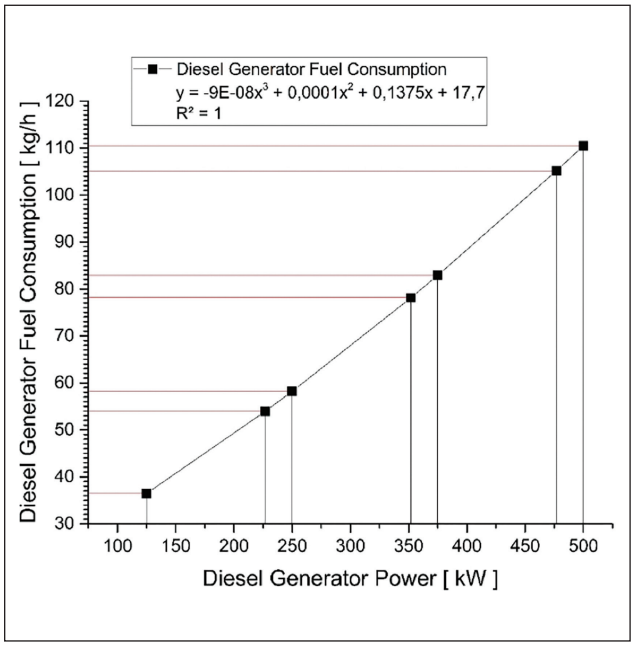

Figure 2. Fuel consumption dependent on diesel generator power in IMO mode.

Table 4. Calculation of the BWTS operation cost

Total ballast tanks volume	28930 (m^3)
BWTS capacity	6x167 (m^3/h) or 950 (m^3/h)
Fuel consumption of BWTS	-9×10^{-7} [(P_{dg}^3-P_{bwts3})+(0,0001 × P_{dg}^2-P_{bwts}^2)]+[(0,1375 × P_{dg}-P_{bwts})] (kg/h)
Number of ballast operation	b
Average fuel price	VLSFO - 760.50 $/MT, MGO - 1201 $ and IFO 380 -481 $
BWTS operation cost	($)

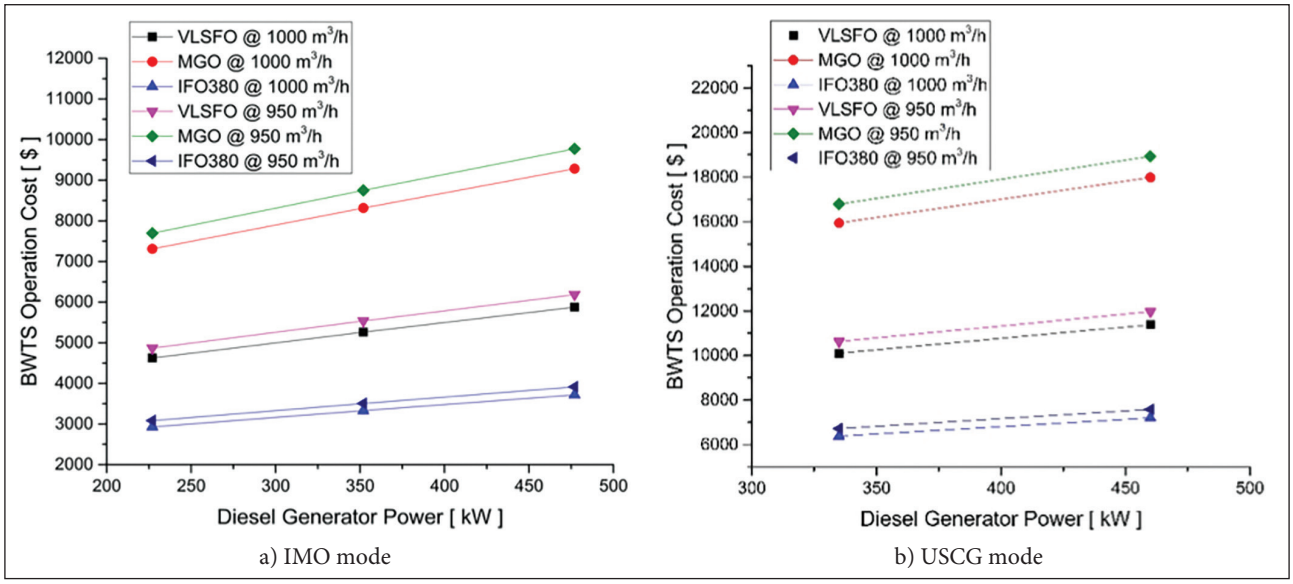

Figure 3. Cost of operating BWTS at variable loads with different fuels.

RESULTS AND DISCUSSION

In ballast operations on ships, when there was no BWTS, the operation cost was incurred by the fuel consumption of the ballast pump(s). When UV-based BWTS is used, UV systems consume energy in both IMO mode and USCG mode of the USA. According to the capacities of the BWTS and the ballast pumps, calculations were made in this study as 950 m^3/h or 1000 m^3h treatment. Ships generally operate with different fuels according to their voyage regions. Therefore, in this study, cost analysis of BWTS was made according to 3 different fuels and according to the 25%, 50%, and 75% load of the diesel generator. In Figure 3, in case of running BWTS at 3 different generator loads, a cost analysis is made regarding three different fuels. It is assumed that the system operates in IMO and USCG modes and performs 12 ballast operations in 1 year.

Figure 3 shows the annual cost of BWTS, when used at different loads of the generator in IMO and USCG modes. Calculations are made for the ship to fully fill the ballast tanks 12 times a year. It is also seen in the figure that the ballast operation is carried out at two different flow rates and the use of different fuels during the operations. The reason for choosing these two different flow rates is that the maximum flow rate of the BWTS system is 1000 m^3/h and the maximum flow of a ballast pump on board is 950 m^3/h. It is seen that the minimum cost in IMO mode is $2928 when using the cheapest fuel, IFO380, and operating at the maximum flow rate of the BWTS. In addition, it is seen that the highest cost is $9773 when the most expensive fuel, MGO, is used and operation is performed with a single ballast pump. In USCG mode, the minimum cost is $6382 and the maximum cost is $18929 under the same conditions. Considering the highest cost case, i.e., using MGO in USCG mode, the extra cost of not using the maximum capacity of the BWTS appears to be $946.

Figure 4 shows the cost of using BWTS with different fuel prices for IMO and USCG modes. Calculations are made for the ship to fully fill the ballast tanks 12 times a year. In addition, as seen in Figure 3, it is seen that the cost increases as the load of the generator increases. It is seen that if the fuel price increases to 1.4 $/kg, the cost of using BWTS in IMO mode can increase to $11392, and if it drops to 0.3 $/kg, the cost of using BWTS in IMO mode can decrease to $1826. It is seen that the highest cost can go up to $22066 and the lowest cost can go down to $3983, with the change of fuel prices in the use of BWTS in USCG mode.

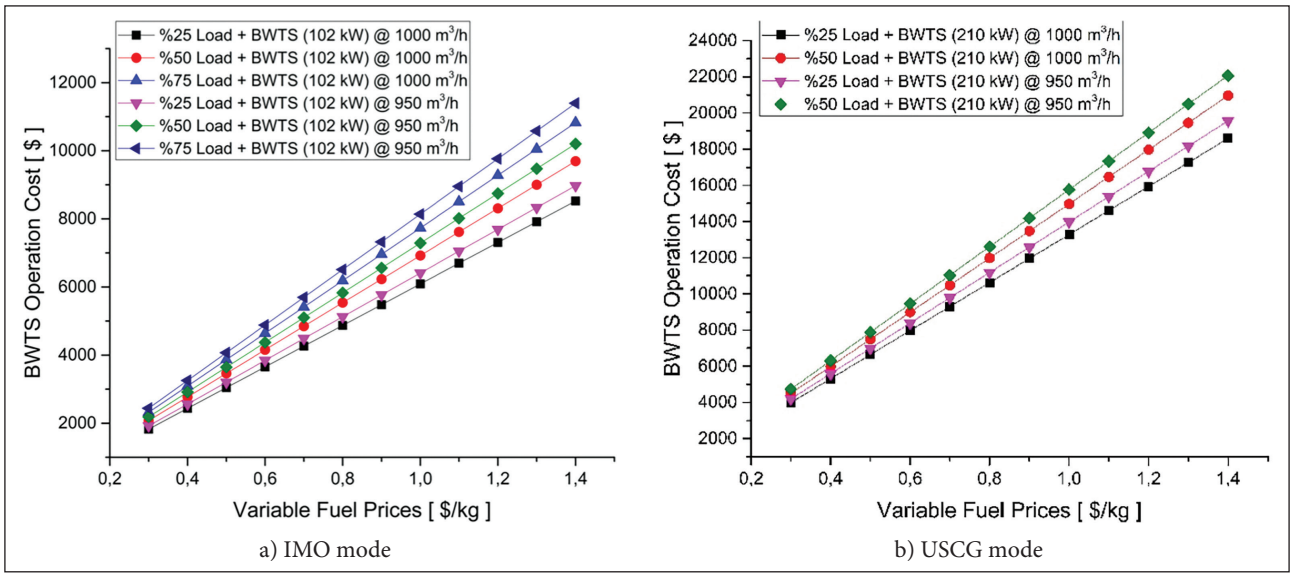

a) IMO mode b) USCG mode

Figure 4. BWTS operation cost at different loads for variable fuel prices.

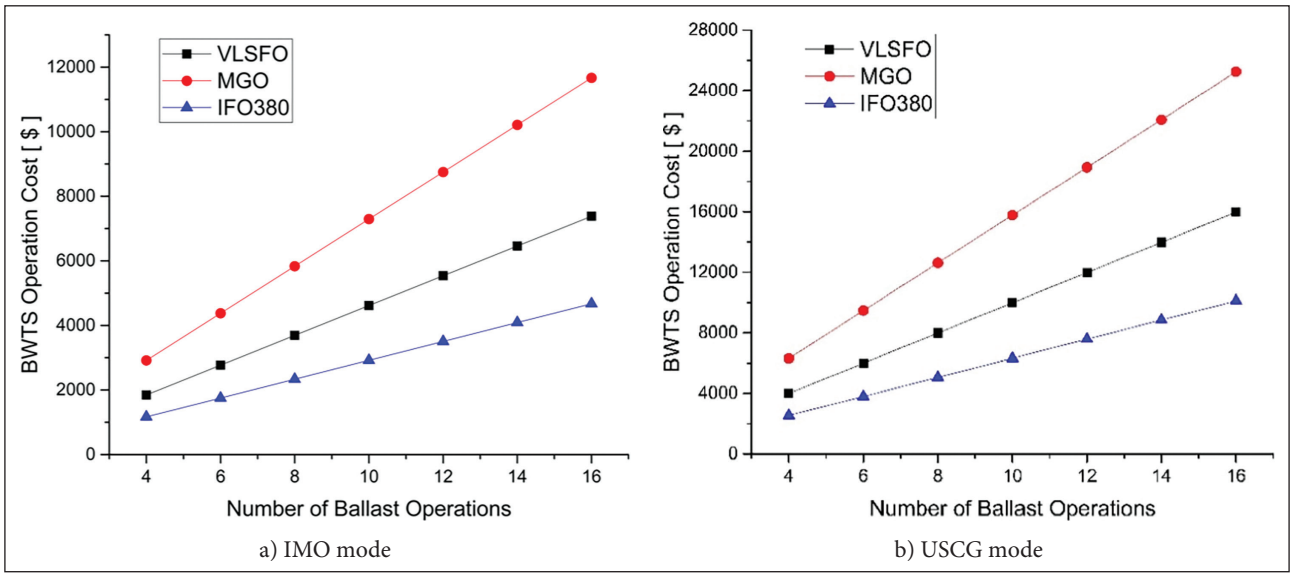

a) IMO mode b) USCG mode

Figure 5. BWTS operation cost with different fuels for variable numbers of ballast operations.

Figure 5 shows the annual costs of using BWTS in IMO and USCG modes, depending on the number of ballast operations per year. Calculations are made for the case that the generator is at 50% load excluding BWTS and the ballast operation is carried out with a flow rate of 950 m³/h. With the annual number of ballast operations increasing to 16, the cost of using BWTS in annual IMO mode increased to $11693 with MGO. In addition, it was observed that when the number of operations decreased to 4 while using IFO380, the cost decreased to $1168.

Figure 6 shows the annual cost of operating the BWTS in USCG mode, depending on the load on the single generator when two generators are running. The fuel consumption by the BWTS is covered by two generators while the generators are operating in parallel, that is, in synchronization, and therefore the extra fuel consumption has been calculated. Under these conditions, it is seen that the annual cost of using BWTS increases up to a maximum of $20146 and decreases to a minimum of $6039.

CONCLUSIONS

There are BWTSs developed with many different mechanical, physical, and chemical methods for ballast water treatment. Each of these methods has its own advantages and disadvantages. In addition to complying

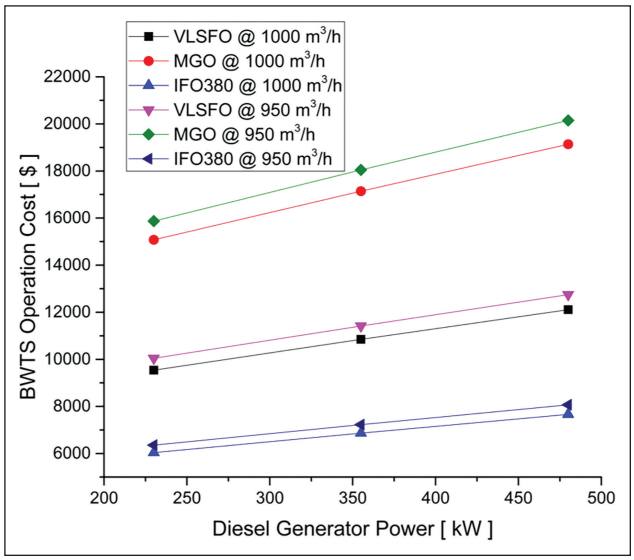

Figure 6. Cost of operating BWTS at variable loads on 2 generators with different fuels.

with the standards set by the IMO, shipowners want the BWTSs they will integrate on their ships to be systems with high energy efficiency, low fuel consumption, and therefore low operational cost. Therefore, the additional operational cost of integrating a UV-based BWTS, which is frequently preferred in the maritime market, into a bulk carrier ship has been calculated in different scenarios. As the load of the diesel generator increases, fuel consumption also increases. However, as the load increases, the specific fuel consumption decreases to a certain level. Therefore, calculations were made at different generator loads. In addition, calculations were made considering VLSFO, MGO and IFO380 fuel prices as ships use different fuels. Since fuel prices are constantly changing in the world, fuel prices have been parametrically changed and it has been shown how much BWTS operation costs can increase in case of an increase in fuel prices. Since the number of ballast operations may vary depending on the voyage area of the ship and the load it carries, cost analysis has also been carried out for different ballast operations to give an idea. In addition, these analyzes were repeated according to both IMO and USCG situations. Because the manufacturer stated that BWTS consumes more power to meet the standards in USCG mode. Thanks to all these calculations and formulation, shipping companies can similarly be able to deduct the operating cost of the UV-based BWTSs they plan to integrate into their ships.

ACKNOWLEDGMENTS

Authors would like to thank to the İnce Shipping and technical manager & DPA Mr. Ahmet Yaşar CANCA for providing technical data.

DATA AVAILABILITY STATEMENT

The authors confirm that the data that supports the findings of this study are available within the article. Raw data that support the finding of this study are available from the corresponding author, upon reasonable request.

CONFLICT OF INTEREST

The authors declared no potential conflicts of interest with respect to the research, authorship, and/or publication of this article.

ETHICS

There are no ethical issues with the publication of this manuscript.

REFERENCES

[1] E. Tsolaki, and E. Diamadopoulos, "Technologies for ballast water treatment: A review," Journal of Chemical Technology and Biotechnology, Vol. 85(1), pp. 19–32, 2010. [CrossRef]

[2] S. Olenin, S. Gollasch, S. Jonušas, and I. Rimkutė, "En-route investigations of plankton in Ballast water on a ship's voyage from the Baltic sea to the open Atlantic coast of Europe," International Review of Hydrobiology, Vol. 85(5–6), pp. 577–596, 2000. [CrossRef]

[3] International Marine Organization. "Ballast water management - the control of harmful invasive species." https://www.imo.org/en/MediaCentre/HotTopics/Pages/BWM-default.aspx Accessed Oct. 09, 2022.

[4] O. Casas-Monroy, R. D. Linley, P. S. Chan, J. Kydd, J. Vanden Byllaardt, and S. Bailey, "Evaluating efficacy of filtration + UV-C radiation for ballast water treatment at different temperatures," Journal of Sea Research, Vol. 133, pp. 20–28, 2018. [CrossRef]

[5] B. Sayinli, Y. Dong, Y. Park, A. Bhatnagar, and M. Sillanpää, "Recent progress and challenges facing ballast water treatment – A review," Chemosphere, Vol. 291, Article 132776, 2022. [CrossRef]

[6] T. Makkonen and T. Inkinen, "Systems of environmental innovation: Sectoral and technological perspectives on ballast water treatment systems," WMU Journal of Maritime Affairs, Vol. 20(1), pp. 81–98, 2021. [CrossRef]

[7] U. Ozdemir, "A quantitative approach to the development of ballast water treatment systems in ships," Ships and Offshore Structures, pp. 1–8, 2022. [CrossRef]

[8] E. Lakshmi, M. Priya, and V. S. Achari, "An overview on the treatment of ballast water in ships," Ocean & Coastal Management, Vol. 199, Article 105296, 2021. [CrossRef]

[9] W. A. Gerhard, K. Lundgreen, G. Drillet, R. Baumler, H. Holbech, and C. K. Gunsch, "Installation and use of ballast water treatment systems – Implications for compliance and enforcement," Ocean & Coastal Man-

agement, Vol. 181, Article 104907, 2019. [CrossRef]
[10] G. Altug, S. Gurun, M. Cardak, P. S. Ciftci, and S. Kalkan, "The occurrence of pathogenic bacteria in some ships' ballast water incoming from various marine regions to the Sea of Marmara, Turkey," Marine Environmental Research, Vol. 81, pp. 35–42, 2012. [CrossRef]
[11] A. Vorkapić, R. Radonja, and D. Zec, "Cost efficiency of ballast water treatment systems based on ultraviolet ırradiation and electrochlorination," Promet-Traffic & Transportation, Vol. 30(3), pp. 343–348, 2018. [CrossRef]
[12] I. Animah," A fuzzy analytical hierarchy process–weighted linear combination decision-making model for prioritization of ballast water treatment technologies by ship owners in Ghana." Proceedings of the Institution of Mechanical Engineers, Part M: Journal of Engineering for the Maritime Environment). United Kingdom: SAGE Publications Ltd. pp. 1276-1286, 2019. [CrossRef]
[13] M. Dogru, S. M. E. Demirci, R. Canımoglu, and H. Elcicek, "An overview of environmental impacts and treatment systems of ship ballast waters," Journal of Marine and Engineering Technology, Vol. 1(1), pp. 13–23, 2021.
[14] G. Vural and F. Yonsel, "Application of key performance indicators (KPI) to the selection of ballast water treatment systems," Gemi ve Deniz Teknolojisi, Vol. 208, pp. 5–30, 2017. [Turkish]
[15] H. Elcicek, A. Parlak, and M. Cakmakci, (2013)."Effect of ballast water on marine and coastal ecology," In C. Ozdemir, S. Sahinkaya, E. Kalıpcı, and M. K. Oden (Eds.), Digital Proceeding Of THE ICOEST'2013, Selcuk University Institute of Natural & Applied Science, pp. 454-463, 2013.
[16] J. Ren, "Technology selection for ballast water treatment by multi-stakeholders: A multi-attribute decision analysis approach based on the combined weights and extension theory," Chemosphere, Vol. 191, pp. 747–760, 2018. [CrossRef]
[17] P. G. Jang, B. Hyun, and K. Shin, "Ballast water treatment performance evaluation under real changing conditions," Journal of Marine Science and Engineering, Vol. 8(10), Article 0817, 2020. [CrossRef]
[18] W. A. M. Hijnen, E. F. Beerendonk, and G. J. Medema, "Inactivation credit of UV radiation for viruses, bacteria and protozoan (oo)cysts in water: A review," Water Research, Vol. 40(1), pp. 3–22, 2006. [CrossRef]
[19] S. Viitasalo, J. Sassi, J. Rytkönen, and E. Leppäkoski, "Ozone, ultraviolet light, ultrasound and hydrogen peroxide as ballast water treatments-experiments with mesozooplankton in low-saline brackish water," Journal of Marine Environmental Engineering, Vol. 8(1), pp. 35–55, 2005.
[20] E. Joyce, S. S. Phull, J. P. Lorimer, and T. J. Mason, "The development and evaluation of ultrasound for the treatment of bacterial suspensions. A study of frequency, power and sonication time on cultured Bacillus species," Ultrasonics Sonochemistry, Vol. 10(6), pp. 315–318, 2003. [CrossRef]
[21] C. B. Güney, "Balast suyu arıtım sistemlerinin incelenmesi," [Rep. No: DEN 2017/2], 2017. [Turkish]
[22] E. Mesbahi, "Latest results from testing seven different technologies under the EU MARTOB project: Where do we stand now?" In J. Matheickal, & S. Raaymakers (Eds.), 2nd International Ballast Water Treatment: R&D Symposium London, United Kingdom: Global Ballast Water Management Programme, International Maritime Organization. pp. 210–230, 2003.
[23] V. Başhan, H. İ. Sönmez, and G. Gonca, "Bir Yük gemisinin balast operasyonunun ekonomik ve ekolojik analizi," 1st International Congress on Ship and Marine Technology, İstanbul, Turkey, 2016, pp. 659–670. [Turkish]
[24] Optimarin, "Ballast water treatment," https://optimarin.com/ Accessed on Nov 27, 2022.
[25] Ship &Bunker, "Average bunker prices," https://shipandbunker.com/prices/av Accessed on Nov 27, 2022.

Environ Res Tec, Vol. 5, Issue. 4, pp. 357–368, December 2022

Environmental Research and Technology
https://ert.yildiz.edu.tr - https://dergipark.org.tr/tr/pub/ert
DOI: https://doi.org/10.35208/ert.1160713

Environmental Research & Technology

Research Article

Evaluation of Bartın river water quality index and suitability as irrigation water with physicochemical parameters

Gülten GÜNEŞ*

Department of Environmental Engineering, Bartın University, Bartın, Türkiye

ARTICLE INFO

Article history
Received: 11 August 2022
Revised: 19 November 2022
Accepted: 01 December 2022

Key words:
Water quality index, Irrigation water quality, Sodium adsorption ratio, Kelly index, Bartın River

ABSTRACT

In this study, it was aimed to determine the water quality of Bartın River and its usability as irrigation water. In order to evaluate the change of water quality according to the precipitation the samples were collected from 4 points in December and July months. pH, NO_3, SO_4, Cl^-, total phosphorus (TP), chemical oxygen demand (COD), suspended solid (SS), turbidity, some cations and metals were analyzed in the collected samples. The assessment of physicochemical parameters was made according to the Surface Water Quality Regulation. It was determined that SS and turbidity parameters increased after precipitation and 98% of turbidity was caused by SS. Cl^-, Na^+, K^+, Ca^{+2}, Mg^{+2}, SO_4^{-2}, TP were determined higher in the dry period. Although COD, total dissolved solid (TDS), electrical conductivity (EC), NO_3 were higher in the rainy season, the difference between the two periods is not much. According to the water quality index, water quality was poor at all sampling points during the rainy season. In the dry period, good quality was also determined at only 1 sampling point. COD is the parameter with the greatest effect on effective weight and water quality. Irrigation water suitability was evaluated with the indexes sodium adsorption ratio (SAR), (EC), %Na, magnesium ratio (MR), Kelly index (KI), potential salinity (PS) and total hardness (TH). River water is suitable as irrigation water in both periods according to SAR, %Na, MR, KI indexes. However, since the potential salinity (PS) value is greater than 3 μeq/L at the SP4 in the dry period, it is not suitable as irrigation water. Its total hardness value is >180 mg/L, so it is in the very hard water class.

Cite this article as: Güneş G. Evaluation of Bartın river water quality index and suitability as irrigation water with physicochemical parameters. Environ Res Tec 2022;5:4:357–368.

INTRODUCTION

Water resources are an important part of the ecological system and one of the natural resources necessary for the survival of humans and other living things [1, 2]. Today, as a result of rapid industrialization and rapid population growth, increasing domestic and industrial discharges and agricultural activities cause deterioration of water quality in natural water resources [3]. Water quality is closely related to human health, and organic compounds, toxic metals, nutrients, suspended solids and pathogens in water are important parameters that affect water quality [4]. Agricultural activities (excessive use of fertilizers), industrial and domestic wastewater discharges are the main

***Corresponding author.**
*E-mail address: ggunes@bartin.edu.tr

causes of nitrogen and phosphorus pollution in natural waters [5, 6]. Heavy metals are another type of pollutant found in natural waters and cause environmental problems by accumulating in the food chain [7]. The most important metals in terms of water pollution are zinc (Zn), arsenic (As), copper (Cu), lead (Pb), cadmium (Cd), mercury (Hg), nickel (Ni) and chromium (Cr). Heavy metals enter the river system through natural and anthropogenic activities [8]. The most important anthropogenic sources are industrial discharges, domestic wastewater, metal-containing fertilizers and pesticides [9, 10]. Since heavy metals cannot be decomposed in nature, they accumulate in animals and humans and cause undesirable effects. As, Pb, Cd are highly toxic even at low concentrations [11, 12]. Protection of water quality is also important in terms of determining the usability of river water as irrigation water. Irrigation water quality affects soil structure and plant growth. Especially in arid environments, low precipitation amount, high evaporation and use of inappropriate irrigation water cause salinity problem in soils [13] and excessive salinity causes soil degradation [14]. The chemical components in the irrigation water affect the plant in different ways, such as having a direct toxic effect on the plant, causing the plant to be without nutrients, or preventing the plant from taking nutrients from the soil [15, 16]. For this reason, irrigation water quality should be determined by different indexes such as electrical conductivity (EC), potential salinity (PS), sodium adsorption rate (SAR), sodium percentage (%Na), Kelly's Index (KI), magnesium ratio (MR). In this study, it was aimed to determine the water quality of the Bartın River with physicochemical parameters. Physicochemical water quality parameters were analyzed in water samples taken from different points of the river in rainy and dry periods, and the water quality index was calculated and the water quality classes were determined. The assessment of physicochemical parameters was made according to the Surface Water Quality Regulation (SWQR) [17]. In addition, the suitability of river water as irrigation water was evaluated by using indexes defined in the literature such as sodium adsorption rate, sodium percentage, magnesium ratio, potential salinity, Kelly's index.

MATERIALS AND METHODS

Sampling Area

Bartın River is located within Bartın Province in Turkey. Bartın is located in the western Black Sea Region and has a rugged geography. Its heights are covered with mountain rows reaching 1736 meters. The mountains are very steep, steep and rocky towards the beaches, although not high. The average rainfall is 69.3 mm and 111.3 mm for the summer and winter seasons. Sampling locations are shown in (Fig. 1) [18]. SP1, SP2 (water dept ≈ 2 m) and SP3 sampling points are located in the area of the river passing through the city center. At these three points, domestic wastewater discharges are effective. SP4 sampling point is on a different tributary of the river. At this point, water depth and bed width are higher (>5 m) than other points [18].

Sample Collection and Analysis

Water samples were collected immediately after heavy rain and snowfall in winter, in December, when the water level and flow rate increased. In the summer season, the samples were collected in July, when the rains were very ineffective and the river water level and flow rate decreased. Water samples were collected in high density polyethylene bottles. Bottles were washed within a solution of 10% nitric acid followed by repeated rinsing with distilate water and finally rinsing with ultrapure water prior to sampling [18]. Details on heavy metal analyzes have been explained in detail in the author's previous work [18]. For physicochemical analyzes, water samples were collected in accordance with the ISO 5667-3: 2018 [19] method. Before the water samples were collected, the plastic bottles were rinsed 3 times with distilled water and 1 time with sample water. All physicochemical analyzes were performed in accordance with the American Public Health Association Method [20]. Nitrate and sulfate analyzes were performed by UV VIS Spectrophotometer (HACH Lange 6000 DR) device according to spectrophotometric method, and chloride and COD analyzes were performed by titrimetric method. Turbidity was determined by the turbidimeter (Hach 2100 Q Portable Turbidimeter) according to the nephelometric method, and the color was determined by the Hach Lico 620 device according to the photometric method. pH, electrical conductivity, total dissolved solids (TDS) values were measured with Hanna (HI 9812-5) multi parameter probe. Suspended solid (SS) analysis was done by gravimetric method.

Evaluation of Data

River water quality was evaluated with the water hazard index [21] and water quality indexes [22]. The usability of river water as irrigation water was evaluated by sodium adsorption rate (SAR), magnesium ratio, sodium percentage, Kelly's index (KI), potential salinity (PS), and total hardness (TH) and electrical conductivity (EC) indexes. All calculations were made with Microsoft Excel 2016 and SPSS 26 programs.

Suitability of River Water as Irrigation Water

Salinity causes deterioration of soil quality [23]. For this reason, the suitability of river water as irrigation water was evaluated with the indexes sodium adsorption ratio (SAR), electrical conductivity (EC), sodium percentage (%Na), magnesium ratio (MR), kelly's index (KI), potential salinity (PS) and total hardness (TH). The formulas of the indexes and water quality classifications are shown in Table 1.

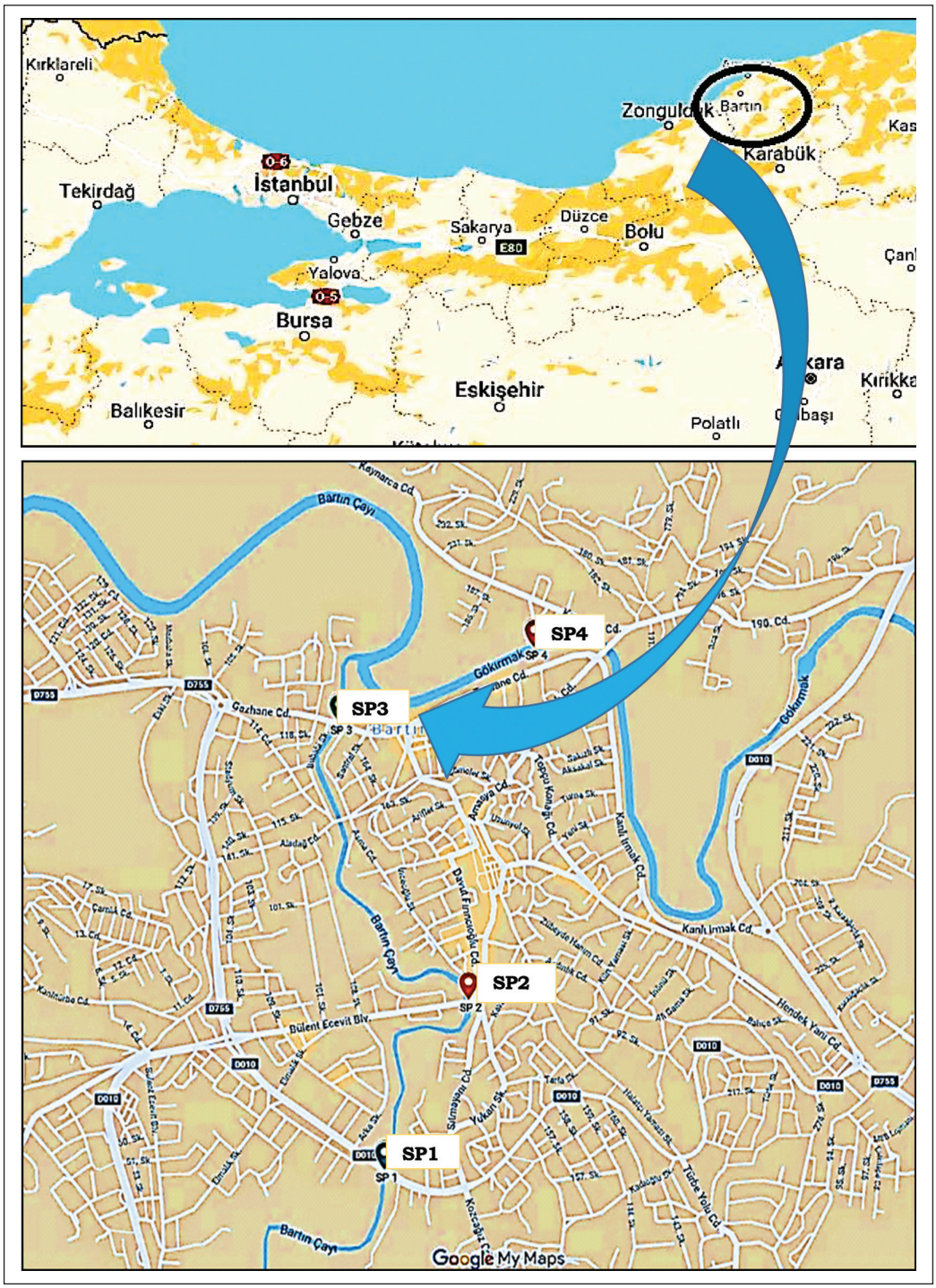

Figure 1. Location of sampling points [18].

Water Quality Index

The water quality index is used to determine and evaluate water quality. The influence of many water quality parameters is reduced to a single value. In other words, the water quality index can be defined as an indicator of the combined effect of many water quality parameters [30]. The WQI value calculated for each sampling point allows the sampling points to be classified according to different quality categories. Different water quality indexes have been used in the literature [22, 31]. In this study, WQI was calculated according to equation (1) [22]. The grading of water quality according to water quality indexes is shown in Table 2.

$$WQI = \sum SI_i \quad (1)$$

Table 1. Quality indexes for irrigation water (concentrations of all parameters are meq/L except EC (µs/cm) and TH (mg/L)

Index	Formula	Classification	Reference
Kelly Index	$KI = \frac{Na^{+1}}{Ca^{+2} + Mg^{+2}}$	<1 safe >1 unsafe	[24]
Sodium adsorption ratio (SAR)	$SAR = \frac{Na^{+1}}{\sqrt{\frac{Ca^{+2} + Mg^{+2}}{2}}}$	<10 excellent 10–18 good 18–26 doubtful >26 unsuitable	[25]
Sodium percentage (%Na)	$\% Na = \left(\frac{Na^{+} + K^{+}}{Ca^{+2} + Mg^{+2} + K^{+} + Na^{+}}\right) \times 100$	<20 excellent 20–40 good 40–60 permissible 60–80 doubtful >80 unsuitable	[26]
Magnesium ratio (MR)	$MR = \frac{Mg^{+2} \times 100}{Ca^{+2} + Mg^{+2}}$	<50 suitable >50 unsuitable	[27]
Potential salinity (PS)	$PS = Cl^{-} + 0.5SO_4^{-2}$	<3 suitable >3 unsuitable	[28]
Total hardness (TH)	$TH = (2.497Ca^{+2}) + (4.11Mg^{+2})$	<60 soft 60–120 medium hard 120–180 hard >180 very hard	[29]
Electrical conductivity (EC)		EC<250 excellent 250–750 good 750–2000 permissible 2000–3000 doubtful >3000 unsuitable	[25]

$$\boldsymbol{WQI} = \sum \boldsymbol{SI_i} \quad (2)$$

Where, W_i: the relative weight of ith parameter, w_i: the weight of ith parameter [22, 32–35] (Table 3), n: the number of parameters.

$$q_i = \frac{C_i}{S_i} \times 100 \quad (3)$$

Where, q_i: quality rating of ith parameter, C_i: concentration of each chemical parameter in each water sample in mg/l, S_i: drinking water standard for each chemical parameter in mg/L except for conductivity (µS/cm) and pH turbidity and colour.

$$SI_i = W_i \times q_i \quad (4)$$

SI_i: Sub-index of ith parameter;

The effective weight of each water quality parameter was calculated according to equation (5) to determine the parameter that has the greatest effect on the water quality index.

$$\boldsymbol{EW_i} = \frac{\boldsymbol{SI_i}}{\boldsymbol{WQI}} \boldsymbol{x100} \quad (5)$$

Where EW_i: Effective weight of i water quality parameter, SI_i: Subindex value of i water quality parameter.

Table 2. Water quality classification according to WQI values

WQI value	Water quality
<50	Excellent
50–100	Good water
100–200	Poor water
200–300	Very poor water
>300	Water unfit for drinking

Water Hazard Index

One of the indexes used to evaluate the impact of heavy metals on water quality is the water hazard index [21]. As shown in equation (6), this index is calculated by dividing the measured concentration of the metal by the maximum allowable value for drinking water [36]. According to the hazard index, the toxicity of water is categorized into 4 classes [21, 38]: WHI <5 (low to minimal toxicity), 5≤ WHI ≤10 (slightly toxic), 10≤ WHI ≤15 (moderately toxic) and WHI >15 (extremely toxic).

Table 3. Weight factors, unit weight values and effective weights (EW) of water quality parameters

	Si [36, 37]	wi (weight)	Wİ (relative weight)	EW% rainy	EW% dry	Mean EW %
pH	8.5	4	0.100	7.39	7.5	7.45
TDS	1000	4	0.100	3.09	2.85	2.97
EC	2500	1	0.025	0.62	0.57	0.6
SO_4^{-2}	200	4	0.100	1.35	1.86	1.6
NO_3^-	50	5	0.125	0.3	0.14	0.22
COD	10	4	0.100	80.38	77.81	79.09
Cl^-	250	3	0.075	0.15	1.46	0.8
Ca^{+2}	200	2	0.05	1.26	1.85	1.55
Mg^{+2}	30	2	0.05	0.8	1.78	1.29
Na^+	200	2	0.05	0.16	1.04	0.6
K^+	200	2	0.05	0.04	0.13	0.08
Mn	0.05	4	0.1	4.53	3.16	3.85
Cu	1	3	0.075	0.01	0.01	0.01
		Σwi= 40	ΣWi= 1.0			

Concentrations of all parameters are mg/L except for pH, EC (µs/cm).

$$WHI = \left\{\frac{Al}{0.2} + \frac{Fe}{0.3} + \frac{Mn}{0.05} + \frac{Cu}{1} + \frac{Zn}{0.3} + \frac{Cr}{0.05}\right\}/6 \quad (6)$$

RESULTS AND DISCUSSION

Evaluation of Physicochemical Water Quality Parameters

The results of physicochemical water quality parameters are shown in Table 4. It was determined that the suspended solid (SS) and turbidity parameters increased considerably after precipitation and 98% of the turbidity was caused by suspended solids. Suspended solid concentrations were determined to be 14.5 mg/L and 41.5 mg/L for dry and rainy periods, respectively [18]. In the previous study, although the dry period concentration was higher than the rainy period, it was determined that there was no significant difference between the two periods [39]. For this reason, it is thought that the soil particles carried from the surrounding land together with the precipitation waters increase the SS and turbidity. In addition, topographic features (slope, altitude) can partially affect the transport of pollutants from diffuse sources to the river [40]. The fact that the mountains around Bartın are quite steep and the land is quite rugged may affect the transport of materials from diffuse sources to the river during the rainy season. At the same time, the increased water flow rate after precipitation may cause resuspension of compounds from the sediment to the water column, thus increasing suspended solids and turbidity [41]. The highest values for SS and turbidity in the rainy season were determined in SP4. This point is located at a point where soil transport from the surrounding land is effective.

Electrical conductivity (EC) is a parameter directly related to dissolved solids in water. Total dissolved solids include inorganic salts (calcium, magnesium, potassium, sodium, bicarbonate, chloride, sulfates) and dissolved organic matters [42]. Salts can be of geogenic origin (decomposition of rocks) as well as anthropogenic origin (domestic/industrial wastewater discharge) [43]. EC was determined as 730 µs/cm in the dry period and 800 µs/cm after precipitation. According to the Surface Water Quality Regulation [17], the river is in the second quality water class in terms of EC. Although the average EC value is higher for the rainy season, there is no significant difference between the two periods. The highest average EC and TDS values were determined in SP4 in the dry period and in SP3 in the rainy period (Table 4). Precipitation waters can cause soil erosion and increase in the EC and TDS values in the river, and sometimes cause a decrease in these parameters with the effect of dilution [44]. In the dry season, the concentrations of EC, TDS, Na^+, Cl^-, K^+, Ca^{+2}, SO_4^{-2} were quite high in SP4 compared to other sampling points. This situation can be explained by the geological features of the river bed at this point. The same parameters were determined higher in SP 3 during the rainy period. This situation can be explained by 2 reasons: 1) due to the high flow rate, the compounds in the sediment move back to the water column 2) the composition of the soil particles carried around the sampling point. Contrary to this study, in a previous study in the river, TDS, EC values were determined to be higher in the dry period [39]. The difference between the results of both studies can be explained by the fact that the sampling points were different in this study and the rainy period samples were taken just after the precipitation.

Table 4. Results of physicochemical parameters

	Dry period					Rainy period					Irrigation[a] guideline
	SP1	SP2	SP3	SP4	Mean	SP1	SP2	SP3	SP4	Mean	
Suspended solid	24	9	12	13	14.5	35	39	37	55	42	
Temperature	26	25	26	26	26	6.0	6.0	6.0	7.0	6.3	
Turbidity	22.90	8.39	9.62	5.16	11.5	40	33	39	85	49	
Filtrate turbidity	0.33	0.81	0.29	1.09	0.6	1.06	0.50	0.88	2.32	1.19	
pH	8.20	7.90	7.90	8.30	8.1	8.30	8.50	8.30	8.60	8.4	8.5
EC	600	530	520	1270	730	660	570	1350	620	800	3000
TDS	290	260	260	640	363	330	290	670	310	400	2000
$NO3^-N$	0.17	0.17	0.13	0.17	0.16	0.37	0.34	0.36	0.38	0.36	10
SO_4^{-2}	40	40	40	70	48	48	37	35	27	37	960
Total phosphorus (TP)	0.10	0.29	0.20	ND	0.20	ND	ND	0.08	0.06	0.07	
COD	64	192	96	96	112.0	168	84	84	126	116	
Cl^-	18	20	22	196	64.0	15.0	6.93	4.50	2.50	7.2	1063
Na^+	28	26	26	135	54	8.79	8.68	9.19	6.24	8.2	919
K^+	6.50	6.42	5.22	8.43	6.6	2.22	2.20	2.39	1.53	2.1	2
Ca^{+2}	113	89.2	89.6	72.8	91.2	68	68.2	70	62	67	400
Mg^{+2}	12.2	9.58	8.85	23.5	13.53	5.86	5.77	6.12	8.14	6.47	60
Al	0.112	0.019	0.027	0.013	0.043	0.24	0.303	0.365	0.567	0.369	5
Fe	0.476	0.04	0.09	ND	0.202	0.307	0.323	0.41	0.47	0.378	5
Mn	0.017	0.013	0.043	0.00445	0.019	0.025	0.027	0.03	0.04	0.031	0.2
Ni	ND	ND	ND	ND	ND	0.009	ND	0.0058	0.0083	0.008	0.2
Cu	0.0029	0.0022	0.0043	ND	0.003	0.0018	0.0016	0.0021	0.0024	0.002	0.2
Zn	0.0062	0.0052	0.0117	ND	0.008	0.0072	0.0073	0.0076	0.0066	0.007	2

a [15], All units are mg/L except pH, turbidity (NTU) and EC (µs/cm).

Sulphate was determined to be 47 mg/L and 37 mg/L for the dry and rainy periods, respectively. The most important sources of sulfate in surface waters are atmospheric storage, bacterial oxidation of sulfur compounds, and sulfate-containing fertilizers [45]. In addition, wastewater discharges and the degradation of sediment and organic materials in the soil can cause sulfate compounds [46]. In this study, the decreasing SO_4^{-2} concentration during the rainy season can be explained by the diluting effect of precipitation.

Nitrogen and phosphorus are nutrients that cause eutrophication in surface waters [47]. In this study, NO_3^-N was determined to be 0.17 mg/L and 0.36 mg/L for dry and rainy periods, respectively. Since NO_3^-N is <3 mg/L, the river is in I. quality water class according to SWQR [17]. The seasonal variation of NO_3^-N depends on the amount of precipitation and the residence time of the water [48]. The water solubility of nitrate is high [49]. The transport of soil particles to the river by erosion is generally considered to be the most important nutrient source for rivers [50]. For this reason, the high concentration determined for the rainy period in this study can be explained by soil erosion from agricultural areas and the transport of animal wastes stored in open areas to the river with rainfall waters. The absence of soil erosion in the dry period when the water temperature is high and the increase in the rate of biochemical reactions may cause a decrease in NO_3^-N. It has also been reported by [51] that water temperature may have an effect on the decomposition rate of NO_3^-. Again, in the rainy period, the transition of the compounds in the sediment to the water column may cause an increase in nitrate concentration. Reference [52] reported that the NO_3^- concentration is higher in the summer season, when precipitation is effective, compared to the winter season. In the previous study in the river [39], it was reported that the NO_3^- concentration was 0.91 mg/L and 0.96 mg/L for the rainy and dry periods, respectively. For this reason, soil erosion and resuspension from the sediment to the water column during the rainy period are considered to be important.

Since the TP concentration was determined to be 0.2 mg/L and 0.1 mg/L for dry and rainy periods, respectively. According to SWQR [17], it is in the water class in the 2th quality class. Wastewater discharges and agriculture and livestock have been reported as the most important sources of phosphates [53]. In this study, domestic wastewater discharges, animal wastes and fertilizers are considered as the most important sources of total phosphorus. TP concentration could not be detected in SP4 during the dry period. It is a far point from wastewater discharges, and the depth and amount of water is higher than other points. The highest concentration in the dry period was determined in SP2 and SP3, where domestic wastewater discharges are intense. It is thought that detergents, which are the most important source of phosphorus in domestic wastewater, cause an increase in TP concentration in the dry period. Similar results have been reported by [48], and [52] in the literature. In the rainy season, it is thought that leaks from manure and animal wastes, which are defined as diffuse sources, will cause TP in the river. In the rainy season, it is thought that leakages from manure and animal wastes, which are defined as diffuse sources, cause TP in the river.

Chemical oxygen demand (COD) is the parameter used to determine organic pollution in waters [54]. In this study, the average COD concentration was determined as 112 mg/L and 116 mg/L for dry and rainy periods. According to SWQR [17], it is in the water class in the 4th quality class. Domestic wastewater discharges and natural organic substances carried by precipitation waters are considered as the causes of organic pollution in water. During the dry period, the highest concentration was determined in SP2. Domestic wastewater discharges are effective at this sampling point, and at the same time, the water depth and flow rate decrease in summer. COD concentrations in the rainy season were arranged as SP1>SP4>SP2=SP3. It is thought that natural organic materials carried into the river from the surrounding land during the rainy season affect the COD parameter [55]. The concentration of natural organic matter varies depending on many factors such as topography, season, flood, drought, and human activity [37]. In a previous study in the Bartın River, the rainy season concentration (115 mg/L) was slightly higher [39], and close to the concentration measured in this study. In another study conducted in the Aksu River, it was reported that the average COD concentrations for the rainy and dry periods were 28.81 mg/L (13.40–157.6 mg/L) and 32.55 mg/L (15.14–178.09) mg/L, respectively [56]. The mean concentrations for Pazarsuyu Stream (Giresun) and Karasu (Aksaray) and Coruh Rivers (Bayburt) were reported as 7.07 (1.54–17.67) mg/L [57], 9.42 (<10–45.38) mg/L [58] and 3.59 mg/L [59], respectively.

It has been reported that the COD concentration in the Umguza River (Zimbabwe), where wastewater discharges are made, varies in the range of 55–381.2 mg/L [53]. In a study conducted in the Nile river, COD was reported as 11.8 mg/L and 9.7 mg/L in winter and summer seasons, respectively [13]. It was determined to be 114.7 mg/L and 151 mg/L in the summer (rainy period) and winter seasons, respectively in Karnaphuli River (Bangladesh) [44].

Table 5. WQI values and quality classification

Sampling point	WQI Rainy		WQI Dry	
1	193	Poor	89	Good
2	108	Poor	214	Very poor
3	113	Poor	124	Poor
4	153	Poor	133	Poor

Statistical Evaluation

It was determined whether there was a statistically significant difference between the concentrations determined for the rainy and dry periods at the sampling points. According to Shapiro-Wilk normality test, it was determined that Temperature (T), EC, TDS, NO_3^-, Mg^{+2}, Cl^-, Ni, Na^+, Cu and Zn did not show normal distribution ($p<0.05$). In addition, since the Skewness-Kurtosis coefficients for T, EC, TDS, NO_3^-, Ni, Cu varied in the range of -2 and +2 [60, 61], these parameters were considered to have a normal distribution. It was determined that suspended solid (SS), turbidity, pH, SO_4^{-2}, Ca^{+2}, Al, Fe, TP, COD, K^+, Mn showed normal distribution ($p>0.05$). According to the Mann-Whitney U test, the concentration difference between rainy and dry periods for Mg^{+2}, Cl^-, and Na^+ was statistically significant ($p<0.05$), while for Zn it was insignificant ($p>0.05$). Independent Sample T-Test, which is a parametric test, was applied for other parameters. According to the independent sample T-test, the concentration difference between rainy and dry periods for suspended solid, turbidity, pH, Ca^{+2}, Al, K^+, temperature and NO_3^- is statistically significant ($p<0.05$). The concentration difference between the two periods for Fe, Mn, TP, COD, EC, TDS is not statistically significant ($p>0.05$).

Evaluation of Water Quality Index

In order to determine the suitability of river water as drinking water, the water quality index was calculated in both periods and the results are shown in Table 5. According to WQI values, water quality was determined in the poor category at all sampling points during the rainy season. It was determined that the water quality was lower in SP1 and SP4. In the dry period, it was determined that it was good only in SP1, poor in SP3 and 4, and very poor in SP2. The effective weights (EW) of water quality parameters are shown in Table 3. The parameter with the highest EW value is COD (79%). Although the nitrate relative weight is the highest parameter, the EW value is low. These results show that COD, in other words organic pollution, is the main parameter affecting the water quality of the river.

Table 6. Irrigation water quality index values for the rainy season

Rainy	SP1	SP2	SP3	SP4	Mean
SAR	0.27	0.27	0.28	0.20	0.26
KI	0.10	0.10	0.10	0.07	0.09
%Na	10.20	10	10.30	7.60	9.53
MR	12	12	13	18	13.75
PS	0.34	0.34	0.36	0.24	0.32
TH	194	194	200	189	194.25
EC	660	570	1350	620	800

Table 7. Irrigation water quality index values for the dry season

Dry	SP1	SP2	SP3	SP4	Mean
SAR	0.68	0.69	0.70	3.52	1.40
KI	0.19	0.21	0.22	1.05	0.42
%Na	17.4	19.6	19.6	52.2	27.2
MR	15	15	14	35	19.75
PS	1.10	0.99	1.01	5.22	2.08
TH	332	262	260	278	283
EC	600	530	520	1270	730

Evaluation of the Water Hazard Index

In order to evaluate the toxicity of heavy metals in river water, the water hazard index was calculated according to the concentrations of Al, Fe, Mn, Cu, Cr, Zn [18]. Since Cr could not be detected at any sampling point during the dry period, it was not included in the calculation. The water hazard index was calculated to be 0.23 (0.03–0.5) for the dry period and 0.83 (0.46–0.88) for the rainy period. The lowest WHI value in the dry period was determined for SP4. At this point, determination of only Al and Fe may result in lower WHI value. The highest WHI was determined in SP1 (WHI=0.5) and the contribution of Fe was higher. In the rainy period, on the contrary to the dry period, the highest WHI value (0.88) was determined in SP4 and the lowest in SP1 (0.46). The elements with the highest impact at both sampling points are Al and Fe, which is thought to be related to the transported soil particles carried into the river. It was determined that metals could cause minimal toxicity since WHI <5 determined for both periods. In a study conducted in Ghana, WHI values were reported in the range of 0.68–5.9 for surface waters [38].

Evaluation of Suitability as Irrigation Water

According to the irrigation water criteria, the K^+ concentration exceeded the limit value (2 mg/L) at all sampling points. In the dry season, the average concentration (6.6 ml/L) is approximately 3 times the limit value (2 mg/L) (Table 4). For the rainy season, the average K^+ concentration (2.1 mg/L) is acceptable at the limit value. All other parameters are suitable for irrigation water criteria (Table 4). When the suitability of EC values in terms of irrigation water was evaluated, it was determined that 3 of the sampling points for each period were good (EC=250–750 µs/cm) and one of them was permissible (EC=750–2000 µs/cm). In another study conducted in Porsuk and Felent Streams, 3 of the surface water samples in the rainy period and 5 in the dry period were determined to be of good quality [62].

The results of the irrigation water quality indexes are shown in Table 6 and Table 7. Concentrations of all parameters were used as meq/L in calculations except EC (µs/cm) and TH (mg/L). Sodium percentage (%Na) is an index used to determine the sodium hazard in irrigation water [63]. Excess sodium in the irrigation water is adsorbed by the ion exchange points in the soil matrix, and as a result of this process, Ca^{+2} and Mg^{+2} ions are released into the soil. This causes a decrease in the infiltration capacity of the soil [23]. For this reason, %Na is calculated to determine the suitability of water as irrigation water [26]. In this study, the average %Na was determined to be 9.5% and 27% for the rainy and dry periods, respectively. Since the %Na values were <20% at all sampling points during the rainy season, it was determined that the river water was of excellent quality as irrigation water at all sampling points. In the dry period, it was determined to be of good quality in SP4 and other permissible sampling points. In another study, the %Na value was reported as 20% for rainy and dry periods [62]. In the study conducted at 5 sampling points in the Murat River (Euphrates basin), it was reported that the %Na values varied between 23.1 and 58.7 [64]. In another study, %Na values were reported in the range of 52.8 to 54.6 in Güllübağ irrigation pond (Uşak) [65].

As explained above, excess Na^+ ion causes a decrease in soil permeability and deterioration of soil structure. The sodium adsorption rate (SAR) is important in determining the Na^+ ion to be adsorbed by the soil. If the SAR ratio of the irrigation water is high, the ability of the soil to form stable aggregates will decrease [66], and its infiltration and permeability properties will decrease and cause problems with plant growth [65]. In this study, the SAR value varied between 0.68–3.52 (1.4) in the dry period and between 0.2–0.28 (0.26) in the rainy period. Since SAR<10 at all sampling points, Na^+ does not pose a hazard in water samples. It can be said that river water is suitable for all crops and all kinds of soils [67] except for sodium sensitive crops. SAR values for Porsuk and Felent streams have been reported in the range of 0.25–0.8 in the rainy season and 0.21–0.56 in the dry season. For the Murat River, SAR values have been reported in the range of 0.68–4.19 meq/L [64]. In the study conducted in the Güllübağ Dam Pond in Uşak, it was reported that the SAR values ranged from 3.1 to 3.5 [65].

One of the indexes used to determine the suitability of irrigation water is the magnesium ratio (MR). Excess magnesium in the soil increases the salt level of the soil and negatively

affects plant growth [62]. The magnesium ratio was determined to be 19.8 and 13.8 for the dry and rainy periods, respectively. Since the values for both periods were <50, it was determined that the river water was suitable as irrigation water. The highest magnesium ratio was determined in SP 3 in the dry period and in SP 1 in the rainy period. The mean MR was reported as 36 for Güllübağ Irrigation Pond [65], and between 31.52–44.68 for Porsuk and Felent Streams [62].

Kelly's Index is one of the indexes used to evaluate irrigation water quality [68]. Since Kelly index was less than 1 at all sampling points in both periods, it was determined Similarly, other researchers have reported KI in the range of 0.07–0.14 [62] and 0.94–1.0 [65] that river water was suitable as irrigation water.

The potential salinity (PS) index is calculated based on the Cl^- and SO_4^{-2} anions. Potential salinity values varied between 0.99–5.22 meq/L and 0.24–0.36 meq/L in the dry and rainy periods, respectively. Since PS <3 at all sampling points during the rainy season, they are suitable as irrigation water. In the dry season, only the 4th sampling point is not suitable as irrigation water (PS>3 meq/L). The high Cl^- and SO_4^{-2} anions at this sampling point in the dry period caused the PS value to be high. High Cl^- concentration in irrigation water may cause toxicity to plants. Since Cl^- is not adsorbed by the soil, it is transported with soil water and is taken up by plants and accumulated in their leaves [13] and causes toxicity. Similarly, in the study conducted in the irrigation pond, PS values were determined in the range of 4.41–5.72 meq/L, and the value in July was found to be higher than March and May [65]. In another study, mean PS values for December and June were determined as 1 meq/L and 0.79 meq/L [62].

Total hardness is related to $CaCO_3$ compounds of Ca^{+2} and Mg^{+2} in water. TH values were determined to be 283 mg/L and 194 mg/L for the dry and rainy periods, respectively. According to the classification made by [29], river water is in the very hard water class as irrigation water, since TH>180 mg/L at all sampling points in both periods. The widespread presence of dolomite ($CaCO_3$, $MgCO_3$) in the geological formation of the study area is considered to be the most important cause of water hardness.

CONCLUSION

It was determined that the increase in SS and turbidity concentrations after precipitation was significant. While the rainy season concentration of SS is about 3 times of the dry period, the turbidity is about 4 times. Considering the sampling point where these parameters are the highest, it is thought that soil transport from the surrounding land is effective. The fact that 98% of the turbidity is caused by SS also confirms this idea. It is thought that SS concentration is also effective in parameters such as bed width and water flow rate. The larger the bed width and the water depth of SP4, the higher the SS concentration may result. While dissolved salts such as Na^+, Mg^{+2}, K^{+1}, Ca^{+2}, Cl^-, SO_4^{-2} are higher in the dry period, the higher EC and TDS concentrations in the rainy period indicate that natural organic substances are carried by precipitation waters. The higher COD concentration during the rainy season confirms this idea. According to the water quality index, it was determined that the water was of good quality at only SP1 and during the dry period. According to the water hazard index calculated for heavy metals, it has been determined that metals may cause low toxicity. When all physicochemical parameters were compared with the limit values reported for irrigation waters, it was determined that only K^+ exceeded the limit value at all sampling points, especially in the dry period. According to the SAR, %Na, MR, Kelly Indexes related to Na^+, K^+, Ca^{+2}, Mg^{+2} ions, it was determined that the river water was suitable as irrigation water. However, according to the potential salinity (PS) index related to Cl^- and SO_4^{-2}, the river is not suitable as irrigation water at the SP4 in the dry period. According to the total hardness index, the river water was categorized at the very hard water class (>180 mg/L) at all sampling points. River water, NO_3^-, TP, Al, Fe, Mn, Ni, Cu, Zn in terms of 1st quality water class according to the Regulation on Surface Water Quality Management. In terms of electrical conductivity, the second quality is in the water class. According to the regulation, the 1st and 2nd class waters are defined as high quality and low-contaminated waters, respectively. According to the water quality index, river water is in the 4th quality water class in terms of COD. 4th grade water is defined as very contaminated water. For this reason, organic pollution was effective in the river. It is thought that domestic wastewater discharge and spread resources (especially in rainy period) affect organic pollution in the river. Fully prevention of domestic wastewater discharge will also reduce organic pollution. According to the statistical analysis, the concentration difference between rainy and dry periods for suspended solid, turbidity, pH, Ca^{+2}, Al, K^+, Mg, Cl^-, Na^+, and NO_3^- is statistically significant unlike Fe, Mn, Zn, TP, COD, EC, TDS ($p>0.05$).

ACKNOWLEDGMENT

This study was supported by Bartın University Scientific Research Coordinator (Project number: 2018-FEN-A-018).

DATA AVAILABILITY STATEMENT

The author confirm that the data that supports the findings of this study are available within the article. Raw data that support the finding of this study are available from the corresponding author, upon reasonable request.

CONFLICT OF INTEREST

The author declared no potential conflicts of interest with respect to the research, authorship, and/or publication of this article.

ETHICS

There are no ethical issues with the publication of this manuscript.

REFERENCES

[1] N. Al-Ansari, "Management of water resources in Iraq: perspectives and prognoses," Engineering, Vol. 5, pp. 667–684, 2013. [CrossRef]

[2] Z. Wang, Q. Su, S. Wang, Z. Gao, and J. Liu, "Spatial distribution and health risk assessment of dissolved heavy metals in groundwater of eastern China coastal zone," Environmental Pollution, Vol. 290, Article 118016, 2021. [CrossRef]

[3] S. N. Sinha, D. Paul, and K. Biswas, "Effects of Moringa oleifera Lam. and Azadirachta indica A. Juss. leaf extract in treatment of tannery effluent," Our Nature, Vol. 14, pp. 47–53, 2016. [CrossRef]

[4] D. Paul, and S. N. Sinha, "Isolation and characterization of phosphate solubilizing bacterium Pseudomonas aeruginosa KUPSB12 with antibacterial potential from river Ganga, India," Annals of Agrarian Science, Vol. 15, pp. 130–136, 2016. [CrossRef]

[5] N. E. Pettit, T. D. Jardine, S. K. Hamilton, V. Sinnamon, D. Valdez, P. M. Davies, M. M. Douglas, and S. E. Bunn, "Seasonal changes in water quality and macrophytes and the impact of cattle on tropical floodplain waterholes," Marine and Freshwater Research, Vol. 63, pp. 788–800, 2012. [CrossRef]

[6] V. Rodrigues, J. Estrany, M. Ranzini, V. Cicco, J. Martín-Benito, J. Hedo, and M. Lucas-Borja, "Effects of land use and seasonality on stream water quality in a small tropical catchment: the headwater of Córrego Água Limpa, São Paulo (Brazil)," Science of the Total Environment, Vol. 622/623, pp. 1553–1561, 2018. [CrossRef]

[7] S. M. Praveena, A. Z. Aris, and M. Radojevic, "Heavy metals dyanamics and source in intertidal mangrove sediment of Sabah, Borneo Island," Environment Asia, Vol. 3, pp. 79–83, 2010.

[8] O. Akoto, T. N. Bruce, and G. Darko, "Heavy metals pollution profiles in streams serving the Owabi reservoir," African Journal of Environmental Science and Technology, Vol. 2(11), pp. 354–359, 2008.

[9] R. Reza, and G. Singh, "Heavy metal contamination and its indexing approach for river water," International Journal of Environmental Science and Technology, Vol. 7(4), pp. 785–792, 2010. [CrossRef]

[10] S. A. Abbasi, N. Abbasi, and R. Soni, "Heavy metals in the environment," Mittal Publications, 1998.

[11] R. Nicolau, C. A. Galera, and Y. Lucas, "Transfer of nutrients and labile metals fromthe continent to the sea by a small Mediterranean river," Chemosphere, Vol. 63, pp. 469–476, 2006. [CrossRef]

[12] K. M. Mohiuddin, K. Otomo, Y. Ogawa, and N. Shikazono, "Seasonal and spatialdistribution of trace elements in the water and sediments of the Tsurumi river in Japan," Environmental Monitoring And Assessment, Vol. 184, pp. 265–279, 2012. [CrossRef]

[13] A. M. Abdel-Satar, H. Manal, A. K. Waed, R. Alahmad, W. M. Yousef, H. R. Alsomadi, and T. Iqbal, "Quality assessment of groundwater and agricultural soil in Hail region, Saudi Arabia," Egyptian Journal of Aquatic Research, Vol. 43, pp. 55–64, 2017. [CrossRef]

[14] H. Alfaifi, A. S. El-Sorogy, S. Qaysi, A. Kahal, S. Almadani, F. Alshehri, and F. K Zaidi, "Evaluation of heavy metal contamination and groundwater quality along the Red Sea coast, southern Saudi Arabia," Marine Pollution Bulletin, Vol. 163, Article 111975, 2021. [CrossRef]

[15] R. S. Ayers, and D. W. Westcot, "Water quality for agriculture," Irrigation and drainage Paper 29. Food and Agriculture Organization of the United Nations. Rome, Vol. 29, pp. 1–117, 1985.

[16] D. R. Rowe, and I. M. Abdel-Magid. "Handbook of Wastewater Reclamation and reuse," CRC Press, Inc. pp. 550, 1995.

[17] Surface Water Quality Regulation (SWQR), "Water quality report," Official Gazette Date/Number: 10.08.2016/29797.

[18] G. Gunes, "The change of metal pollution in the water and sediment of the Bartın River in rainy and dry seasons," Environmental Engineering Research, Vol. 27(2), Article 200701, 2022. [CrossRef]

[19] ISO 5667-3:2018, "Water quality Sampling Part 3: Preservation and handling of water samples," https://www.iso.org/standard/72370.html Accessed on Dec 15, 2022.

[20] APHA, "Standard methods for the examination of water and waste water (22nd ed.)," American Public Health Association, 2012.

[21] T. N. Nganje, A. Edet, S. Cuthbert, C. I. Adamu, and A. S. Hursthouse, "The concentration, distribution and health risk from potentially toxic elements in the soil-plant-water system developed on black shales in SE Nigeria," Vol. 165, Article 103806, 2020. [CrossRef]

[22] P. Tirkey, T. Bhattacharya, S. Chakraborty, and S. Baraik, "Assessment of groundwater quality and associated health risks: A case study of Ranchi city, Jharkhand, India," Groundwater for Sustainable Development, Vol. 5, pp. 85–100, 2017. [CrossRef]

[23] T. G. Alharbi, "Identification of hydrogeochemical processes and their influence on groundwater quality for drinking and agricultural usage in Wadi Nisah, Central Saudi Arabia," Arabian Journal of Geosciences, Vol. 11, Article 359, 2018. [CrossRef]

[24] W. P. Kelley, "Use of saline irrigation water," Soilscience, Vol. 95(6), pp. 385–391, 1963. [CrossRef]

[25] L. A. Richards, "Diagnosis and improvement of saline and alkali soils," United States Department of Agriculture, 1954. [CrossRef]

[26] Wilcox, L. V. "Classification and use of irrigation water," United States Department of Agriculture, Circular, Vol. 696, pp. 19, 1955.
[27] K. V. Paliwal, "Irrigation with saline water," Monogram No. 2 (New Series). IARI, pp. 198, 1972.
[28] L. D. Doneen, "Notes on water quality in agriculture," Published as a water science and engineering paper 4001, Department of Water Science and Engineering, University of California, 1964.
[29] C. N. Dufor, and E. Becker, "Public water supplies of the100 largestcities in the United States, 1962: U.S. Geological Survey," Water-Supply Paper, Article 1812, 1964.
[30] R. K. Horton, "An index number system for rating water quality," Journal Water Pollution Control Federation, Vol. 37, 300–305, 1965.
[31] M. Masocha, T. Dube, and T. Dube, "Integrating microbiological and physico-chemical parameters for enhanced spatial prediction of groundwater quality in Harare," Physics and Chemistry of the Earth, Vol. 112, pp. 125–133, 2019. [CrossRef]
[32] S. M. Khan, and A. R. Kumar, "Geogenic assessment of Water Quality Index for the groundwater in Tiruchengode Taluk, Namakkal District, Tamilnadu, India," Chemical Science Transactions, Vol. 2(3), pp. 1021–1027, 2013.
[33] M. Al-hadithi, "Application of water quality index to assess suitability of groundwater quality for drinking purposes in Ratmao-Pathri Rao watershed, Haridwar District, India," American Journal of Scientific and Industrial Research, Vol. 3(6), pp. 395–402, 2012. [CrossRef]
[34] K. Ambiga, and R. A. Durai, "Use of geographical information system and water quality index to assess groundwater quality in and around Ranipet area," International Journal of Advance Engineering and Researchand Studies, pp. 1–8, 2013.
[35] G. S. Rao, and G. Nageswararao, "Assessment of groundwater quality using water quality index, Archives of Environmental Science, Vol. 7, pp. 1–5, 2013.
[36] World Health Organization. Guidelines for drinking water quality: Fourth edition ıncorporating the first addendum. World Health Organization, 2017.
[37] N. Ibrahim, and H. A. Aziz, "Trends on natural organic matter in drinking water sources and its treatment," International Journal of Scientific Research in Environmental Sciences, Vol.2(3), pp. 94-106, 2014. [CrossRef]
[38] A. Ewusi, E. D. Sunkari, J. Seidu, and E. Coffie-Anum, "Hydrogeochemical characteristics, sources and human health risk asseSSent of heavy metal dispersion in the mine pit water–surface water–groundwater system in the largest manganese mine in Ghana," Environmental Technology & Innovation, Vol. 26, Article 102312, 2022. [CrossRef]
[39] G. Gunes, "The change of physicochemical properties of bartın river in rainy and dry periods," Dokuz Eylul University Faculty of Engineering Journal of Science And Engineering, Vol. 21(63), pp. 761–774, 2019.
[40] M. Shibata, S. Sugihara, A. D. Mvondo-Ze, S. Araki, S. Funakawa, "Effect of original vegetation on nutrient loss patterns from Oxisol cropland in forests and adjacentsavannas of Cameroon," Agriculture, Ecosystems & Environment, Vol. 257, pp. 132–143, 2018. [CrossRef]
[41] N. Ejaz, H. N. Hashmi, and A. R. Ghumman, "Water quality assessment of effluent receiving streams in Pakistan: a case study of Ravi river," Mehran University Research Journal of Engineering and Technology, Vol. 30(3), pp. 383–396, 2011.
[42] C. N. Sawyer, P. L. McCarty, and G. E. Parkin, "Chemistry for environmental engineering," 4th ed., Mc Graw-Hill, 1994.
[43] N. J. Raju, P. Patel, D. Gurung, P. Ramb, W. Gossel, and P. Wycisk, "Geochemical assessment of groundwater quality in the Dun valley of central Nepal using chemometric method and geochemical modelling," Groundwater for Sustainable Development, Vol. 1, pp. 135–145, 2015. [CrossRef]
[44] M. Ali, L. Ali, S. Islam, and Z. Rahman, "Preliminary assesment of heavy metals in water and sediment of Karnaphuli River, Bangladesh," Environmental Nanotechnology, Monitoring & Management, Vol. 5, pp. 27–35, 2016. [CrossRef]
[45] K. Wayland, D. Long, D. Hyndman, B. Pijanowski, S. Woodhams, and K. Haack, "Identifying relationships between Baseflow geochemistry and land use with synopticsampling and R-mode factor analysis," Journal of Environmental Quality, Vol. 32, pp. 180, 2003. [CrossRef]
[46] S. Varol, and A. Davraz, "Evaluation of the groundwater quality with WQI (Water Quality Index) and multivariate analysis: a case study of the Tefenni plain (Burdur/ Turkey)," Environmental Earth Sciences. Vol. 73, pp. 1725–1744, 2015. [CrossRef]
[47] O. Minareci, M. Ozturk, O. Egemen, and E. Minareci, "Detergent and phosphate pollution in Gediz River, Turkey," African Journal of Biotechnology, Vol. 8(15), pp. 3568–3575, 2009.
[48] J. D. Pérez-Gutiérrez, J. O. Paz, and M. L. M. Tagert, "Seasonal water quality changes in on-farm water storage systems in a south-central U.S. agricultural watershed," Agricultural Water Management, Vol. 187, pp. 131–139, 2017. [CrossRef]
[49] Y. Anteneh, G. Zeleke, and E. Gebremariam, "Assessment of surface water quality in Legedadie and Dire catchments," Acta Ecologica Sinica, Vol. 38, pp. 81–95, 2018. [CrossRef]

[50] H. Blanco, and Lal, R., (Eds.), "Principles of soil conservation and management," Springer, 2008.
[51] C. J. Mikan, J. P. Schimel, and A. P. Doyle, "Temperature controls of microbial respiration in arctic tundra soils above and below freezing," Soil Biology and Biochemistry, Vol. 34 (11), pp. 1785–1795, 2002. [CrossRef]
[52] G. Xu, P. Li, K. Lu, Z. Tantai, j. Zhang, Z. Ren, X. Wang, K. Yu, P. Shi, and Y. Cheng, "Seasonal changes in water quality and its main influencing factors in the Dan River basin," Catena, Vol. 173, pp. 131–140, 2019. [CrossRef]
[53] A. Chinyama, R. Ncube, and W. Ela, "Critical pollution levels in Umguza River, Zimbabwe," Physics and Chemistry of the Earth, Vol. 93, pp.76–83, 2016. [CrossRef]
[54] S. A. M. Ali, T. W. Hsiang, R. Tair, A. A. Naser, and F. Sualin, "Surface sediment analysis on heavy metals in coastal area of Ums – Tuaran, Sabah," Borneo Science, Vol. 34, pp. 6–10, 2014.
[55] C. J. Hwang, S. Krasner, and M. Sclimenti, "Polar NOM: characterization, DBPs, treatment," American Water Works Association. 2002.
[56] Ş. Şener, E. Şener, and A. Davraz, "Evaluation of water quality using water quality index (WQI) method and GIS in Aksu River (SW-Turkey)," Science of the Total Environment, Vol. 584–585, pp. 131–144, 2017. [CrossRef]
[57] F. Ustaoğlu, and Y. Tepe, "Water quality and sediment contamination assessment of PazarsuyuStream, Turkey using multivariate statistical methods and pollution indicators," International Soil and Water Conservation Research, Vol 7, pp. 47–56, 2019. [CrossRef]
[58] A. Alver, and E. Baştürk, "Evaluation of Karasu River water quality in terms of different water quality indexes," Süleyman Demirel University Journal of Natural and Applied Sciences, Vol. 23, pp. 488–497, 2019.
[59] N. Birici, G. Karakaya, T. Şeker, M. Küçükyılmaz, M. Balcı, N. Özbey, and M. Güneş, "Evaluation of Coruh river (Bayburt) water quality in accord with water pollution control regulation," International Journal of Pure and Applied Sciences, Vol. 3(1), pp. 54–64, 2017.
[60] J. Hair, W. C. Black, B. Babin, and R. E. Anderson, "Multivariate data analysis (7th ed.)." Upper Saddle River, Pearson Educational International, 2010.
[61] B. M. Byrne, "Structural equation modeling with AMOS: Basic concepts, applications, and programming," Routledge, 2010
[62] B. A. Berhe, M. Çelik, and U. E. Dokuz, "Investigation of irrigation water quality of surface and groundwater in the Kutahya plain, Turkey," Journal of Mineral Research and Exploration, Vol. 150, pp. 147–163, 2015. [CrossRef]
[63] E.K. Maskooni, M. Naseri-Rad, R. Berndtsson, and K. Nakagawa, "Use of heavy metal content and modified water quality index to assess groundwater quality in a semiarid area," Water, Vol. 12, Article 1115, 2020. [CrossRef]
[64] A. D. Demir, Ü. Şahin, and Y. Demir, "Trend analysis and agricultural perspective availability of water quality parameters at Murat river," Yuzuncu Yıl University Journal of Agricultural Sciences, Vol. 26, pp. 414-420, 2016.
[65] E. B. Kapdı, and B. B. Aşık, "Evaluation of irrigation pond water in terms of surface water quality and irrigation water quality; Sample of Güllübağ pond in Usak province," Journal of Biosystems Engineering, Vol. 2 (1), pp. 52–69, 2021.
[66] S.V. Sarath Prasanth, N.S. Magesh, K.V. Jitheshlal, N. Chandrasekar, and K. Gangadhar, "Evaluation of groundwater quality and its suitability for drinking and agricultural use in the coastal stretch of Alappuzha District, Kerala, India," Applied Water Science, Vol. 2 pp.165–175, 2012. [CrossRef]
[67] C. A. Vishwakarma, R. Sen, N. Singh, P. Singh, V. Rena, K. Rina, and S. Mukherjee, "Geochemical characterization and controlling factors of chemical composition of spring water in a part of Eastern Himalaya," Journal Geological Society of India, Vol. 92, pp.753-763, 2018. [CrossRef]
[68] J. Wu, H. Zhou, S. He, and Y. Zhang, "Comprehensive understanding of groundwater quality for domestic and agricultural purposes in terms of health risks in a coal mine area of the Ordos basin, north of the Chinese Loess Plateau," Environmental Earth Sciences, Vol. 78(15), Article 446, 2019. [CrossRef]

Environ Res Tec, Vol. 5, Issue. 4, pp. 369–379, December 2022

Environmental Research and Technology
https://ert.yildiz.edu.tr - https://dergipark.org.tr/tr/pub/ert
DOI: https://doi.org/10.35208/ert.1163939

Environmental Research & Technology

Research Article

Characterization and dye adsorption effectiveness of activated carbon synthesized from olive pomace

Fatma DENİZ*[1], Öyküm BAŞGÖZ[2], Ömer GÜLER[3], Mehmet Ali MAZMANCI[1]

[1]*Department of Environmental Engineering, Mersin University, Mersin, Türkiye*
[2]*Department of Metallurgical and Material Engineering, Mersin University, Mersin, Türkiye*
[3]*Department of Machinery and Metal Technologies, Munzur University, Tunceli, Türkiye*

ARTICLE INFO

Article history
Received: 18 August 2022
Revised: 23 November 2022
Accepted: 07 December 2022

Key words:
Activated carbon; Adsorption; Aqueous solution; Dye removing; Olive pomace

ABSTRACT

Studies, about products obtained from agricultural wastes, have increased within the scope of zero waste studies. The olive pomace is produced as a result of olive oil production. In the present study, activated carbon was synthesized using the olive pomace taken from the olive pomace processing plant operating with a three-phase process. The synthesized activated carbon characterization was performed using Scanning Electron Microscope (SEM), Fourier-Transform Infrared Spectroscopy (FT-IR), Brunauer – Emmett – Teller (BET), and X-Ray Crystallography (XRD) devices. Olive pomace activated carbon (OPAC) was used for the adsorption of dye from an aqueous solution. The adsorption efficiency of the OPAC was investigated. The initial pH value of dye solution (6–9), the amount of activated carbon (0.5 and 1.0 g/L), and initial dye concentration (600–1200 mg/L) were optimized. Also, adsorption kinetic and isotherm calculations were evaluated. The optimum parameters were found as the original pH value (pH=8) of dye solutions, OPAC amount of 1.0 g/L and the initial concentration of 1000 mg/L. The Langmuir isotherm model and the pseudo-second-order kinetic model were found as the most suitable models. It can be said that the synthesized material can be used at dye removing from wastewater.

Cite this article as: Deniz F, Başgöz Ö, Güler Ö, Mazmancı MA. Characterization and dye adsorption effectiveness of activated carbon synthesized from olive pomace. Environ Res Tec 2022;5:4:369–379.

INTRODUCTION

The olive oil production is one of the important agro-industries [1]. There are 900 million olive trees on an area of approximately 10 million hectares in the world. According to the averages in last five seasons, olive oil production is around 2.91 million tons [2]. Olive oil production process generates wastewater and pomace, which are difficult to treat. The amount and characteristics of wastes vary according to the production method. Two different processes, classical and continuous, are applied in olive oil production. In the classical production process, oil is extracted using hydraulic presses. Olives are washed with water, crushed and kneaded by adding water. The olive paste is then pressed

***Corresponding author.**
*E-mail address: fatmadeniz@mersin.edu.tr

and oil, wastewater (black water) and solid phase (olive pomace) are separated. The continuous production process is based on the separation of the oil from the olive paste by centrifugation. It consists of feeding, washing, crushing and olive paste preparation units. Depending on the centrifuge used during production, there are two different processes: three-phase and two-phase. In the three-phase process, water is used. After the process, three phases are formed: oil, black water and olive pomace. Since process water is added, three times more wastewater is generated than in the conventional process. In the two-phase process, no process water is added. After the process, two phases are formed as oil and olive pomace. Black water is not formed. Most of the black water is in the pomace [3].

Pomace consists of olive, seed, and pulp. Approximately, 270 and 250 kg of anhydrous pomace is produced per ton of olive in two-phase and three-phase processes, respectively [4]. An average of 3.3 million tons of pomace waste in two-phase systems and 3.06 million tons in three-phase systems (at 5% humidity) are produced annually. The results show that every year a high amount of pomace is produced in the world. Pomace has been used to synthesize activated carbon after various processes to reuse. The effectiveness of olive pomace activated carbon (OPAC) in removing various pollutants such as cadmium II, chromium III, arsenic III, phenol, toluene, iodine, methylene blue, etc. from wastewater has been investigated [5]. Dyes are one of these pollutants. If the wastewater containing dye is discharged to the receiving environment without treatment, the dyes in the wastewater are also released to the receiving environment. Dyes are toxic to living organisms. Since it gives color to the water and prevents sunlight from entering the water, it hinders the vital activities of aquatic organisms. For this reason, discharging wastewater containing dye to receiving environments without treatment causes a critical environmental problem. Many studies have been carried out on treating wastewater containing dye [6–9]. Methods such as adsorption, sedimentation, filtration, coagulation, electrocoagulation, biodegradation, electrochemical oxidation, Fenton process, ozonation, sonolysis, wet air oxidation, electrical discharges, photocatalysis, photolysis were applied for the treatment of such wastewaters [6]. Among these methods, adsorption is an effective, simple, and frequently preferred purification technique [10]. The type of adsorbent and the method of synthesis of adsorbent affect the cost of adsorption processes. Activated carbon is generally used in adsorption processes for high porosity, sufficient pore size, large specific surface area, and high mechanical strength. These properties of activated carbon make it one of the reliable adsorbents since it provides a high-efficiency treatment of many organic and inorganic pollutants [11–14]. However, the high price of commercial activated carbons increases the cost of treatment. Therefore, agricultural wastes are used to synthesize the activated carbon for reducing the cost [11]. There are studies in which agricultural wastes are used as activated carbon after various processes. Rice husk, citrus peel, eggshells, sawdust, cigarette waste, alfalfa, by-products from industries (e.g., sugar cane, paper, tea leaves, and others), palm tree cob, plum kernels, nutshell, wood, corn cob cottonseed shell, rubber seed shell, almond shell, coconut shell, bamboo powder, sunflower seed shell, peach kernel, and olive pomace can be given as examples of these agricultural wastes [11, 15]. These wastes are used as adsorbent to treat wastewater.

The aim of this study was to demonstrate the effectiveness of reusing an agricultural waste as an adsorbent in removing dye from an aqueous solution. OPAC synthesized from pomace was used as an adsorbent. The novelty of this study is that commercial dyes used at paper industry were studied.

EXPERIMENTAL

Carbonization Experiments

The olive pomace used in this study was taken from the three-phase pomace processing plant located in Mersin, Türkiye. The moisture content of olive pomace was calculated from the weight loss after drying at 103–105 °C for 3 hours and determined as 3.7%. Next, dried pomace (49.83 gr) was calcined in a specially produced metal screwed crucible at 800 °C for 1440 minutes using a muffle-type furnace.

The flow chart of the OPAC synthesis was given in Figure 1. It was determined that there was a weight loss of 21.41% in the pomace after the calcination process. Before the calcination process, as a result of the carbon-sulfur (Eltra CS-580) analysis, it was determined that the pomace contained 52.01% carbon and 0.025% sulfur. It was determined that the calcined pomace had 88.98% carbon and 0.038% sulfur.

Adsorption Experiments

Three different water-based dyes (DS-00102:WB dispensing yellow base: JR05 (DS-00102); DS-00203:WB dispensing orange base: JR05 (DS-00203); DS-00502:WB dispensing blue base: JR05 (DS-00502)) and the mixture of three water-based dyes solution (V: V: V; 1: 1: 1) were used. The dyes were taken from a cardboard factory in Mersin, Türkiye.

The pH, OPAC amount, and initial dye concentration effect were studied (Table 1). The sample volume was 200 mL. The original pH level of the aqueous solutions of the dyes was approximately 8. The pH values of solutions were adjusted using 0,1 and 0,01 M H_2SO_4 and NaOH solutions. OPAC was added to the samples after pH adjustment. The magnetic stirrer (at 150 rpm) was used for the mixing process, and samples were taken for color measurement at intervals of 15 minutes. Collected samples were centrifuged at 6000 rpm for 5 minutes for the color measurement of the supernatant. The color measurement was carried out using Hach Lange, DR3900 model spectrophotometer.

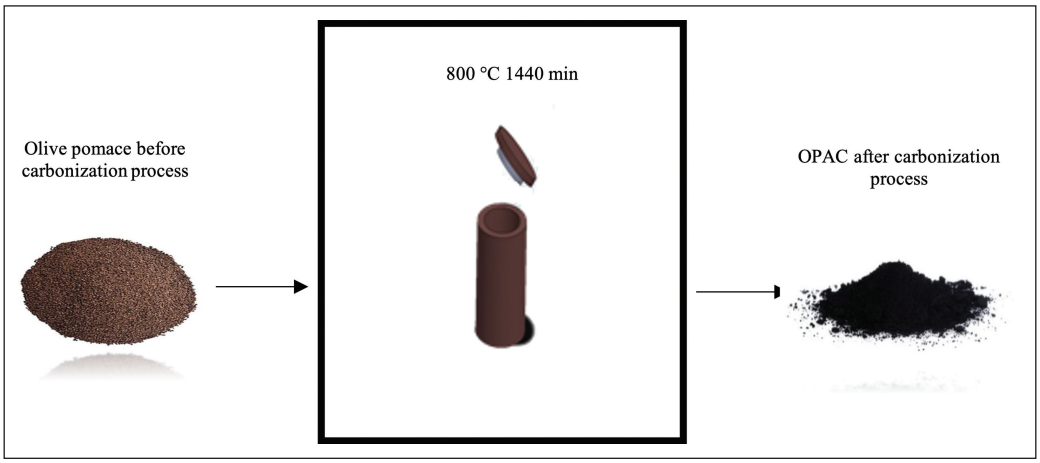

Figure 1. OPAC synthesis flow chart.

Table 1. Adsorption experiments conditions

	The effect of pH	The effect of OPAC amount
pH	6, 8*, 9	Optimum pH
AC amount (g AC/200 mL)	0,5	0.5, 1.0

*: Original pH value of aqueous solutions of dyes.

The dye removal efficiency was calculated using Equation 1.

$$Removal\ \% = \frac{C_0 - C_t}{C_0} \times 100 \quad (1)$$

where C_t (mg/L) is the concentration at t time, and C_0 (mg/L) is the initial concentration.

Isotherm (Langmuir and Freundlich) and kinetic models (pseudo-first and second order, and intraparticle diffusion) were calculated.

RESULTS AND DISCUSSION

Characterization of the OPAC

Structural properties of OPAC were analyzed with a Scanning Electron Microscope (SEM) (FEI-Quanta 650). Surface functional groups were investigated with Fourier Transform Infrared Spectrometer (FT-IR) (Jasco-6700). The surface area and pore volume of the OPAC were determined using The Brunauer – Emmett – Teller (BET) method by N_2 adsorption at -196 °C with surface area-pore size analyzer (Micrometrics Surface Area and Porosity-TriStar II). The structural feature of OPAC was examined by X-Ray Diffraction Measurement (XRD) (PANalytical-EMPYREAN) using Cu Kα as a radiation source.

The SEM images of OPAC was given in Figure 2. The surface of the OPAC was smooth. This is the reason that total surface area was low as mentioned below. The sizes of the chars changed at wide range. Carbonization parameters such as the temperature, time and pressure affect the textural properties of synthesized material [16, 17]. At this study carbonization method was not optimized. The optimization of carbonization conditions can develop surface properties and adsorption capacity of material.

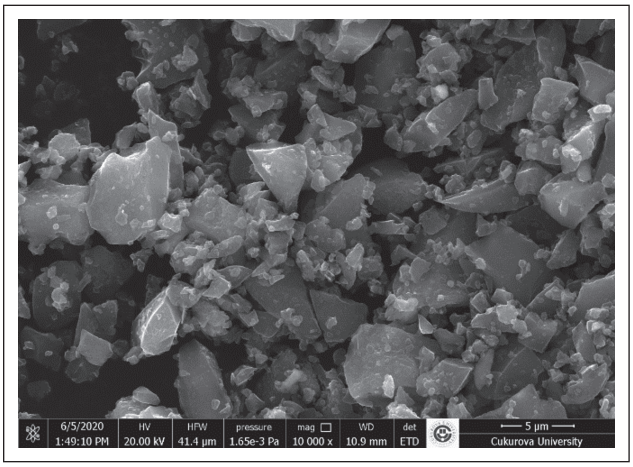

Figure 2. SEM images of OPAC.

The FT-IR spectra for OPAC were shown in Figure 3. For the O-H bond of most carboxylic acids, a characteristic broad property is observed in the range 3300–2500 cm^{-1}, with a secondary absorption close to 2600 cm^{-1} and overlapping the C-H stretching region [18]. Highly non-absorbent peaks above the region between 2700 and 2400 are not associated with any compound has multiple bounds. Hydride vibrations such as thiols and sulfides (SH), boranes (BH), phosphines (PH), silanes (SiH) and arsines (AsH) often cause these absorptions [18]. The peak at 2663 cm^{-1} is indicative for O-H stretching [19]. The peak at 2330 cm^{-1} can represent CO_2 [19]. The religion between 2260–2100 cm^{-1} (2113 cm^{-1}) represents C≡C stretch [18]. The peak at 1995 cm^{-1} may represent transition metal carbonyl that has the bands between 2100–1800 cm^{-1}. The multi-bonded CO group gives an intense absorption band

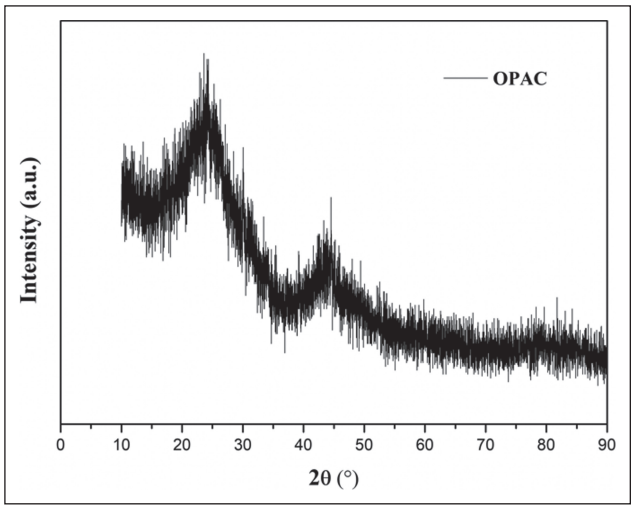

Figure 4. XRD plot of OPAC.

in regions close to 2000 cm^{-1}. The complexity and actual location of bands depend on the compounds nature [18]. C=O stretching vibrations at 1769 cm^{-1} peak represents of aldehydes, ketones, lactones or carboxyl groups [20]. Between 2000–1660 cm^{-1} is the aromatic combination in general [18]. Bands range between 1650 and 1750 cm^{-1} represent esterified and free carboxyl groups that may be convenient to identify pectins [21].

BET analysis results were given in Table 2. When the results were compared with other studies, it was seen that the calculated values for OPAC were lower [11, 12, 22]. It was thought that this situation was caused by the carbonization method applied. Temperature change, carbonization time, and used chemicals create differences in the surface properties of the obtained activated carbon [22].

XRD graph of OPAC was given in Figure 4. In the XRD graph, strong and weak peaks were observed at 2θ=25° and 2θ=45° respectively. The pores formed by the decomposition of carbon along the direction of the graphic structures form the peak at 2θ=25°. This structure produces an more stable aromatic carbon than amorphous carbon [23, 24].

Table 2. Properties of OPAC

Total pore volume (cm^3/g)	Total pore area (m^2/g)	Surface area BET (m^2/g)
0,04976	26,962	17,5958

Adsorption Experiments

The Effect of Initial pH

One of the essential parameters in adsorption experiments is the pH value of solution [25]. The ionization degree of the pollutant compound and the adsorbent surface charge are affected by the pH of the solution [12, 26]. In addition, hydronium (H_3O^+) and hydroxide (OH^-) ions in the solution are adsorbed by the adsorbent, which affects the removal capacity of pollutants [27]. Researchers have studied the adsorption of various pollutants at pH ranging between 2–10.9 in different studies [5]. In this study, three initial pH values (6, 8, and 9) were studied. The experiments were performed at initial concentrations of 912, 820, and 996 mg/L for DS-00102, DS-00203, and DS-00502 dyes, respectively. Color removal findings for each sample were given in Figure 5.

Dye removal efficiencies of pH 6, 8, and 9 were close to each other for each dye. The maximum dye removal was carried out in the first 15 minutes. In the following minutes, the amount of dye remained at approximately the same values. The highest removal efficiencies for DS-00102, DS-00203, and DS-00502 dye solutions were calculated as 32, 37, and 55%, respectively.

The removal efficiencies obtained at pH 6, 8, and 9 indicate that dye removal can be done in this range. The different removal efficiencies for each dye were attributed to the differences in the dye surface load. Since pH 8 was the original pH, it was determined as the optimum pH value. Similar pH values (8.10–8.53) were studied by Pala et al. [28] for color removal. In addition, there are studies using similar [29, 30], acidic [12, 31], and basic [27, 30] pH values in adsorption studies with activated carbon obtained from olive pomace. The difference in pH is attributed to the difference in pollutants and carbonization methods.

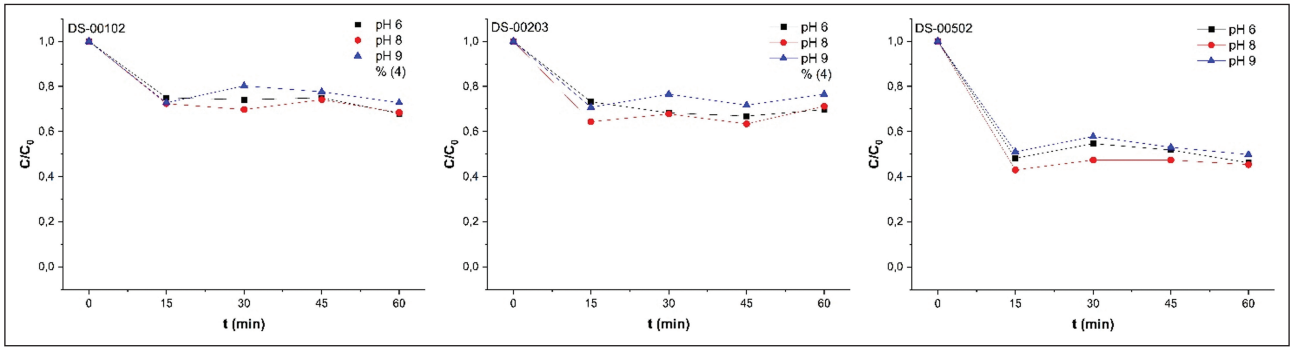

Figure 5. pH value optimization for color removal from DS-00102, DS-00203, and DS-00502 dye solutions (0.5 g OPAC/200 mL).

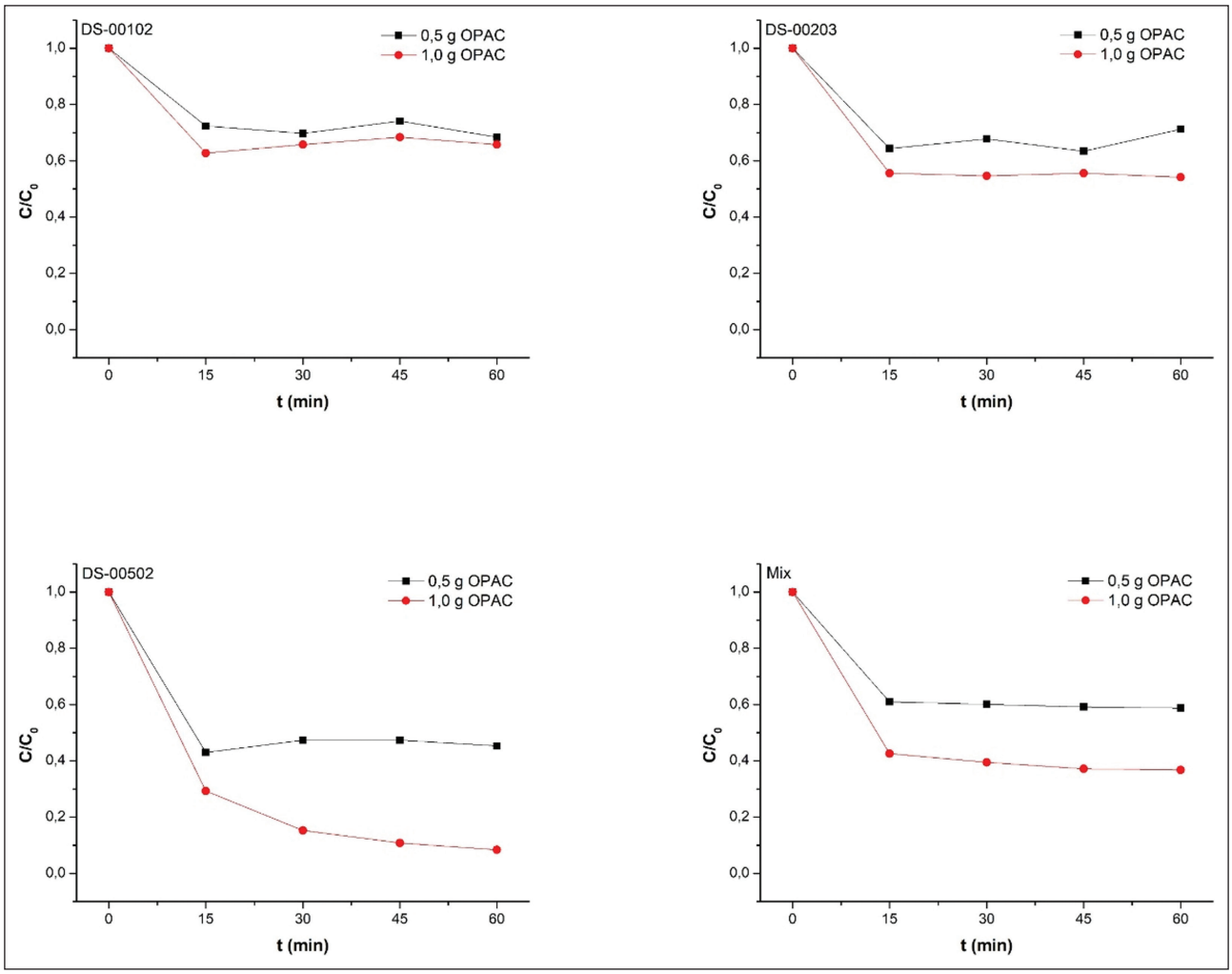

Figure 6. OPAC amount optimisation for colour removal from DS-00102, DS-00203, DS-00502, and mix dye solutions (pH=8).

The pH change was monitored during the experiment. After 60 minutes, the pH increased from 6 and 8 to 8.3 and 9.6, respectively.

The Effect of OPAC Amount

The experiments investigating the effect of OPAC amount (0.5 and 1.0 g/200 mL) were carried out at pH 8. The initial dye concentrations were 912, 820, 996, and 892 mg/L for the DS-00102, DS-00203, DS-00502, and mix samples (V: V: V; 1: 1: 1), respectively. Color removal efficiencies for different amounts of OPAC (0.5 and 1.0 g/200 mL dye solution) for each dye were given in Figure 6.

As the OPAC amount was increased from 0.5 g to 1.0 g, the color removal efficiency increased. The highest removal efficiencies with 1.0 g OPAC for DS-00102, DS-00203, DS-00502, and mixture samples were calculated as 37, 46, 92, and 63%, respectively. Among all dye solutions, the highest removal was achieved in DS-00502 (92%). Increasing the OPAC amount from 0.5 to 1.0 g increased the removing efficiency of the DS-00102 and DS-00203 dyes by 5 and 9%, respectively. However, the increasing amount of OPAC in the DS-00502 dye solution increased the removal from 55% to 92%. Compared to previous studies, it was seen that higher removal efficiency was performed in a shorter time [5].

The Effect of Initial Dye Concentration

To examine the effect of initial dye concentration, DS-00502 dye solutions were prepared as 600, 800, 1000, and 1200 mg/L concentrations. OPAC (1.0 g/200 mL) was added to the solutions. Removal of 97, 93, 92 and 85% was obtained for 600, 800, 1000 and 1200 mg/L, respectively. When the initial dye concentration increased from 600 mg/L to 1200 mg/L, the adsorption capacity of OPAC increased from 110 to 207 mg/g. The highest dye removal was achieved at 1200 mg/L (1020 mg/L). If the remaining dye amount considered, the least amount of dye (18 mg/L) remained from initial concentration of 600 mg/L. However, the most effective removal was achieved with 1000 mg/L. In all experiments, 15 minutes was enough for the system to reach equilibrium. Time-dependent removal results were given in Figure 7.

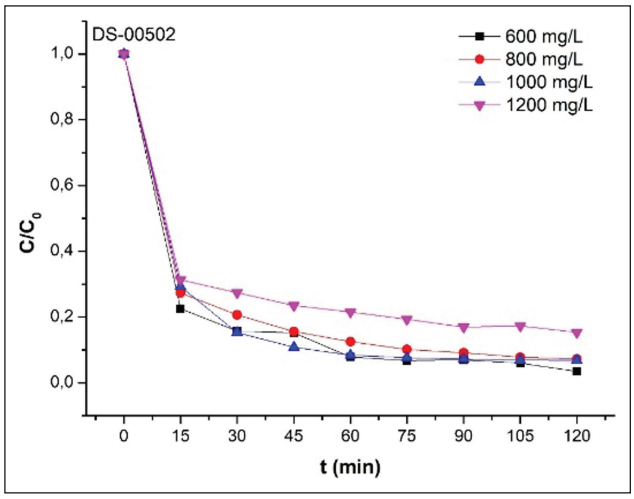

Figure 7. Initial dye concentration optimization for color removal from DS-00502 (pH=8 and 1.0 g OPAC /200 mL).

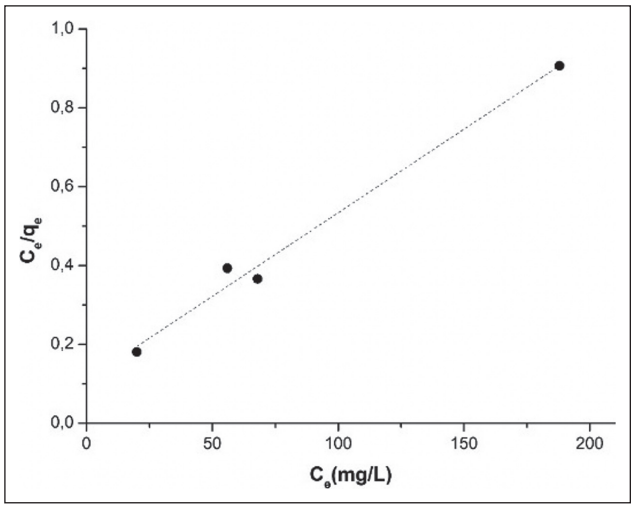

Figure 8. Langmuir isotherm curve.

For isotherm and kinetic calculations, DS-00502 dye solutions in four different initial concentrations (600, 800, 1000, and 1200 mg/L) were used. Experiment conditions were determined as pH 8, 1.0 g/200 mL OPAC and a reaction time of 120 minutes. The capacity of OPAC at equilibrium was calculated using Equation 2.

$$q_e=(C_0-C_e)V/W \quad (2)$$

where C_e (mg/L) is the equilibrium concentration and C_0 is the initial concentration, W (g) OPAC amount and V (L) the sample volume. The capacity of OPAC at time t was calculated using Equation 3.

$$q_t=(C_0-C_t)V/W \quad (3)$$

where C_t (mg/L) is the concentration at time t.

Adsorption Isotherms

Langmuir [32] and Freundlich [33] isotherms were calculated in this study.

Table 3. Parameters of isotherm models

Langmuir isotherm			Freundlich isotherm		
q_{max} (mg/g)	R^2	K_L (L/mg)	n	R^2	K_F
238.09	0.9886	0.0382	3.4530	0.8877	47.5663

Table 4. The comparison of maximum adsorption capacity with previous studies

Activated carbon material	Removed pollutant	Max. adsorption capacity (mg/g)	References
This study	Dye	238.09	
Olive Stones	Phenol	58.8	[12]
Clay	Acid blue 29	104.83	
	Methylene blue	178.64	[17]
Olive Stone	Phenol	51	[31]
	Methylene blue	714	
Olive-seed waste residue	Methylene blue	263	[41]
Acorns		127	
Olive seeds	Methylene blue	115	[42]
Olive-waste cakes	Iodine	1495	[43]
	Methylene blue	490	

Langmuir isotherm states that the surface of the adsorbent has a certain number of active sites with the same energy, and the adsorption is reversible. According to this model, adsorption is limited to a single molecular layer [12]. Equilibrium is reached when the adsorption rate is equal to the desorption rate. The Langmuir isotherm accepts adsorption in a single layer, and the surface is homogeneous. It fills the homogeneous surface until the equilibrium moment. At equilibrium, the maximum amount of adsorption is reached [12, 34].

The Langmuir equation was given in Equation 4.

$$C_e/q_e=1/(q_{max}K_L)+C_e/q_{max} \quad (4)$$

where K_L is the Langmuir constant and q_m (mg/g) is the maximum adsorption capacity of OPAC [35].

The graph of C_e versus C_e/q_e was given in Figure 8.

$1/q_{max}$ obtained from Figure 8 gives the slope [36]. Langmuir parameters were shown in Table 3.

Freundlich isotherm is applied to determine adsorption characteristics on heterogeneous surfaces [36]. Equations were given in Equations 5 and 6.

$$q_e=K_F C^{1/n} \quad (5)$$

$$Logq_e=LogK_F+1/n\ LogC_e \quad (6)$$

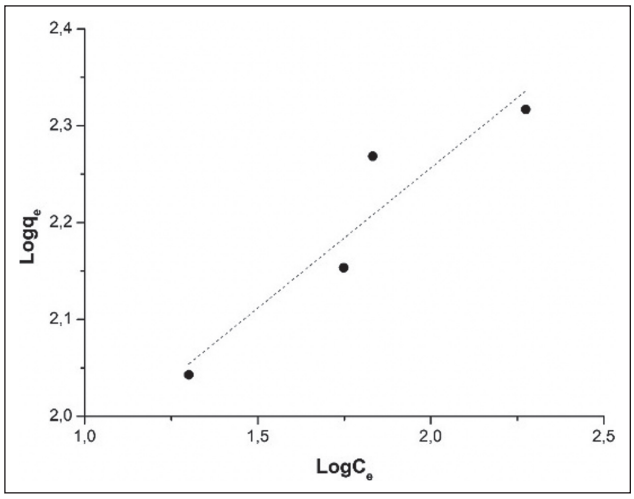

Figure 9. Freundlich isotherm curve.

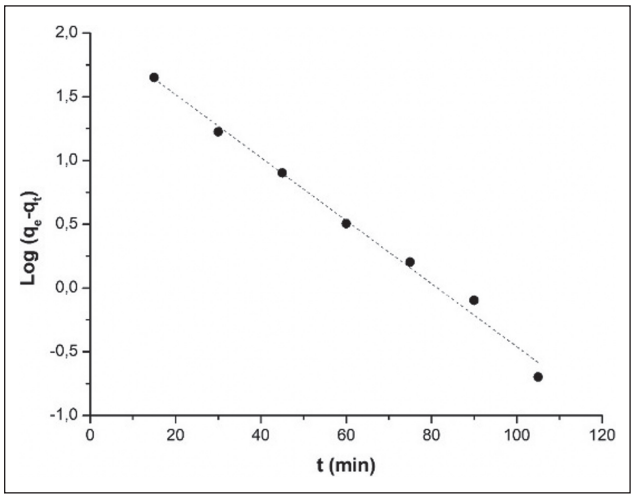

Figure 11. Pseudo-first-order curve.

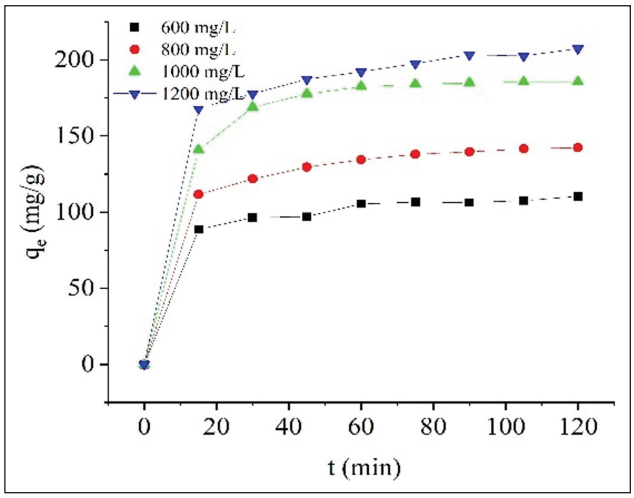

Figure 10. Adsorption capacities of OPAC.

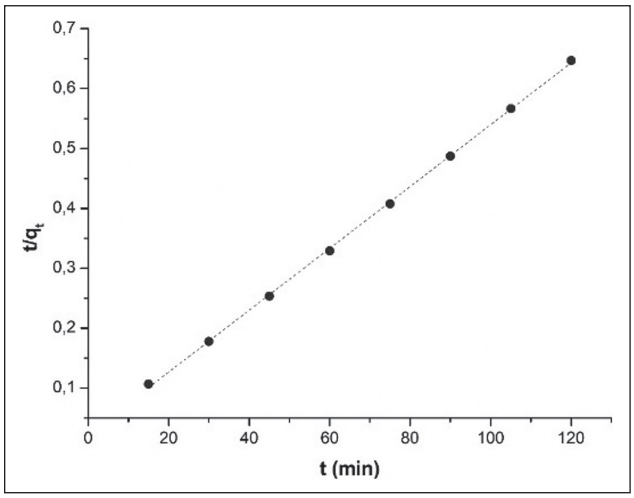

Figure 12. Pseudo-second-order curve.

where 1/n is heterogeneity factor and K_F (L/g) is the Freundlich constant [36].

The logarithmic form of Freundlich equation can be expressed as a line equation whose slope is 1/n and where it intersects the axis Log K_f [12]. The graph of Log C_e versus Log q_e was given in Figure 9, and the parameters of the Freundlich isotherm were shown in Table 3.

The R^2 value obtained with the Langmuir isotherm is higher (R^2=0.9886) than Freundlich isotherm (Table 1). Adsorption occurs equally on the active sides of adsorbent, according to the Langmuir isotherm [37]. Similar findings were obtained in the color removal study of Pala et al. [28] and the phenol removal study of Bohli et al. [12].

The adsorption capacity of OPAC according to initial dye concentration was given in Figure 10. The maximum adsorption capacities were found as 110.4, 142.4, 185.6 and 207.4 for 600, 800, 1000 and 1200 mg/L initial dye concentrations, respectively. The results showed that the dye adsorption capacity increased with increasing initial dye concentration. In Langmuir isotherm calculations, maximum adsorption capacity q_{max} was

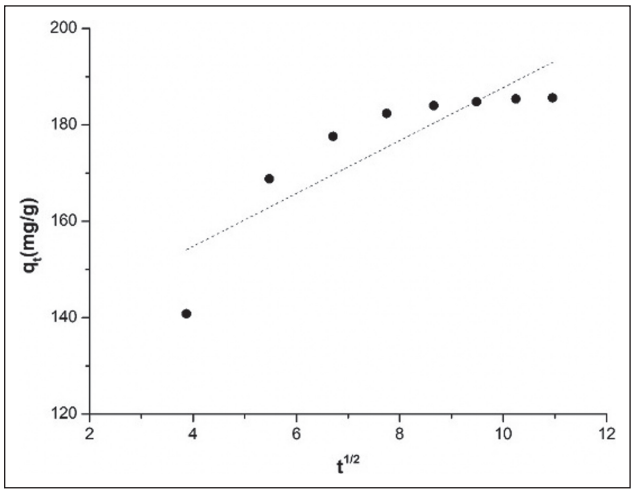

Figure 13. Intraparticle diffusion curve.

Table 5. Parameters of kinetic models

Initial concentration (mg/L)	Pseudo-first-order				Pseudo-second-order				Intra particle diffusion	
	q_e (mg/g) cal.	q_e (mg/g) exp.	k_1 (min^{-1})	R^2	q_e (mg/g) cal.	q_e (mg/g) exp.	k_2 (min^{-1})	R^2	k_d (mg/g.min)	R^2
600	29.11	110.4	0.0237	0.9178	113.63	110.4	0.0015	0.9988	2.9485	0.9262
800	66.51	142.4	0.0382	0.9644	149.25	142.4	0.001	0.9997	4.3481	0.9506
1000	102.92	185.6	0.0568	0.9919	192.3	185.6	0.0011	0.9997	5.4924	0.7553
1200	63.22	207.4	0.0262	0.9492	217.39	207.4	0.0007	0.9991	5.5461	0.9810

found as 238.09 (Table 3). Adsorption isotherm models give the theoretical maximum adsorption capacity [38, 39]. OPAC did not reach the theoretical maximum adsorption capacity. It means that OPAC was not fully covered by dye and still has surface area for more adsorption [38, 40].

There are dye removal studies with similar q_{max} values [41]. In dye removal studies, methylene blue removal has been mostly studied. The maximum adsorption capacities of other studies were shown Table 4. The removal capacities of activated carbon can be different according to some properties or conditions such as used material, carbonization temperature, carbonization time, removed pollutant, initial dye concentration, initial pH, surface area of activated carbon, the amount of activated carbon, etc.

Adsorption Kinetics

Pseudo-first and second-order, and intraparticle diffusion model kinetic parameters were calculated.

According to Lagergren, the rate of adsorption is directly proportional to the number of pores on the adsorbent surface. The equation that gives the relation between adsorption capacity and contact time was given in Equation 7 [44].

$$Log(q_e-q_t)=Log\ q_e-k_1\times t/2.303 \quad (7)$$

where k_1 (min^{-1}) is the pseudo-first-order rate constant. The parameters were calculated using the graph of Log (q_e-q_t) versus t [34]. The pseudo-first-order curve was given in Figure 11. The parameters were shown in Table 5.

According to pseudo-second-order model, valence forces are formed by exchanging electrons or joint use of electrons between adsorbent and adsorbate during adsorption [34, 45].

Calculations were made according to Equation 8.

$$t/q = 1/K_2q_e^2 + (1/q_e)\,t \quad (8)$$

where K_2 (min^{-1}) refers to the pseudo-second-order rate constant. The parameters were calculated using the graph of t/q_t versus t (Fig. 12) and shown in Table 5.

The kinetic model defined by Weber was applied to evaluate the diffusion mechanism and speed control steps [46]. The intraparticle diffusion kinetic equation was given in Equation 9.

$$q_t=k_dt^{1/2}+C \quad (9)$$

where C (mg/g) is the constant depending on the boundary layer thickness and k_d (mg/g.min) is the intraparticle diffusion rate constant [47].

Boundary layer diffusion occurs in the first few minutes, and intraparticle diffusion occurs in the time left. The step determining the adsorption rate is intraparticle diffusion [48]. The qt versus $t^{1/2}$ was drawn to determine the effect of intraparticle diffusion (Fig. 13). The slope of the obtained equation gives the velocity constant [49, 50]. An intraparticle diffusion plot was drawn using the data obtained after the 15th minute.

Results showed that R^2 value closest to 1 were obtained with pseudo-second-order kinetic. Therefore, the adsorption was carried out by the pseudo-second-order kinetic.

CONCLUSIONS

Activated carbon was synthesized from the pomace obtained by the three-phase process. Synthesized activated carbon was used to adsorption four different dyes (DS-00102, DS-00203, DS-00502, and mix) from the aqueous solution. The pH value of dye solution, the amount of activated carbon, and the initial dye concentration parameters were optimized. Adsorption kinetics and isotherm models were compared. The most effective removal (92%) was obtained in DS-00502 dye. The optimum parameters were the original pH value (pH=8), 1.0 g/L OPAC, 1000 mg/L initial concentration. The Langmuir isotherm and pseudo-second-order kinetic have been found as the most suitable models. As a result, it can be said that the synthesized material can be used at dye removing from wastewater.

ACKNOWLEDGMENT

The authors thank the Mersin University Scientific Research Projects Department to provide the financial support (Project Number: 2015-AP4-1368).

DATA AVAILABILITY STATEMENT

The authors confirm that the data that supports the findings of this study are available within the article. Raw data that support the finding of this study are available from the corresponding author, upon reasonable request.

CONFLICT OF INTEREST

The authors declared no potential conflicts of interest with respect to the research, authorship, and/or publication of this article.

ETHICS

There are no ethical issues with the publication of this manuscript.

REFERENCES

[1] N. Gholamzadeh, M. Peyravi, and M. Jahanshahi, "Study on olive oil wastewater treatment: Nanotechnology impact," Journal of Water and Environmental Nanotechnology, Vol. 1, pp. 145-161, 2016.

[2] Republic of Turkey Ministry of Trade, "2019 olive and olive oil report," Republic of Turkey Ministry of Trade, Turkey, 2020.

[3] F. Şengül, A. Özer, E. Çatalkaya, E. Oktav, H. Evcil, O. Çolak, and Y. Sağer, "A project on the purification of olive processing waste," T. C. Dokuz Eylül University, Engineering Faculty, Department of Environment Engineering, 2003. [Turkish]

[4] Republic of Turkey Ministry of Trade, "Comparison of olive oil production processes," Republic of Turkey Ministry of Environment and Urbanization Turkey, 2020.

[5] J. Saleem, U. B. Shahid, M. Hijab, H. Mackey, and G. McKay, "Production and applications of activated carbons as adsorbents from olive stones," Biomass Conversion and Biorefinery, pp. 1–28, 2019. [CrossRef]

[6] C. Fernández, M. S. Larrechi, and M. P. Callao, "An analytical overview of processes for removing organic dyes from wastewater effluents," TrAC Trends in Analytical Chemistry, Vol. 29, pp. 1202–1211, 2010. [CrossRef]

[7] S. Ahmed, S. Aktar, S. Zaman, R. A. Jahan, and M. L. Bari, "Use of natural bio-sorbent in removing dye, heavy metal and antibiotic-resistant bacteria from industrial wastewater," Applied Water Science, Vol. 10, pp. 1–10, 2020. [CrossRef]

[8] V. Selen and Ö. Güler, "Modeling of congo red adsorption onto multi-walled carbon nanotubes using response surface methodology: Kinetic, isotherm and thermodynamic studies," Arabian Journal for Science and Engineering, Vol. 46, pp. 6579–6592, 2021. [CrossRef]

[9] V. D. Pakhale and P.R. Gogate, "Removal of rhodamine 6g from industrial wastewater using combination approach of adsorption followed by sonication," Arabian Journal for Science and Engineering, Vol. 46, pp. 6473–6484, 2021. [CrossRef]

[10] M. Bahrami, M. Amiri, and F. Bagheri, "Optimization of crystal violet adsorption by chemically modified potato starch using response surface methodology," Pollution, Vol. 6, pp. 159–170, 2020.

[11] M. Berrios, M. A. Martin, and A. Martin, "Treatment of pollutants in wastewater: Adsorption of methylene blue onto olive-based activated carbon," Journal of Industrial and Engineering Chemistry, Vol. 18, pp. 780–784, 2012. [CrossRef]

[12] T. Bohli, N. Fiol Santaló, I. Villaescusa Gil, and A. Ouederni, "Adsorption on activated carbon from olive stones: Kinetics and equilibrium of phenol removal from aqueous solution," Journal of Chemical Engineering and Process Technology, Vol. 4, pp. 165, 2013.

[13] M. Uğurlu, A. Gürses, and M. Açıkyıldız, "Comparison of textile dyeing effluent adsorption on commercial activated carbon and activated carbon prepared from olive stone by ZnCl2 activation," Microporous and Mesoporous Materials, Vol. 111, pp. 228–235, 2008. [CrossRef]

[14] K. Mohanty, D. Das, and M. Biswas, "Adsorption of phenol from aqueous solutions using activated carbons prepared from tectona grandis sawdust by ZnCl2 activation," Chemical Engineering Journal, Vol. 115, pp. 121-131, 2005. [CrossRef]

[15] N. Hossain, M.A. Bhuiyan, B.K. Pramanik, S. Nizamuddin, and G. Griffin, "Waste materials for wastewater treatment and waste adsorbents for biofuel and cement supplement applications: A critical review," Journal of Cleaner Production, Vol. 255, pp. Article 120261, 2020. [CrossRef]

[16] N. Howaniec, "Olive pomace-derived carbon materials—effect of carbonization pressure under CO_2 atmosphere," Materials, Vol. 12, Article 2872, 2019. [CrossRef]

[17] F. Marrakchi, M. Bouaziz, and B. Hameed, "Activated carbon–clay composite as an effective adsorbent from the spent bleaching sorbent of olive pomace oil: Process optimization and adsorption of acid blue 29 and methylene blue," Chemical Engineering Research and Design, Vol. 128, pp. 221–230, 2017. [CrossRef]

[18] J. Coates. "Interpretation of infrared spectra, a practical approach," John Wiley & Sons, Inc., Newtown, USA, 2006. [CrossRef]

[19] R. Rotaru, P. Samoila, N. Lupu, M. Grigoras, and V. Harabagiu, "Ferromagnetic materials obtained through ultrasonication. 1. Maghemite/goethite nanocomposites," Revue Roumaine de Chimie, Vol. 2017, pp. 131–138, 2017.

[20] S. M. Yakout and G. Sharaf El-Deen, "Characterization of activated carbon prepared by phosphoric acid activation of olive stones," Arabian Journal of Chemistry, Vol 9(Suppl 2), pp. S1155–S1162, 2011. [CrossRef]

[21] H. Arslanoglu, H. Altundogan, and F. Tumen, "Preparation of cation exchanger from lemon and sorption of divalent heavy metals," Bioresource Technology, Vol. 99, pp. 2699–2705, 2008. [CrossRef]

[22] I. H. Aljundi and N. Jarrah, "A study of characteristics of activated carbon produced from jordanian olive cake," Journal of Analytical and Applied Pyrolysis, Vol. 81, pp. 33–36, 2008. [CrossRef]

[23] L. J. Kennedy, J. J. Vijaya, and G. Sekaran, "Effect of two-stage process on the preparation and characterization of porous carbon composite from rice husk by phosphoric acid activation," Industrial & Engineering Chemistry Research, Vol. 43, pp. 1832–1838, 2004. [CrossRef]

[24] T.-H. Liou, "Development of mesoporous structure and high adsorption capacity of biomass-based activated carbon by phosphoric acid and zinc chloride activation," Chemical Engineering Journal, Vol. 158, pp. 129–142, 2010. [CrossRef]

[25] E. I. Ugwu, and J. C. Agunwamba, "A review on the applicability of activated carbon derived from plant biomass in adsorption of chromium, copper, and zinc from industrial wastewater," Environmental Monitoring and Assessment, Vol. 192, pp. 1–12, 2020. [CrossRef]

[26] A. Maleki, A. Mahvi, R. Ebrahimi, and K. Jamil, "Evaluation of barley straw and its ash in removal of phenol from aqueous system," World Applied Sciences Journal, Vol. 8, pp. 369–373, 2010.

[27] M. Bahrami, M.J. Amiri, and F. Bagheri, "Optimization of the lead removal from aqueous solution using two starch based adsorbents: Design of experiments using response surface methodology (RSM)," Journal of Environmental Chemical Engineering, Vol. 7, Article 102793, 2019. [CrossRef]

[28] A. Pala, P. Galiatsatou, E. Tokat, H. Erkaya, C. Israilides, and D. Arapoglou, "The use of activated carbon from olive oil mill residue, for the removal of colour from textile wastewater," European Water, Vol. 13, pp. 29–34, 2006.

[29] G. Cimino, R. Cappello, C. Caristi, and G. Toscano, "Characterization of carbons from olive cake by sorption of wastewater pollutants," Chemosphere, Vol. 61, pp. 947–955, 2005. [CrossRef]

[30] A. Türkyılmaz, and K. Işınkaralar, "Removal of antibiotics (tetracycline and penicillin g) from water solutions by adsorption on activated carbon," Journal of Engineering Sciences and Design, Vol. 8, pp. 943–951, 2020.

[31] N. Soudani, S. Souissi-najar, and A. Ouederni, "Influence of nitric acid concentration on characteristics of olive stone based activated carbon," Chinese Journal of Chemical Engineering, Vol. 21, pp. 1425–1430, 2013. [CrossRef]

[32] I. Langmuir, "The adsorption of gases on plane surfaces of glass, mica and platinum," Journal of the American Chemical Society, Vol. 40, pp. 1361–1403, 1918. [CrossRef]

[33] H. Freundlich, "Über die adsorption in lösungen," Zeitschrift für physikalische Chemie, Vol. 57, pp. 385–470, 1907. [Deutsch] [CrossRef]

[34] N. Abdel-Ghani, E. Rawash, and G. El-Chaghaby, "Equilibrium and kinetic study for the adsorption of p-nitrophenol from wastewater using olive cake based activated carbon," Global Journal of Environmental Science and Management, Vol. 2, pp. 11, 2016.

[35] J.-J. Gao, Y.-B. Qin, T. Zhou, D.-D. Cao, P. Xu, D. Hochstetter, and Y.-F. Wang, "Adsorption of methylene blue onto activated carbon produced from tea (camellia sinensis l.) seed shells: Kinetics, equilibrium, and thermodynamics studies," Journal of Zhejiang University Science B, Vol. 14, pp. 650–658, 2013. [CrossRef]

[36] G. Vijayakumar, R. Tamilarasan, and M. Dharmendirakumar, "Adsorption, kinetic, equilibrium and thermodynamic studies on the removal of basic dye rhodamine-b from aqueous solution by the use of natural adsorbent perlite," Journal of Materials and Environmental Science, Vol. 3, pp. 157–170, 2012.

[37] E. Musin, "Adsorption modelling," Environmental Engineerin Thesis, Mikkeli University of Applied Sciences, Finland, 2013.

[38] I. Anastopoulos, and G. Z. Kyzas, "Agricultural peels for dye adsorption: A review of recent literature," Journal of Molecular Liquids, Vol. 200, pp. 381–389, 2014. [CrossRef]

[39] K. Bharathi and S. Ramesh, "Removal of dyes using agricultural waste as low-cost adsorbents: A review," Applied Water Science, Vol. 3, pp. 773–790, 2013. [CrossRef]

[40] O. Lawasl, A. Sanni, I. Ajayi, and O. Rabiu, "Equilibrium, thermodynamic and kinetic studies for the biosorption of aqueous lead (ii) ions onto the seed husk of calophyllum inophyllum," Journal of Hazardous Materials, Vol. 177, pp. 829–835, 2010. [CrossRef]

[41] G. Stavropoulos, and A. Zabaniotou, "Production and characterization of activated carbons from olive-seed waste residue," Microporous and Mesoporous Materials, Vol. 82, pp. 79–85, 2005. [CrossRef]

[42] W. K. Lafi, "Production of activated carbon from acorns and olive seeds," Biomass and Bioenergy, Vol. 20, pp. 57–62, 2001. [CrossRef]

[43] A. Baçaoui, A. Yaacoubi, A. Dahbi, C. Bennouna, R. P. T. Luu, F. Maldonado-Hodar, J. Rivera-Utrilla, and C. Moreno-Castilla, "Optimization of conditions for the preparation of activated carbons from olive-waste cakes," Carbon, Vol. 39, pp. 425–432, 2001. [CrossRef]

[44] S. Lagergren, "Zur theorie der sogenannten adsorption geloster stoffe, kungliga svenska vetenskapsakademiens," Handlingar, Vol. 24, pp. 1–39, 1898. [Deutsch]

[45] S. Deng, R. Ma, Q. Yu, J. Huang, and G. Yu, "Enhanced removal of pentachlorophenol and 2, 4-d from aqueous solution by an aminated biosorbent," Journal of Hazardous Materials, Vol. 165, pp. 408–414, 2009. [CrossRef]

[46] W. J. Weber, and J. C. Morris, "Kinetics of adsorption on carbon from solution," Journal of the sanitary engineering division," Vol. 89, pp. 31–60, 1963. [CrossRef]

[47] T. A. Saleh, M. N. Siddiqui, and A. A. Al-Arfaj, "Kinetic and intraparticle diffusion studies of carbon nanotubes-titania for desulfurization of fuels," Petroleum Science and Technology, Vol. 34, pp. 1468–1474, 2016. [CrossRef]

[48] O. Keskinkan, M. Z. L. Goksu, A. Yuceer, M. Başibüyük, and C. F. Forster, "Heavy metal adsorption characteristics of a submerged aquatic plant (myriophyllum spicatum)," Process Biochemistry, Vol. 39, pp. 179–183, 2003. [CrossRef]

[49] P. Waranusantigul, P. Pokethitiyook, M. Kruatrachue, and E. Upatham, "Kinetics of basic dye (methylene blue) biosorption by giant duckweed (spirodela polyrrhiza)," Environmental Pollution, Vol. 125, pp. 385–392, 2003. [CrossRef]

[50] P. Ramachandran, R. Vairamuthu, and S. Ponnusamy, "Adsorption isotherms, kinetics, thermodynamics and desorption studies of reactive orange 16 on activated carbon derived from ananas comosus (l.) carbon," Journal of Engineering and Applied Sciences, Vol. 6, pp. 15–26, 2011.